AD_____

Award Number: W81XWH-04-1-0906

TITLE: Delineating the Effects of Tumor Therapies on Prostate Cancer Using Small Animal Imaging Technologies

PRINCIPAL INVESTIGATOR: Jason S. Lewis, Ph.D.

CONTRACTING ORGANIZATION: Washington University
St. Louis, MO 63130-4899

REPORT DATE: November 2007

TYPE OF REPORT: Final

PREPARED FOR: U.S. Army Medical Research and Materiel Command
Fort Detrick, Maryland 21702-5012

REPORT DOCUMENTATION PAGE

Form Approved
OMB No. 0704-0188

1. REPORT DATE *(DD-MM-YYYY)*	**2. REPORT TYPE**	**3. DATES COVERED** *(From - To)*
01-11-2007	Final	15 OCT 2004 - 14 OCT 2007

4. TITLE AND SUBTITLE

Delineating the Effects of Tumor Therapies on Prostate Cancer Using Small Animal Imaging Technologies

5a. CONTRACT NUMBER

5b. GRANT NUMBER
W81XWH-04-1-0906

5c. PROGRAM ELEMENT NUMBER

6. AUTHOR(S)
Jason S. Lewis, Ph.D.

E-Mail: j.s.lewis@wustl.edu

5d. PROJECT NUMBER

5e. TASK NUMBER

5f. WORK UNIT NUMBER

7. PERFORMING ORGANIZATION NAME(S) AND ADDRESS(ES)

Washington University
St. Louis, MO 63130-4899

8. PERFORMING ORGANIZATION REPORT NUMBER

9. SPONSORING / MONITORING AGENCY NAME(S) AND ADDRESS(ES)
U.S. Army Medical Research and Materiel Command
Fort Detrick, Maryland 21702-5012

10. SPONSOR/MONITOR'S ACRONYM(S)

11. SPONSOR/MONITOR'S REPORT NUMBER(S)

12. DISTRIBUTION / AVAILABILITY STATEMENT
Approved for Public Release; Distribution Unlimited

13. SUPPLEMENTARY NOTES

14. ABSTRACT
This final report presents the data generated under the grant awarded to Jason S. Lewis, PhD (W81XWH-04-1-0906). This proposal was aimed at delineating the relationship between androgen ablation and hypoxia as well as monitoring changes in blood flow, metabolism, oxygenation, vascular permeability and cellular proliferation in animal models of prostate cancer using small animal PET. In this final report we detail the advances made in relation to the original Statement of Work. During this funding period we have shown that, (1) it is not possible to delineate changes in prostate tumor glucose utilization with 2-[18F]Fluoro-2-deoxyglucose (FDG) and microPET following androgen ablation treatment; (2) it is not possible to monitor alterations in cellular proliferation with 18F-3'-deoxy-3'-fluorothymidine (18F-FLT) and microPET following treatment; (3) 64Cu-ATSM uptake is affected by the presence of fatty acid synthase (FAS) and, therefore, may not be suitable for the imaging of hypoxia in prostate tumors as the redox balance is changed, and (4) that 1-11C-acetate is a marker for FAS. This work has led to the presentation of six abstracts at international meetings and two peer-reviewed manuscripts. These findings are promising as they suggest a possible biomarker for more effective treatments in prostate cancer patients, and possibly others, since FAS expression has shown links to poor prognosis in other cancers as well. Moreover, since FAS inhibitors are being developed as anti-tumor agents, this technology also provides a unique opportunity to monitor the effectiveness and the validation of new FAS inhibitors for translation into a clinical setting.

15. SUBJECT TERMS
Prostate tumors, small animal imaging, radiopharmaceuticals

16. SECURITY CLASSIFICATION OF:			**17. LIMITATION OF ABSTRACT**	**18. NUMBER OF PAGES**	**19a. NAME OF RESPONSIBLE PERSON**
a. REPORT	**b. ABSTRACT**	**c. THIS PAGE**			USAMRMC
U	U	U	UU	100	**19b. TELEPHONE NUMBER** *(include area code)*

Table of Contents

INTRODUCTION

This final report presents the progress made in months 1-36 of the grant awarded to Jason S. Lewis, Ph.D. (W81XWH-04-1-0906; Delineating the Effects of Tumor Therapies on Prostate Cancer Using Small Animal Imaging Techniques). In this final report we detail the advances made in relation to the Statement of Work, the data collected, and the results obtained. The Research Plan to be achieved during the funding period was as follows;

Table 1. Original Research Plan

CWR22, LAPC-4 and PC-3 tumor bearing mice				
		Months 1-12	**Months 12-24**	**Months 24-36**
Animals Implanted	3 tumor models (50 each line)	150	150	120
Animals for Imaging	Take rate of 80%	120	120	96
RaPh	**Imaging Protocol**	**Months 1-36**		
^{18}F-FDG	1 h post	Months 1-18,140 mice (2 compounds, baseline and post-treatment time points, in 3 tumor models lines, 50% controls)		
^{18}F-FLT	1 h post			
^{64}Cu-ATSM	0–30 min dynamic	Months 12-30, 140 mice (2 compounds, baseline and post-treatment time points, in 3 tumor models lines, 50% controls)		
^{64}Cu-PTSM	0–30 min dynamic			
^{18}F-FDHT	1 h post injection	Months 24-36, 140 mice (2 compounds, baseline and post-treatment time points, in 3 tumor models lines, 50% controls)		
^{45}Ti-transferrin	2 and 4 h post			

BODY – PROGRESS

1. Imaging of Prostate Cancer Tumor Models undergoing Androgen Ablation

1.1. Cell lines and Tumor Models

At the start of the grant we had successfully established the three prostate cancer cell lines, CWR22, LAPC-4 and PC-3 as outlined in the original proposal. During the funding period two additional prostate adenocarcinomas were acquired by our lab. It was felt important to include these lines in our studies in order to present a more complete picture of the response of prostate tumors to flutamide treatments. 22Rv1 is an androgen-independent form of the CWR22 tumor line developed after treatment, regression, and regrowth of tumor to androgen independence (*2*). The LNCaP tumor model is a human prostate carcinoma metastasis and is being maintained in-house.

1.2. Optimizing Androgen Ablation Treatments (Flutamide Therapy)

The treatment of tumors in the imaging experiments was done as outlined in the original proposal. Briefly, flutamide (Sigma) was put into solution in peanut oil by sonication for 30 minutes at 37°C prior to treatment. Treatments were given at 1000 μg/200 μL injection subcutaneously every other day (~20 mg/kg per day) for a total of 6-8 treatments, depending on tumor progression. In all cases, substantial oil remained between injections and accumulated over the course of the treatment schedule. To improve solubility, the flutamide was dissolved in ethanol and subsequently diluted to 10% with peanut oil and vortexing. Although this allowed a smaller injection volume (100 μL), oil still

remained under the skin of the animals. The pockets of oil did not appear to affect the animal, but there was concern that there was inadequate uptake of the pharmaceutical due to sporadic results in tumor size after treatment. With their wild-type androgen receptors, LNCaP tumors should show have shown a response to flutamide treatments, where CWR22 would grow more quickly as the flutamide acts as an agonist. PC-3 tumors should have shown no response since they do not contain androgen receptors.

It was deemed necessary to switch the method of treatment, and diethylstilbestrol was chosen as the replacement based on literature and previous studies performed in our group. Tumor-bearing mice were treated with diethylstilbestrol (DES) to suppress endogenous androgen synthesis. The treated animals were injected subcutaneously with 200 μg DES in 0.1 mL of sunflower seed oil every other day for a total of seven treatments.

1.3. Imaging the Effect of Androgen Ablation on Prostate Tumors with ^{18}F-FDG (Task 1.1)

The task was to delineate changes in tissue glucose utilization with 2-[^{18}F]Fluoro-2-deoxyglucose (FDG) and microPET following androgen ablation treatment. Although it is known that the glycolytic metabolism of prostate cancers is lower than most malignancies (*3*), the lowered uptake was still visible and images could be effectively analyzed. In separate studies, CWR22, LAPC-4, PC-3, LNCaP, and 22Rv1 prostate tumors were implanted subcutaneously into male athymic mice and allowed to grow until palpable. Treatments of flutamide were administered *via* the subcutaneous, peanut oil method every other day for a total of 6-8 treatments. Single position, whole body microPET imaging was performed on mice in pairs in a supine position at the conclusion of treatment. ^{18}F-FDG was prepared using the Coincidence Technologies ^{18}F-FDG synthesis module based on the methods of Hamacher et al.(*4*) Post-imaging, the mice were euthanized and tumors excised for further analysis. MicroPET images (Figure 1) were evaluated by analysis of the standardized uptake value (SUV) of the tumor. No significant differences of uptake of ^{18}F-FDG were seen between the treated and control mice in any of the tumor models (Figure 2).

Task 2.1.was to correlate and validate the imaging results with histological markers (Months 1-36). We felt since there was no observable changes with ^{18}F-FDG imaging to perform histological correlatives with the ^{18}F-FDG imaging would be time consuming and would use valuable resources.

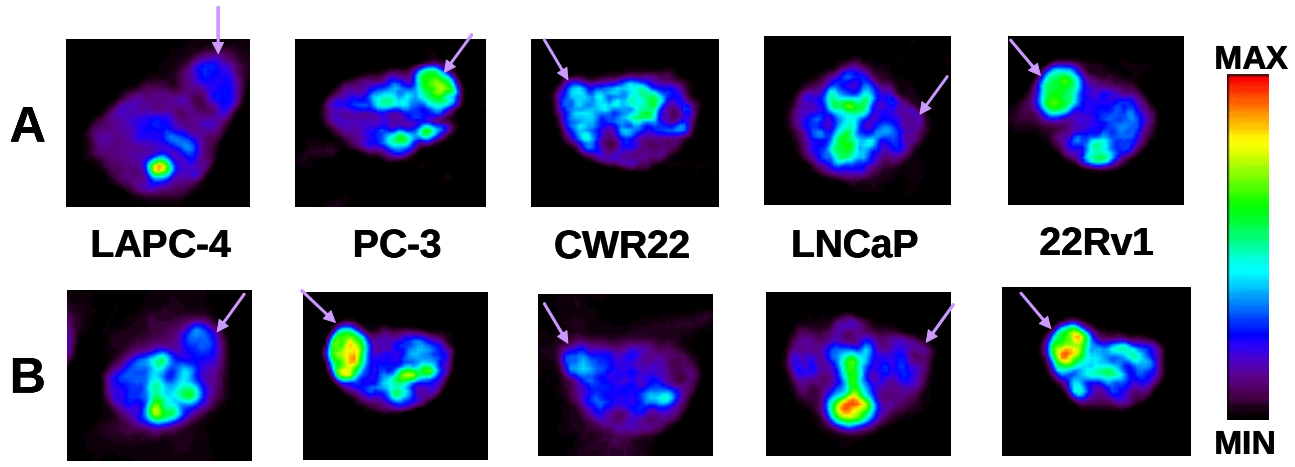

Figure 1. Small animal PET image slices (transaxial) of flutamide treated (A) and control (B) athymic mice bearing prostate tumors and imaged with ^{18}F-FDG. Tumors designated by purple arrows.

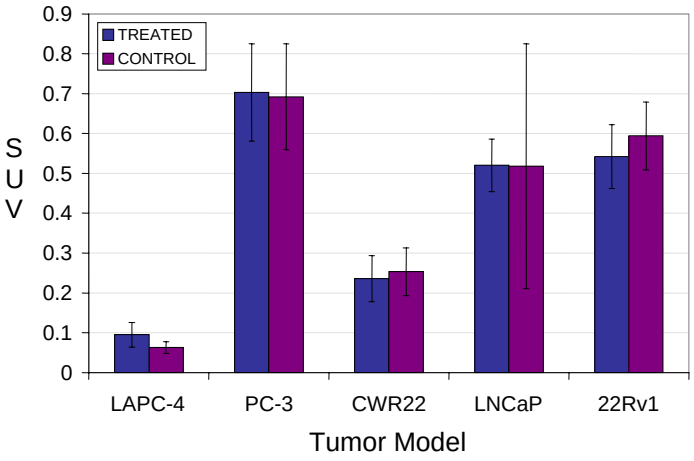

Figure 2. Average SUV values for LAPC-4 (n = 2-3), PC-3 (n = 4-5), CWR22 (n = 2-3), LNCaP (n = 4), and 22Rv1 (n = 5) tumors at 1 hour p.i. of ^{18}F-FDG after 6-8 treatments of flutamide.

These studies were also repeated in PC-3 tumor bearing mice (n = 10) undergoing DES treatment. Again, there were no significant differences of uptake of ^{18}F-FDG were seen between the treated and control mice in any of the tumor models

1.4. Imaging the Effect of Androgen Ablation on Prostate Tumors with ^{18}F-FLT (Task 1.2)

3'-Deoxy-3'-^{18}F-fluorothymidine (^{18}F-FLT) is a marker of cell proliferation (*5-7*). CWR22 and PC-3 tumor bearing mice were treated with flutamide (injection in peanut oil every two days) and imaged with ^{18}F-FLT after 4 and 8 treatments. Results demonstrate no statistical difference in uptake between the treated and control mice in these two tumor lines (Figure 3). The post treatment data has not been analyzed in the CWR22 tumors due to close proximity to the bladder. Activity in the bladder was extremely high, causing artifacts and dead spots where the tumors were located.

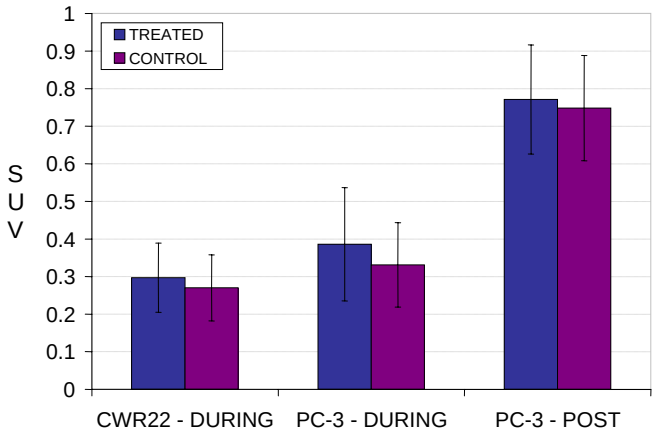

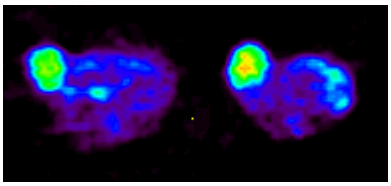

Figure 3. (left) SUV values for PC-3 and CWR22 tumors at 1 hour p.i. of ^{18}F-FLT after 4 and 8 treatments of flutamide. (n = 4-5 for PC-3, n = 3-4). (above) MicroPET transaxial image slices of PC-3 tumor-bearing mice, treated (left) and control (right) at 1 hour p.i. with ^{18}F-FLT.

These studies were also repeated in PC-3 tumor bearing mice (n = 10) undergoing FES treatment. Again, there were no significant differences of uptake of ^{18}F-FLT were seen between the treated and control mice in any of the tumor models

1.5. Imaging the Effect of Androgen Ablation on Prostate Tumors with ^{64}Cu-ATSM (Task 1.3)

Androgen ablation therapy for advanced prostate cancers induces a rapid reduction of blood flow to the prostate and prostate tumor tissue and the concomitant onset of a hypoxic environment in these tissues. Copper(II)-diacetyl-bis(N^4-methylthiosemicarbazone), Cu-ATSM, labeled with a positron-emitting isotope of copper (^{60}Cu, ^{61}Cu, ^{62}Cu or ^{64}Cu) has been shown, *in vitro* and *in vivo*, to be

selective for hypoxic tissue (*8-10*). The clinical use of Cu-ATSM for delineating hypoxic human tumors using PET has provided valuable information in cervical, lung and rectal cancers (*11-13*). Although a rapid >4-fold increase in retention of Cu-ATSM in hypoxic over normoxic cells was observed with overall retention at around 90% in hypoxic compared to 25% in normoxic cells (*1,9*), these investigations did not include the use of prostate tumor cell lines. The year after this grant was funded, Burgmann *et al.* reported diminished hypoxic selectivity of Cu-ATSM *in vitro* in a rat prostate cancer cell line, R3327-AT (*14*). In their analysis of 6 different cell lines, ratios of hypoxic or anoxic uptake of ^{64}Cu-ATSM to normoxic uptake showed that the retention into the two prostate lines were consistently the lowest of the six lines examined. The same group also reported *in vivo* imaging studies comparing ^{64}Cu-ATSM and ^{18}F-MISO in two animal models of cancer (*15*). In the FaDu human squamous cell carcinoma tumor model, the early (~1-4 h) and late (~19 h) ^{64}Cu-ATSM images were similar and were in general accordance with ^{18}F-MISO scans. However, their data did not support using Cu-ATSM as an indicator of hypoxia at early timepoints in the R3327-AT prostate model, with a negative correlation with ^{18}F-MISO at 1 hour after administration. Therefore, although the use of Cu-ATSM had been validated *in vitro* and *in vivo* in multiple tumor models and clinically in various human cancers, there was a concern that its ability to delineate hypoxia in **prostate** tumors may be suspect. In this work, we aimed to investigate and to begin to explain the causes for the reduction of Cu-ATSM hypoxia-selectivity in prostate tumor lines. Given that the mechanism of Cu-ATSM hypoxia-selectivity is reliant on a chemical reduction of Cu(II) and that in prostate cancer the fatty acid synthesis pathway harnesses its oxidizing power for improving the redox balance (i.e., lower NADH/NAD+ ratios) despite conditions of extreme hypoxia (*16*), we wanted to explore these relationships as a potential reason for the lack of Cu-ATSM hypoxia-selectivity in prostate tumors. It was therefore decided to undertake a series of studies exploring the *in vitro* characteristics of Cu-ATSM in hypoxic tumor cells prior to animal studies with flutamide to validate the use of this tracer. The results of these studies are currently being published in Nuclear Medicine and Biology (see Appendix).

1.5.1. Methods

1.5.1.a. In vitro ^{64}Cu-ATSM uptake. A comparison of ^{64}Cu-ATSM uptake under anoxic and normoxic conditions was made in three prostate cell lines – 22Rv1, LNCaP, and PC-3. The apparatus and methods used in the *in vitro* uptake study are based on those previously described in the literature (*9*). Viability of the cells was measured with a hemocytometer utilizing trypan blue staining. Briefly, two three-neck flasks containing cells in suspension were immersed in a 37°C water bath by a rod connected to a stand rotating on an external orbital mixer. An anoxic (5% CO_2, 95% N_2) and normoxic (20% O_2, 5% CO_2, 95% N_2) gas mixture were humidified and brought to 37°C before being passed continuously through each of the flasks. 30-50 mL of cell suspension (1×10^6 cells/mL) was added to each flask and given 1 hour to equilibrate to the environment. After equilibration, 100 μCi ^{64}Cu-ATSM was added to each of the flasks in a small amount (~5 μL) of ethanol. At 1, 5, 15, 30, 45, and 60 minutes, 200 μL of cell suspension was removed *via* pipet and placed in a 1.5 mL Eppendorf tube which was immediately centrifuged for 30 s at 3000 rpm to pellet the cells. 180 μL of the supernatant was then pipetted off and deposited in a separate tube. This was done in triplicate at each timepoint. All pellet and supernatant samples were counted on a gamma counter. Percent uptake was calculated as activity in the pellet (corrected for remaining supernatant) divided by the sum of the pellet and supernatant.

C75 treatment studies were performed in four prostate cell lines – 22Rv1, LNCaP, PC-3, and LAPC-4 following similar methods. In this case, both flasks were under anoxic conditions, while one flask received C75 for FAS inhibition. During the hour of equilibration, C75 was added to the cells (in 10 μL or less of DMSO) so that the final concentration in the flask was 100 μM, while the other flask received DMSO alone. At 1, 5, 15, 30, 45, and 60 minutes the same procedure of sample collection and analysis was performed.

1.5.1.b. FAS expression by ELISA. FAS expression of each tumor line was quantified using a FAS-detect™ ELISA kit (FASgen, Inc.) based on a two-site ELISA technique to quantitatively measure FAS

in human serum. Cells were pelleted and lysed by addition of 1 mL of cell lysis buffer containing protease inhibitors and incubated on ice for 30 minutes. The cell debris was then repelleted and the final supernatant was analyzed. Results were compared to a standard curve of varying concentrations of FAS to determine the concentration in ng/mL. These values were normalized by protein concentration as determined by using a standard copper reduction/bicinchoninic acid assay (Pierce) with bovine serum albumin as the standard, resulting in a ratio with units of ng FAS/µg protein.

1.5.1.c. In vitro C75 dose response on ^{64}Cu-ATSM uptake. These *in vitro* studies were performed using the same apparatus and methods as previously described in the initial *in vitro* experiments. In this study however, various amounts of C75 were added to the cells (in 10 µL or less of DMSO) so that the final concentration of C75 in each flask was 100, 20, 4, or 0.8 µM.

1.5.2. Results

For each cell line, two three-neck flasks containing cells (35 mL) in suspension were placed under anoxic and normoxic conditions with or without pretreatment with C75 (100 µM). Uptake of ^{64}Cu-ATSM was measured over time to determine if FAS inhibition (by C75) restored the cells' ability to trap Cu-ATSM under low oxygen conditions. Inhibition of FAS with C75 resulted in a dramatic increase in ^{64}Cu-ATSM retention into prostate tumor cells *in vitro* under anoxic conditions (Figure 4). The treated cells demonstrated higher uptake values at 15 minutes of 20.93 ± 3.271, 103.0 ± 32.57, 144.2 ± 32.28, and 200.1 ± 79.27 % over control values for LAPC-4, PC-3, LNCaP, and 22Rv1 cell lines, respectively. These values would later be correlated to FAS expression of each cell line.

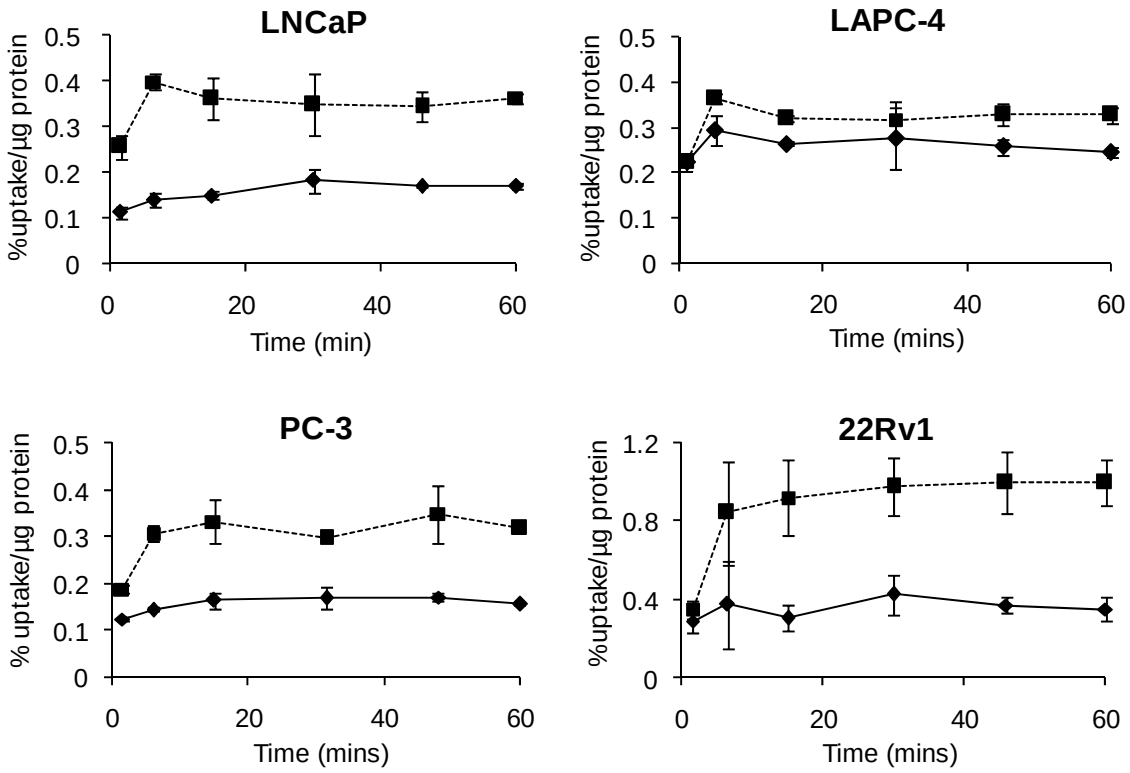

Figure 4. Uptake of ^{64}Cu-ATSM into prostate tumor cells (in suspension) under anoxic conditions (5% CO_2 + 95% N_2) treated with C75 (dashed) and compared to control (solid). (n = 3 at each timepoint)

Ratios of anoxic to normoxic ^{64}Cu-ATSM uptake demonstrate the selectivity of the tracer in a particular model, and so these were also compared over the 60 minute experiment (Figure 5, 15 min data shown). The value obtained for the retention of ^{64}Cu-ATSM into EMT-6 murine mammary

carcinoma cells at 15 min is included for comparison (*1*). The 15 minute time point was chosen since Cu-ATSM in these cells was shown to plateau at this point (Fig. 4). Similar kinetics were shown in Lewis et al., (*1*) and Dearling et al., 1998 (*9*). Also given that this is entirely an *in vitro* study, the potential blood flow issues associated with *in vivo* studies was not felt to be a factor. It is also worth pointing out that in the human ^{60}Cu-ATSM studies uptake in tumors (*11,12*) resulted in high contrast levels between hypoxic and normoxic tissues by as little as 10-15 minutes post injection, and yielded clinically relevant information about tumor oxygenation that was predictive of tumor behavior and response to therapy. In this current study, values in all three of the cell lines examined under normoxic conditions, were lower than the EMT-6 ratios suggesting that visualization of solid tumors, derived from these prostate cancer cell lines may be difficult due to normoxic background retention in the surrounding tissue.

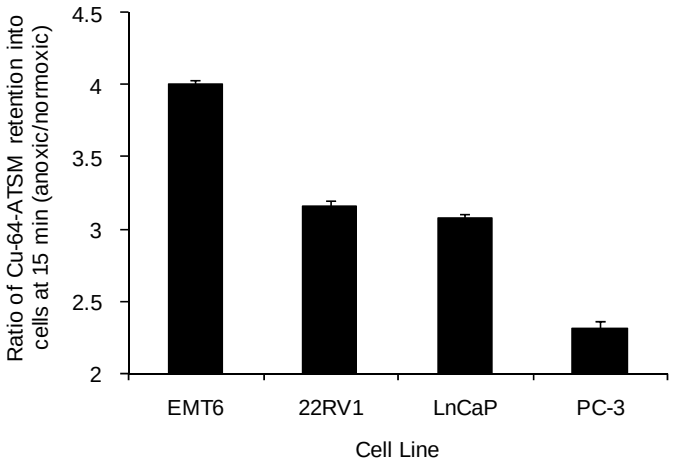

Figure 5. Ratios of anoxic to normoxic ^{64}Cu-ATSM uptake in prostate cancer cells lines at 15 mins demonstrating differing selectivity of the tracer in different models. The value obtained for the retention of ^{64}Cu-ATSM into EMT-6 murine mammary carcinoma cells at 15 mins is included for comparison (*1*).

Samples of each cell line were analyzed to determine if relative amounts of FAS were related to the magnitude of Cu-ATSM retention at 15 min post-incubation. Quantification of FAS expression, by ELISA, resulted in values of 0.00438 ± 0.00024, 0.00832 ± 0.00038, 0.01877 ± 0.00092, and 0.02679 ± 0.00224 ng FAS/µg total protein for LAPC-4, PC-3, LNCaP, and 22Rv1, respectively. As expected, a correlation is seen (R^2 = 0.911) with FAS expression plotted against the change in hypoxic retention resulting from inhibition of FAS (Fig. 6).

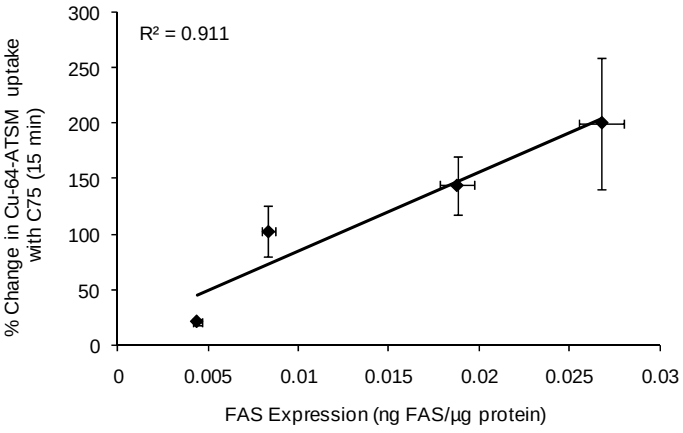

Figure 6. Correlation of FAS expression as determined by ELISA to % change in ^{64}Cu-ATSM uptake between C75 treated (100 µM) and control cells under anoxic conditions (5% CO_2, 95% N_2) at 15 min post-incubation. Points on the graph represent LAPC-4, PC-3, LNCaP, and 22Rv1 from left to right. (n = 3 at each timepoint)

The dose response effect of C75 on the restoration of hypoxic retention of Cu-ATSM was measured in PC-3 cells utilizing the same cell suspension apparatus and anoxic gas mixture. During a 1-hour equilibration period, the four flasks were treated with varying concentrations of C75 (100, 20, 4, or 0.8

μM). Confirming the effect of FAS inhibition on ^{64}Cu-ATSM uptake, the experiment showed increasing retention directly related to C75 for 100, 20, 4, and 0.8 μM respectively at 15 mins (Fig. 7).

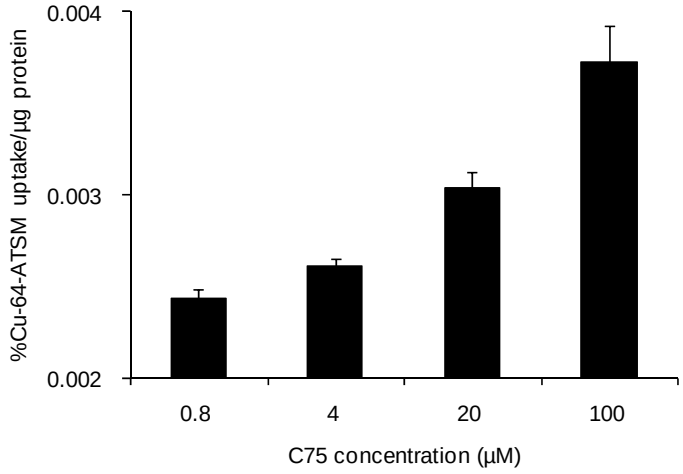

Figure 7. Dose response of ^{64}Cu-ATSM uptake at 15 mins (under anoxic conditions) in PC-3 cells following FAS inhibition by C75. p = 0.0026 (100-20), p = 0.0002 (20-4).

1.5.3. Discussion

Low oxygen levels are a hallmark of malignant processes, leading to a cascade of oncogenic properties that support tumor growth and invasion (*17-21*). Existing in this harsh environment, the cells go into survival mode and do not easily respond to DNA damaging chemotherapeutics or agents that promote apoptosis (*22,23*). In the absence of oxygen, the damaging radicals created by traditional radiation therapy recombine resulting in little damage to the target tissue (*21,24,25*). Levels of tumor hypoxia have also been correlated to overall patient survival and tumor aggressiveness (*17,18,26-28*).

^{64}Cu-ATSM (*8*), which targets hypoxia as opposed to metabolism, has already been confirmed as a clinically important PET agent in the prediction of prognosis in several cancers. It has been shown to be a useful clinical PET imaging tracer that can distinguish responders to conventional therapies from non-responders in patients with lung (*12*), cervical (*11*), rectal (*13*) and head and neck (data not published) cancer. It has also been suggested as a potential tool for radiation oncologists to tailor the radiation dose based on hypoxic regions, giving the resistant regions an increased dose (*29*).

Recently, Yuan *et al*, showed that the regional ^{64}Cu-ATSM retention in two tumors types (R3230Ac and 9L) correlated closely with intrinsic markers for hypoxia, but in a third tumor type (FSA) a correlation was not observed (*30*). The suggested reason for this low correlation between Cu-ATSM uptake and hypoxic distribution was the differing redox statuses of the tumor types. FSA tumors may have a lower-than-average redox potential with high concentrations of electron donors. If the speculated mechanism of Cu-ATSM uptake holds, then reduction, release and ultimate cellular trapping of Cu(I) would be caused by a decrease in the redox potential of the cell (*8,10,14,31,32*). In the FSA tumor line, the lower-than-average redox potential caused reduction and trapping of ^{64}Cu-ATSM in both hypoxic and normoxic areas. It was also suggested that the higher perfusion levels surrounding the hypoxic regions of the FSA tumor could contribute to the higher level of retention of Cu-ATSM in normoxic FSA cells. *In vitro* and *in vivo* experiments have also revealed inconsistencies in the hypoxic selectivity of Cu-ATSM in **prostate** cancer models (*14,15*). Although a very limited number of other tumor cell lines such as FSA have shown inconsistencies, prostate tumors clearly stand out as the primary tumor type that Cu-ATSM hypoxia-selectivity is reduced to low or even undetectable levels (*14,15*). This current study was undertaken in human prostate tumor lines to better examine the reasons for the lack of hypoxia-selectivity of Cu-ATSM in prostate tumors.

Biologically, prostate tumors have some unique characteristics when compared to other malignancies. Prostate cancer is known to have low metabolism, and the most common PET tracer for detecting malignancies, ^{18}F-FDG, is not effective in delineating it from surrounding tissue (*33*) and also goes to sites of inflammation. Fatty acid synthase (FAS) is a multi-functional enzymatic protein involved in many stages of fatty acid synthesis and has been found to be overexpressed in prostate carcinomas as well as other cancers (*34-42*). It is an androgen-regulated enzyme that is overexpressed in the vast majority of prostate tumors and its expression defines distinct molecular signatures in prostate cancer (*43*). An increased level of FAS has been found to be indicative of aggressive and late-stage prostatic adenocarcinomas (*44*) as well as a prognostic indicator for overall survival (*45*).

As a defense mechanism in prostate cancer cells, the fatty acid synthesis pathway harnesses its oxidizing power for improving the redox balance (i.e., lower NADH/NAD^+ ratios) despite conditions of extreme hypoxia (*16*). This pathway is able to consume reducing equivalents (i.e., NADPH) as part of its normal processes. Under hypoxic conditions, anaerobic glycolysis creates excessive levels of lactate, which limits the respiratory chain and reduces its oxidizing power. The relationship between the fatty acid synthesis pathway and prostate tumors has been superbly reviewed by Hochachka et al., (*16*). In regards to the hypoxia-selectivity of Cu-ATSM, it has been shown that Cu-ATSM enters all cells by passive diffusion, and under normoxic conditions freely exits the cell. Under hypoxic or anoxic conditions, the redox potential of the cell is altered such that the Cu(II) in the complex is reduced to Cu(I) and the complex falls apart (*10,14,31,32*). This retention mechanism is reliant on the reduction of the Cu(II) to Cu(I), and if cellular reducing equivalents such as NADPH are consumed by the overexpression of the fatty acid synthesis pathway this chemical reduction, even under conditions of hypoxia, is unlikely to take place.

Analysis of the hypoxic selectivity of the four human prostate models studied shows diminished selectivity when compared to EMT-6 mammary carcinoma (Fig. 5). By dividing the anoxic uptake by the normoxic uptake, a relative selectivity is calculated. Values of approximately 1.5-3.8, which were found in this study, are consistently lower than many other cell lines described in the literature (*14*). In Burgman's study, MCF-7, FSaII, and FaDu cell lines show selectivity of between 7 and 10, with R3327-AT showing no hypoxia selectivity at all (*14*). Interestingly, cancers of the breast (*38,39,42*), colon (*41*) and ovary (*40*) are also known to demonstrate *elevated* levels of FAS. Given that in the Burgmann study (*14*) MCF7 cells demonstrated high hypoxia-selectivity for Cu-ATSM and they are known to express high levels of FAS (*46*), additional pathways may be involved in reducing Cu-ATSM hypoxia-selectivity that are not explained entirely by the presence of over-expression of FAS. However, it is important also to discuss what is meant by the term of 'overexpression' or "express high levels'. Even though the literature often uses these terms, they must be placed in context; in this current study we chose to compare four human prostate cancer cells lines that were shown to have *relatively* low or high expression to one another. It is has been shown that the overexpression of FAS in precursor prostate tumors is significantly higher than that of other tumor types such as breast (*47*). Therefore, even though breast cancer and other malignancies are known to have higher levels FAS than surrounding normal tissue, whether or not this overexpression is at a level that will prevent Cu-ATSM reduction in hypoxic cells has yet to be determined. A full comparative and exhaustive study is therefore required in other cell types (e.g., breast tumor lines) before similar conclusions about the relationship of FAS expression and Cu-ATSM hypoxia-selectivity can be made for those tumor types.

C75 is a small molecule that binds to and inhibits mammalian FAS and inhibits fatty acid synthesis in human cancer cells. Researchers have shown that C75 inhibits FAS by 89-95% (*48*). In this study, C75 was used to inhibit FAS activity in prostate tumor cell lines by blocking this enzymatic cycle's ability to offset the redox balance of a hypoxic cell, therefore, increasing retention of Cu-ATSM under hypoxic conditions. Typically a blocking study is designed to inhibit uptake of the radiotracer; in this case we were attempting to block the FAS so that it is unable to 'stabilize' the redox environment of the cell. Its inhibition should allow the anticipated retention of Cu-ATSM in hypoxic regions of the tumor. *In vitro* results in all cell lines demonstrate that FAS has a significant impact on the retention of

^{64}Cu-ATSM into human prostate tumor cells under oxygen-limited conditions. Inhibition of FAS with a single 1 hour treatment of C75 (50 μM) resulted in increased retention of Cu-ATSM in all four tumor lines tested *in vitro* (Fig.4), but to a limited extent in the low-FAS-expressing LAPC-4. Results also showed that a linear change in uptake correlated directly to the cellular expression of FAS (Fig 6). To demonstrate that restoration of retention is directly related to FAS inhibition, a dose response experiment was undertaken (Fig. 7).

1.5.4. Conclusion

Cu-ATSM has been a valuable tool as a marker of hypoxia, and it's possible that the nature of its mechanism of retention, though not completely understood, could lead us to answers for the incongruences in its selectivity. The uncertainty lies in the possibility that other physiological changes caused by malignant progression and hypoxia within the cell could also affect this redox balance regardless of oxygen concentration. If the suggested mechanism of Cu-ATSM uptake holds, then reduction, release and ultimate cellular trapping of Cu(I) would be caused by a decrease in the redox potential of the cell. And, although in most cases this is directly due to a change (reduction) in oxygen concentration within the cell, there are many other processes that could also alter the redox potential of this environment. In prostate tumors, a reduction of ^{64}Cu-ATSM hypoxia selectivity is demonstrated in a manner that directly correlates to FAS expression. ^{64}Cu-ATSM is a very effective PET agent for clinically delineating many hypoxic human malignancies, but, as with all radiopharmaceuticals, it is not a universal agent. Care should be taken in particular regard to the imaging of prostate tumors.

1.6. Imaging the Prostate Tumors with 1-^{11}C-Acetate

As shown above, the fact that Cu-ATSM as a hypoxia marker was not suitable for imaging prostate tumors and that this was likely related to the expression of FAS, we chose to use ^{11}C-acetate for this task under the Statement of Work. 1-^{14}C-acetate has been used for years for measurement of lipid and cholesterol synthesis by monitoring its uptake into cells, and ^{11}C-acetate is used clinically for imaging prostate cancer in humans. We therefore undertook the following series of studies to evaluate the potential of using ^{11}C-acetate for the purpose of this grant. The results of these studies are currently being published in the Journal of Nuclear Medicine (see Appendix). This work was done in collaboration with Dr. Steve Kridel at Wake Forest University.

^{18}F-fluordeoxyglucose positron emission tomography (^{18}F-FDG PET) has become essential in the diagnosis of many malignancies, but it is not ideal in the detection of prostate cancer. Prostate cancer is one of a handful of tumors with low metabolism and ^{18}F-FDG, being a marker of glucose metabolism, is not highly effective in delineating it from surrounding tissue (*33*). Although FDG has been shown to be effective in the assessment of high grade primary tumors and metastatic disease (*49-53*), other obstacles still leave much to be desired for its use with prostate malignancies, especially at early stages. The bladder clearance of ^{18}F-FDG also poses an obstacle as it is in the same anatomical region as the prostate, and, therefore, the primary tumor. Studies have also shown an inability to differentiate benign hyperplasia in the prostate from malignant disease or post-operative scarring from radical prostatectomy (*54,55*).

Because of the problems associated with ^{18}F-FDG imaging in prostate, alternative modalities must be employed to image prostate cancer. Clinically, 1-^{11}C-acetate has been shown to be an effective tracer for the delineation of prostate cancer and its metastases with PET in humans (*56-60*). Although it is accepted that the metabolic fate of 1-^{11}C-acetate in tumors differs from normal tissue, the exact pathway has not been fully elucidated.

Fatty acid synthase (FAS) is a multi-functional enzymatic protein that catalyzes fatty acid biosynthesis (*61*). FAS is over-expressed in prostate carcinomas as well as other cancers (*34-36,43,62*). On the other hand, FAS levels are low or absent in most normal tissues. FAS levels are associated with tumor aggressiveness in late-stage prostatic adenocarcinomas as well as a prognostic indicator for

overall survival (*44*). Previous studies have demonstrated that FAS inhibitors can reduce ^{14}C-acetate incorporation in human tumor cell lines and in human lung xenografts and mouse prostate tumors *ex vivo* (*63-66*). Because of these facts, we hypothesize that FAS is involved with 1-^{11}C-acetate uptake in prostate cancer. The following reports an examination of the mechanism of 1-^{11}C-acetate uptake in prostate tumor models and its implications for tumor progression and patient survival. Understanding the mechanism of 1-^{11}C-acetate uptake and the relation to FAS expression levels could provide a valuable tool to clinicians for the planning and monitoring of treatments due to increased mortality with raised levels of this protein in prostate cancer. It could also be used in validating the translation of novel FAS inhibitors, as anti-cancer agents, into the clinical setting.

1.6.1. Materials

1.6.1.a. General. Carbon-11 labeled acetate was prepared by the reaction of ^{11}C-labeled carbon dioxide with a Grignard reagent as previously described (*67*). Radiochemical purity was always 99% or greater.

1.6.1.b. In vitro Cell Uptake and Inhibition. PC-3, LNCaP, and 22Rv1 prostate cells were plated in 6-well plates (4.5×10^5, 9×10^5, and 1.2×10^6 cells per well, respectively) 24 hours before the study was initiated. The cells were grown to ~75% confluence at 37°C and 5% CO_2 in appropriate medium and supplemented with 10% heat-inactivated fetal bovine serum. Eighteen hours prior to the uptake experiment, C75 (63.5 μg), an FAS inhibitor (*48*), was added to the growth media (5 mL) in each well in a small amount of DMSO (10 μL) so that the final concentration in each well was 50 μM (controls received DMSO alone). To initiate the study, the culture medium was removed, and cells were rinsed with phosphate buffered saline (PBS). Approximately 0.37 MBq (10 μCi) of 1-^{11}C-acetate was added to the cells in 1.0 mL fresh media to initiate tracer uptake (including C75 or DMSO alone to maintain inhibitor concentration). Incubation was terminated at various times (15, 30, or 60 minutes) by removing the radioactive culture medium. Cell monolayers were washed with 2 mL of cold PBS three times to remove any excess culture medium from the extracellular spaces. Lysis of the cells was achieved by addition of 1 mL of 0.25% sodium dodecyl sulfate. Lysis extracts, as well as 1 mL radioactive culture medium as a standard, were counted in a γ-counter and measured for protein content using a standard copper reduction/bicinchoninic acid assay (Pierce Biotechnology, Rockford, IL), with bovine serum albumin as the protein standard. Cellular uptake data for all experiments were normalized for the amount of protein present and calculated as the percentage uptake (cell-associated). A further inhibition study was performed with TOFA, a potent inhibitor of acetyl-CoA carboxylase (ACC), a key enzyme involved in fatty acid biosynthesis (*68*). Procedures were similar to those stated above, with the final concentration of TOFA being 30 μM and the pretreatment occurring 2 hours prior to addition of 1-^{11}C-acetate. The tracer was added directly to the 5 mL of growth media, rather than changing the media, to ensure continued presence of the pretreatment concentration of TOFA.

To compare the abilities of C75 and TOFA to inhibit fatty acid synthesis, PC-3 cells were seeded in 24-well plates at 1×10^5 cells per well. After 48 hours the cells were treated with either C75 (0, 10, 20, 30 or 60 μM) to inhibit FAS or TOFA (0, 10, 20 or 30 μM) to inhibit ACC for two hours and then 2-^{14}C-acetate (0.037 MBq, 1 μCi) was added for an additional two hours. An additional study was performed in both PC-3 and LNCaP cells, where cells were seeded in 24-well plates at 1×10^5 cells per well. After 48 hours the cells were treated with either C75 (30 μM) to inhibit FAS or TOFA (30 μM) to inhibit ACC for two hours and then 2-^{14}C-acetate (0.037 MBq, 1 μCi) was added for an additional two hours. Control cells received DMSO (0.1 %) only. After the labeling period, the cells were collected, washed and lipids were extracted and quantified by scintillation counting as described previously (*69,70*).

To observe the contribution of the TCA cycle to 1-^{11}C-acetate cellular uptake, an inhibition study with 3-nitroprionic acid, a known inhibitor of succinate dehydrogenase in the TCA cycle, was performed.

PC-3 cells plated in 6-well plates 24 hours prior to uptake, were treated with 100 μM 3-nitropropionic acid 2 hours prior to radiotracer uptake, while control cells received vehicle alone. 1-^{11}C-acetate (1.11 MBq, 30 μCi) was added to the wells followed by a 25 minute incubation. Cells were then washed and collected by trypsin/EDTA for counting in the gamma counter and subsequent protein assay for normalization.

1.6.1.c. Small Animal PET Imaging. All animal experiments were performed in compliance with the Guidelines for the Care and Use of Research Animals established by Washington University's Animal Studies Committee. Single position, whole body imaging was performed using small animal PET (MicroPET®Focus-120 and or 220, CTI-Concorde Microsystems LLC) (*71*). Mice were imaged individually or in pairs in a supine position in a specially designed bed. Isoflurane (1-2%) was used as an inhaled anesthetic to induce and maintain anesthesia during imaging. The bed was placed near the center of field of view of the PET scanner where the highest image resolution and sensitivity are available. Imaging was performed, 20-min post injection, with a single 10 min static scan. Images were reconstructed by Fourier rebinning followed by two-dimensional Ordered Subset Expectation Maximization (OSEM) (*72*).

PET images were evaluated by analysis of the standardized uptake value (SUV) of the tumor and non-target organ (muscle) using the software ASIPRO (Concorde MicroSystems, Inc.). The average radioactivity concentration within the tumor or tissue was obtained from the average pixel values reported in nCi/cc within a volume of interest (VOI) drawn around the entire tumor or tissue on multiple, consecutive transaxial image slices. SUVs were calculated by dividing this value, the decay-corrected activity per unit volume of tissue (nCi/mL), by the injected activity per unit of body weight (nCi/g). Necrotic tissue was excluded by analysis of the images in comparison to serial slices through the tumor post-mortem. Any necrosis in a tumor was noted and those sections (which also had no uptake) were not included in the overall SUV calculation.

An animal imaging study was performed in 22Rv1, PC-3, CWR22 and LAPC-4 tumor bearing mice, to confirm correlation of uptake of 1-^{11}C-acetate to FAS expression in tumors. Two prostatic carcinoma tumor models were prepared in culture (22Rv1 and PC-3) then harvested for implant by trypsin/EDTA and injected in a volume of 100 μL into the right flank of intact, male nu/nu mice (15-20 g) in the appropriate media at a given concentration (5 x 10^6 cells in Matrigel for 22Rv1 and 3 x 10^6 cells in Kaighn's modification of Ham's F12 medium for PC-3). CWR22 and LAPC-4 tumors were obtained from animal to animal passage. Tumors were allowed to grow until palpable, and the time varied by model. PET imaging was performed 20-mins post i.v. injection of 14.8-18.5 MBq (400-500 μCi) 1-^{11}C-acetate (100 μL) via the tail vein. The 20-min post injection time point was chosen given the experience of other researchers (*57,58,60*). Post imaging, the mice were euthanized and the tumors excised and flash frozen to -80°C for subsequent Western blot analysis to determine FAS expression. Images were analyzed for determination of SUV and compared to the Western blots.

1.6.1.d. Western blots. Frozen tumors were thawed over ice, homogenized and the cells lysed with 1X cell lysis buffer (Cell Signaling Technology, Danvers, MA) for determination of protein concentration by BCA protein assay (Pierce, Rockford, IL). 20 μg protein of each sample was run using SDS-PAGE with a 4-20% Tris gradient gel. Standard Western blotting was performed with an anti-FAS primary antibody (rabbit; Novus Biologicals, Littleton, CO) and a goat anti-rabbit secondary antibody (DyLight™647; Pierce Biotechnology, Rockford, IL). Final detection was achieved by using the enhanced chemiluminescence system (Amersham Life Sciences, Piscataway, NJ) according to the manufacturer's instructions. Prestained standards (Kaleidoscope Prestained Standards 161-0324, BIO-RAD Laboratories, Hercules, CA) were used on each Western blot for reference. Blots were traced and intensity and area values were obtained for each band by densitometry using the Image J software (NIH, Bethesda, MD) to quantify expression.

1.6.1.e. PET Imaging of FAS Inhibition. Male, nu/nu mice were injected with either PC-3 (3×10^6 cells/100 μL) (n = 3) or LNCaP (1×10^7 cells/100 μL) (n = 4) tumor cells subcutaneously in the right flank which were allowed to grow until palpable. PET imaging was performed 20 minutes post i.v. injection of 3.7-7.4 MBq (100-200 μCi) 1-^{11}C-acetate (100 μL) followed by a low resolution CT scan for subsequent co-registration and anatomical reference. Following imaging, all mice received an i.p. injection of C75 at 30 mg/kg dissolved in DMSO/RPMI 1640 media (<2% DMSO). Eighteen hours post treatment, the mice were imaged again following the same protocol. Post imaging, the mice were euthanized and the tumors excised and formalin fixed for staining and immunohistochemical analysis.

1.6.1.f. Immunohistochemistry. Following PET imaging to observe inhibition of 1-^{11}C-acetate uptake in prostate tumors by blocking of FAS, immunohistochemical techniques were employed to demonstrate the extent of protein expression. Tumors from the *in vivo* inhibition study were formalin fixed, paraffin embedded, sliced and placed on slides for immunohistochemical analysis by the Histology Core at Washington University, while also staining one slide per section with hemotoxylin and eosin to confirm tissue viability.

1.6.2. Results

Inhibition of fatty acid synthesis reduces 1-^{11}C-acetate in vitro uptake. To confirm the hypothesis that 1-^{11}C-acetate uptake in tumors is related FAS expression, an *in vitro* blocking study was performed. Cells were pretreated with for 18 hours with C75, a known inhibitor of FAS, prior to uptake of 1-^{11}C-acetate to determine if uptake could be blocked. All cells showed a linear increase in uptake over time in both the C75 treated and control tumor cells. In all cases the uptake in the control cells was consistently higher throughout the duration of the study. By 30 min, the C75 treated cells showed inhibition of uptake by 26.4% (p = 0.0005) in the PC-3 cell line, and 16.7% (p = 0.0010) and 26.9% (p = 0.0007) for LNCaP and 22Rv1, respectively (Fig. 8A). Cell viability was measured by trypan blue staining. An average of 95% viability was measured for each of the cell lines, with no decrease in overall cell number due to the presence of C75 (data not shown).

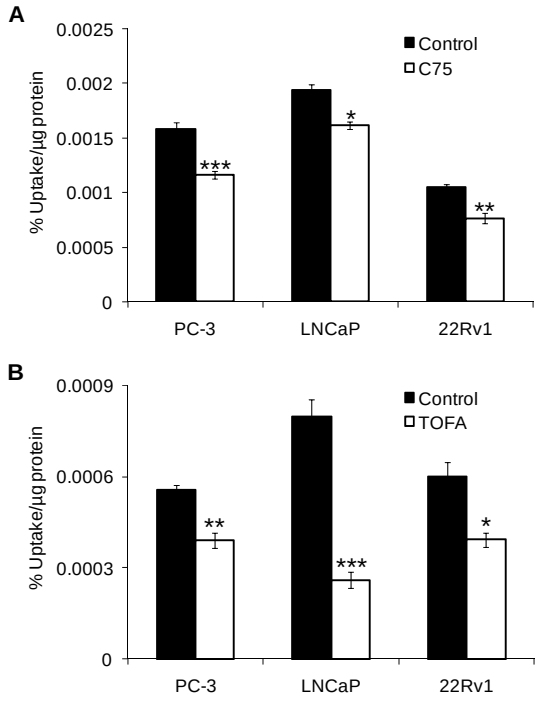

Figure 8. (A) *In vitro* cell association of 1-^{11}C-acetate at 30 min in PC-3, LNCaP, or 22Rv1 prostate cancer cells with and without 18 h prior treatment with C75, a FAS inhibitor. (*p = 0.001, **p = 0.0007, ***p = 0.0005)**;** (B) *In vitro* cell association of 1-^{11}C-acetate at 30 min in PC-3, LNCaP or 22Rv1 prostate cancer cells with and without 2 h prior treatment with TOFA, an ACC inhibitor to block the fatty acid synthesis pathway. (*p = 0.0025, **p = 0.0008, ***p = 0.0001). Error bars are ± SD.

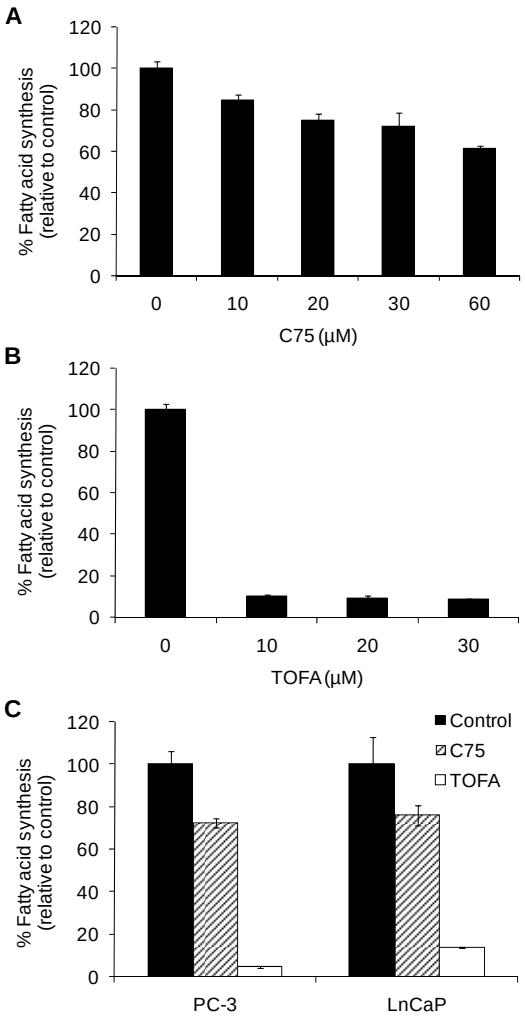

Figure 9. A dose-response comparison of the relative effects of (A) C75 and (B) TOFA on FA synthesis in PC-3 cells, performed with ^{14}C-acetate. (C) Comparison of FA synthesis inhibition with 30 μM of C75 or TOFA in PC-3 and LNCaP cells. Error bars are ± SD.

The role of acetyl Co-A carboxylase (ACC) in 1-^{11}C-acetate uptake was also determined by treating cells with TOFA, a potent inhibitor of ACC; ACC is the rate limiting enzyme in the fatty acid synthesis pathway. After pretreatment with TOFA, cell uptake of 1-^{11}C-acetate was significantly reduced, more so than with C75 (Fig. 8B). The percentage of blocking increased over time in all cases, with values of 29.8 ± 5.75%, 67.4 ± 9.22%, and 34.7 ± 9.31% for PC-3, LNCaP, and 22Rv1, respectively, at 30 minutes. To demonstrate that TOFA is a more potent inhibitor of FA synthesis than C75 a dose-response comparison between TOFA and C75 in PC-3 cells was performed (Fig. 9A and 9B). It is evident that even at concentrations of 10 μM, TOFA has a significantly more pronounced effect on FA synthesis than C75 (10 μM: 10.7 ± 0.59 % vs. 84.9 ± 2.47%). An additional one-point study comparing PC-3 cells with LNCaP cells was undertaken to show that this relationship was observed in more than one cell line. It was shown that 30 μM C75 inhibited about 30% of FA activity in both PC-3 and LNCaP cells while TOFA inhibited FA synthesis about 75-80% (both after a 2 hour treatment) (Fig. 9C). These data demonstrate that 1-^{11}C-acetate uptake is directly related to the degree of FAS inhibition in prostate tumor cell lines.

PET imaging demonstrates an in vivo correlation between 1-^{11}C-acetate uptake and FAS expression. To test the hypothesis that 1-^{11}C-acetate may be imaging FAS expression *in vivo*, an imaging study was performed, with excision of the tumors post imaging for further analysis of FAS levels by Western blot. 1-^{11}C-acetate PET imaging of 4 prostate tumor models (PC-3, 22Rv1, CWR22, and LAPC-4) was performed (Fig. 10A-C). Regions of interest (ROIs) were drawn on the images around the tumors, excluding any necrotic tissue. Standardized uptake values (SUVs) at 20 mins post injection were calculated to normalize these values (nCi/cc) to the injected activity per animal (nCi), as well as body

mass (g). Imaging SUVs were 0.11 ± 0.01 for LAPC-4 (n = 2), 0.26 ± 0.06 for CWR-22 (n = 2), and 0.18 ± 0.02 for 22Rv1 (n = 3). In this case, the PC-3 tumors (n = 2) could not be delineated from the surrounding tissue and, therefore, no SUVs were calculated. Visual inspection of the Western blot results revealed obvious differences in the intensity of the band near 250 kDa (FAS = 267 kDa) with PC-3 showing the lowest levels of expression, 22Rv1 and LAPC-4 with significantly more intensity than PC-3, and CWR22 being the highest of those examined (Fig. 10D). Densitometry analysis confirmed this trend quantitatively. The relative values of expression were averaged for each tumor type resulting in 2354.1 ± 22.8, 9640.9 ± 2552.3, 11160 ± 25.0, and 15798 ± 4057.6 for PC-3, LAPC-4, 22Rv1, and CWR22, respectively. Comparison of the average SUVs from the PET data with Western blot analysis of the homogenized tumor tissue resulted in a correlation (R^2 = 0.974) between tumor uptake of 1-^{11}C-acetate and FAS expression (Fig. 10E).

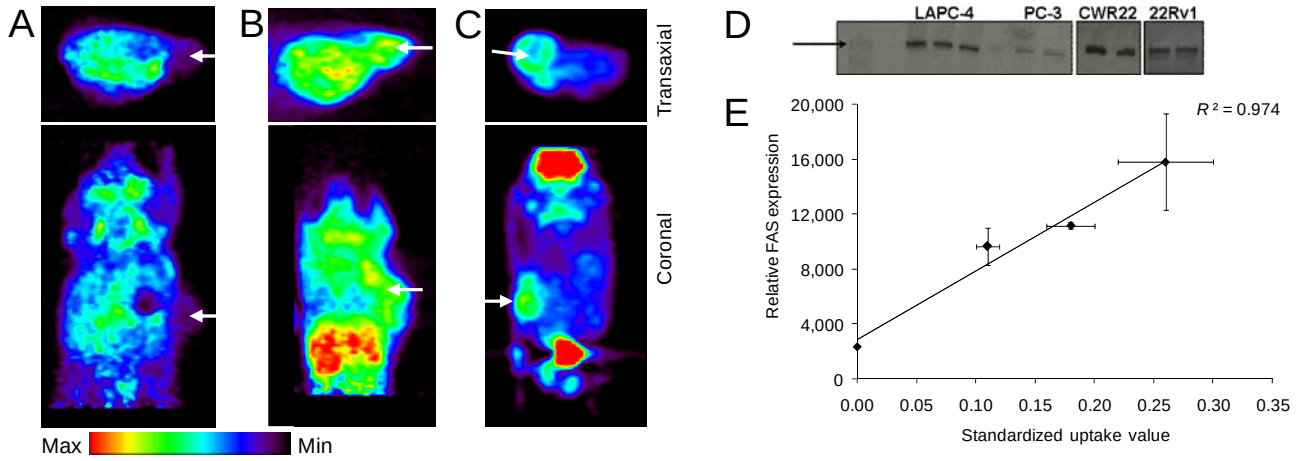

Figure 10. Representative transaxial and coronal PET image slices of LAPC-4 (A), CWR22 (B), and 22Rv1 (C) tumor-bearing mice at 20 minutes post i.v. injection of 14.8-18.5 MBq (400-500 μCi) 1-^{11}C-acetate. Arrows mark tumor location. PC-3 tumors were not visualized. (D) Western blot of tumor lysates to show qualitative levels of FAS expression. Visual inspection of the Western blot results revealed obvious differences in the intensity of the band near 250 kDa (standard band denoted by black arrow; FAS = 267 kDa) with PC-3 showing relatively non-existent bands, 22Rv1 and LAPC-4 with significantly more intensity, and CWR22 being the highest of those examined. Multiplication of the area of the band by its intensity (after subtraction of background intensity) gave a relative value of expression for the sample analyzed. (E) SUV values of 1-^{11}C-acetate uptake in prostate tumor models versus the relative FAS expression (by Western blot) of these samples shows a direct correlation (R^2 = 0.974). Error bars are ± SD.

Small animal PET imaging of FAS inhibition (C75 blocks 1-^{11}C-acetate uptake in vivo). Because the *in vitro* results confirmed that 1-^{11}C-acetate uptake could be diminished by inhibition of FAS, a similar study was pursued *in vivo*. PC-3 (as the low-expressing control) and LNCaP tumor-bearing mice were imaged with 1-^{11}C-acetate before and after treatment with C75 so that each mouse would serve as its own control (Fig. 11A). In 6 out of the 7 image sets analyzed, tumor uptake of 1-^{11}C-acetate decreased following a single treatment with C75. LNCaP tumors showed an average decrease in uptake of 12.3%, with PC-3 SUVs reduced by an average of 49.4% (Fig. 11B). Reasoning for the significant difference in the effect of FAS inhibition on acetate uptake (p = 0.013) between the two tumor types was explored by immunohistochemical analysis of FAS expression (Fig 11C). Visual inspection of the FAS stained slides clearly demonstrated a much higher abundance of the protein in the LNCaP tumors when compared to PC-3 in all cases. H&E stains of all tumor slides confirmed viability of the tissue. The brown staining also co-localized in the same areas as the hemotoxylin stain on subsequent slides, indicating protein-rich portions (data not shown).

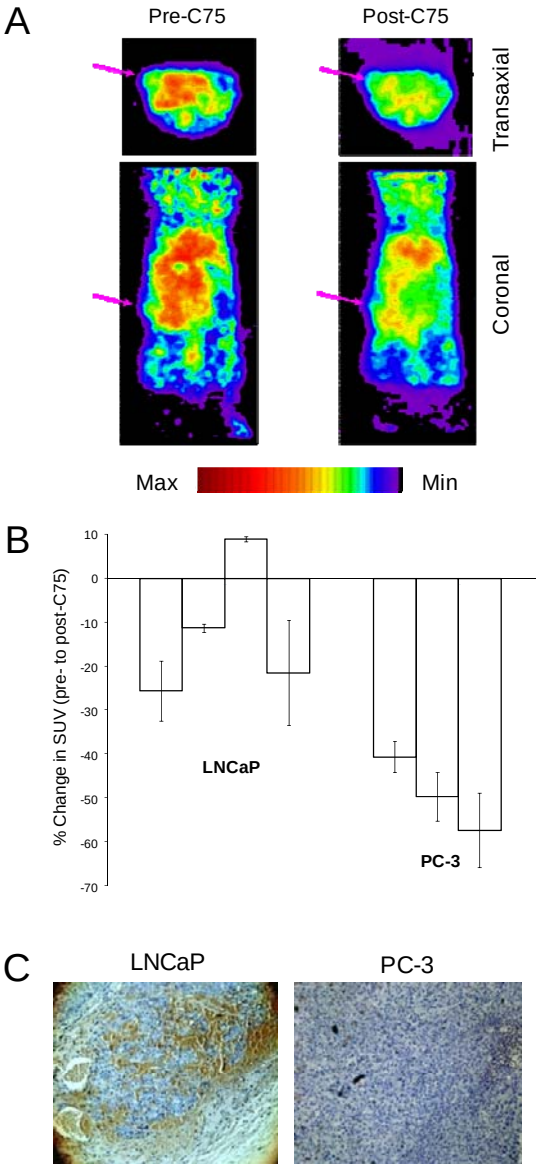

Figure 11. (A) Representative image slices of a LNCaP tumor-bearing mouse post i.v. injection of 3.7-7.4 MBq (100-200 μCi) 1-^{11}C-acetate. Arrows mark tumor location. (B) Overall change in Standardized Uptake Value (SUV) in solid PC-3 and LnCaP tumors in mice pre- and post-treated with C75. Error bars are ± SD. (C) Representative immunohistochemical staining of harvested prostate tumors for FAS (brown) showing a strong reactivity in the LNCaP, while PC-3 has almost none. 10× magnification. Three 3 slices per tumor were analyzed.

1.6.3. Discussion

1-^{11}C-acetate was first examined as a possible tracer for malignancies by Shreve et al. in 1995 (*73*) and has since been extensively investigated in prostate cancer and its metastases (*56-60*). Direct comparisons by researchers have shown greater sensitivity for detection over standard use of ^{18}F-FDG (*33,57*). Most recent work has demonstrated 1-^{11}C-acetate as a useful tool for detecting recurrent disease at PSA relapse in many cases (*56,58,59,74*) and even better results when paired with CT and MRI for anatomical reference and observation of structural changes (*60*). Despite these findings, no definitive explanation for increased uptake has been made.

Acetate can be metabolized by several distinct pathways in cells. Of course, acetate can be metabolized through the TCA cycle. In tumor cells, acetate can also be used as substrate or substrate precursor during fatty acid synthesis. Acetate can be converted to malonyl-CoA by ACC. FAS then uses malonyl-CoA and acetyl-CoA, as substrates for FA synthesis. Acetyl-CoA and malonyl-CoA also provide substrate for fatty acid elongation in the mitochondria and ER, respectively. In addition, acetate is a precursor for cholesterol synthesis. As a result, 1-^{11}C-acetate incorporation could be affected by multiple pathways. Considering that FAS and the fatty acid synthesis pathway are highly

expressed and active in multiple cancers, prostate cancer in particular, this pathway could be a major determinant of 1-^{11}C-acetate uptake in prostate tumors.

Researchers have postulated that increased acetate uptake in malignancies may be due to increased lipid biosynthesis. Accordingly, one study recently observed the uptake and metabolism of ^{14}C-acetate into four non-prostate tumor cell lines (LS174T: human colon adenocarcinoma, RPMI2650: human nasal septum tumor, A2780: human ovary carcinoma, and A375: human malignant melanoma) and one fibroblast model (*75*). They demonstrated that all malignant lines examined had significantly higher uptake over the fibroblasts and that the acetate incorporated into the lipid soluble fractions, and primarily Phosphatidylcholine (PC). Interestingly, Swinnen *et al.* have demonstrated that FAS-derived palmitate primarily partitions to detergent-insoluble lipid fractions where PC is the primary constituent (*76*). Similarly, uptake of 2-^{14}C-acetate has also been measured in CWR22 and PC-3 tumors in castrated and noncastrated mice (*77*). The authors found that acetate uptake correlated with androgen receptor expression, suggesting that acetate uptake can be affected by androgen. FAS has been shown to be overexpressed in prostate cancer (*34-36,43,62*), however, specific examination of FAS levels in correlation to 1-^{11}C-acetate uptake by PET have yet to be reported. Since high levels of FAS expression have also been found to be an indicator of a poor prognosis in patients with prostate cancer, resulting in a 4.45-fold higher risk of death (*78*), we hypothesized that a non-invasive imaging method such as 1-^{11}C-acetate-PET for the determination of FAS in tumors could provide clinicians with an additional tool for individualized therapy.

In this current study, pharmacological inhibition of the FAS pathway was used to demonstrate the specificity of 1-^{11}C-acetate for imaging FAS expression by blocking the protein. C75-treated cells showed a significant decrease in cellular accumulation of 1-^{11}C-acetate when compared to controls, but still showed an appreciable amount of cellular uptake (Fig 8A). It is likely that either all of the FAS was not blocked or other pathways described above are also involved. Inhibition of fatty acid synthesis with TOFA, a pharmacological inhibitor of ACC, the rate-limiting enzyme involved in fatty acid biosynthesis, also had significant impact of the cellular accumulation of 1-^{11}C-acetate (Fig. 8B). The demonstration that TOFA is a more efficient inhibitor of fatty acid synthesis than C75 (Fig. 9A-C) correlates well with differences in 1-^{11}C-acetate uptake. Furthermore, because blockade of the two key enzymes involved in fatty acid synthesis affected acetate uptake, our data demonstrate that a large portion of 1-^{11}C-acetate tumor uptake and retention is related to the fatty acid synthesis pathway.

Demonstrating that *in vivo* uptake of 1-^{11}C-acetate in four prostate tumor models correlated with FAS levels (Fig. 10), it is evident that FAS is at least involved in 1-^{11}C-acetate uptake *in vivo*, the first time this relationship has been demonstrated. After showing that 1-^{11}C-acetate cellular uptake can be diminished with FAS inhibition *in vitro* and that uptake correlates to FAS expression levels *in vivo*, we performed an FAS blocking study *in vivo* with C75 (Fig. 11). With each mouse serving as its own control, specific changes in overall tumor uptake were calculated and showed a small average change in the LNCaP mice (~12%) and a larger effect in the PC-3 model (~49%). LNCaP has a higher expression of FAS (Fig 11C), therefore the amount of C75 given is likely to show less of an effect than in PC-3 where its lower expression of FAS would result in a more extreme response with the same amount of C75.

Inhibition of FAS with C75, Orlistat, triclosan, and many other compounds has led to promising *in vitro* and *in vivo* results confirming FAS as a viable target for cancer therapies (*79,80*). Although FAS represents an important therapeutic target, there has been no *in vivo* demonstration that FAS inhibitors significantly block fatty acid synthesis in tumors. One study with [^{18}F]fluorodeoxyglucose (FDG-PET) to monitor the effects of C75 on tumor glucose metabolism in a rodent model of human A549 lung cancer was recently reported (*65*). It was shown that a transient, reversible decrease in glucose metabolism and tumor metabolic volume after C75 was noted after treatment, with the peak effect seen at 4 h. This, however, was an indirect measure of fatty acid synthesis, while the use 1-^{11}C-

acetate shows a direct measurement. The data presented herein provide validation for further development of 1-^{11}C-acetate PET imaging, as a measure of fatty acid synthesis, and incorporation of the technology into pre-clinical *in vivo* models and clinical studies. Such information could provide important validation of FAS inhibitors efficacy and represents a unique tool in aiding the translation of new FAS inhibitors for the treatment of cancer into the clinical setting.

As mentioned earlier, acetate can be metabolized by other pathways as well. The TCA cycle is a major factor in acetate metabolism throughout the body and its presence in the cells needs to be considered. In one experiment, 3-nitropropionic acid (a known inhibitor of the TCA cycle) was added during cell uptake and showed a reduction of 1-^{11}C-acetate uptake of 14.3 ± 3.7% in the PC-3 model (data not shown). It has been shown that siRNA mediated knockdown of FAS in MDA-MB-435 mammary carcinoma cells can also affect expression of genes related to the TCA cycle and glycolysis and may also influence acetate metabolism indirectly (*81*). This supports in part, the idea that TCA could be a major contributor to the retention of 1-^{11}C-acetate and is regulated by the FA synthesis pathway. Given the role of cholesterol in prostate cancer (*82*), and that in some cell lines increased FA synthesis has been shown to be accompanied by an increase in cholesterol synthesis (*83*), further studies on the ability of the cholesterol synthesis pathway to regulate PET imaging of 1-^{11}C-acetate uptake in prostate cancer may also be warranted. On the other hand, the data presented herein clearly identify FAS and the fatty acid synthesis pathway as an important determinant of 1-^{11}C-acetate uptake in PET imaging of prostate cancer.

1.6.4. Conclusions

These findings are promising as they suggest a possible biomarker for more effective treatments in prostate cancer patients, and possibly others, since FAS expression has shown links to poor prognosis in other cancers as well. Moreover, since FAS inhibitors are being developed as anti-tumor agents, this technology also provides a unique opportunity to monitor the effectiveness and the validation of new FAS inhibitors for translation into a clinical setting.

1.7. Imaging the Prostate Tumors with ^{18}F-FDHT (Task 1.5)

AR mututation and ligand-independent activation are hallmarks of prostate cancer progression and resistance to hormonal therapy. 16β-^{18}F-fluoro-5α-dihydrotestosterone measures AR expression by binding to the receptor as DHT. One set of PC-3 tumor-bearing mice were imaged as a negative control – PC-3 tumors do not have androgen receptors and should show no uptake. Coregistration with CT was performed in this case to locate the tumor, and, as expected, no uptake was visible in this tumor model (Fig. 12).

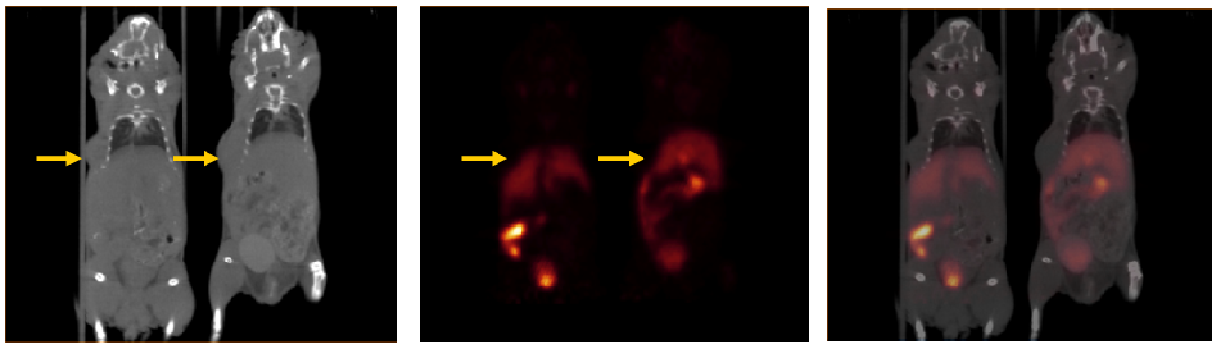

Figure 7. Small animal imaging of 2 PC-3 tumor-bearing mouse at 1 hour post injection of 100 µCi ^{18}F-FDHT. CT (left), microPET (middle), coregistration (right)

KEY RESEARCH ACCOMPLISHMENTS

- We have shown that it was not possible to delineate changes in tissue glucose utilization with 2-[^{18}F]Fluoro-2-deoxyglucose (FDG) and microPET following androgen ablation treatment.
- We have shown it is not possible to delineate alterations in cellular proliferation with ^{18}F-3'-deoxy-3'-fluorothymidine (^{18}F-FLT) and microPET following androgen ablation treatment
- We have demonstrated that, ^{64}Cu-ATSM may not be suitable for the imaging of hypoxia in *prostate* tumors and that 1-^{11}C-acetate may be a reasonable alternative.
- We have demonstrated that, ^{64}Cu-ATSM uptake is affected by the presence of FAS and, therefore, may not be suitable for the imaging of hypoxia in *prostate* tumors as the redox balance is changed. (see Appendix)
- We have provided further confirmation through blocking studies that 1-^{11}C-acetate is a marker for FAS. Since FAS has been shown to be a prognostic indicator, this allows an opportunity for a new imaging paradigm for monitoring prostate cancer response to therapy. (see Appendix)

REPORTABLE OUTCOMES

Abstracts:

1. ”Correlation of [1-^{11}C] Acetate Uptake to Fatty Acid Synthase Expression in Prostate Tumors.” A.L. Vavere, J.S. Lewis, 16th International Symposium on Radiopharmaceutical Chemistry, Iowa City, Iowa; June, 2005 (oral). J. Label Compd. Radiopharm. 2005: 48: S1-S341

2. ”Hypoxia Marker ^{64}Cu-ATSM Shows Diminished Uptake in Prostate Cancer” A.L. Vavere, J.S. Lewis, 2005 International Chemical Congress of Pacific Basin Societies (Pacifichem), Honolulu, Hawaii; December 2005 (oral).

3. ”Correlation of C-11 Acetate Uptake to Fatty Acid Synthase Expression in Prostate Tumors.” A.L. Vavere, J.S. Lewis. American Association of Cancer Research Pathobiology of Cancer Workshop, Snomass, Colorado; July 2005 (poster).

4. ”Relationship of Cu-ATSM Hypoxia Selectivity and Fatty Acid Synthase Activity in Prostate Tumor Models” A.L. Vavere, J.S. Lewis, Society of Molecular Imaging 5th Annual Meeting, Kona, Hawaii; September 2006 (poster)

5. “1-^{11}C-acetate PET imaging as possible surrogate marker for fatty acid synthase expression in prostate cancer” A.L. Vavere, J.S. Lewis, American Association of Cancer Research 97th Annual Meeting, Washington, D.C.; April 2006 (poster)

6. “Imaging of Prostate Cancer and Response to Therapy using Small Animal Imaging” J.S. Lewis, A.L. Vavere, 11th Prouts Neck Meeting on Prostate Cancer, Maine; November 2006 (oral)

7. ”Diminished Cu-ATSM Hypoxia Selectivity and its Relation to Fatty Acid Synthase Expression in Prostate Tumors” A.L. Vāvere, J.S. Lewis, 17th International Symposium on Radiopharmaceutical Sciences, Aachen, Germany; April 2007 (poster)

8. ”The Consequences of Fatty Acid Synthase in Prostate Tumors: PET Imaging of FAS Expression in Vivo” A.L. Vāvere, S. Kridel, J.S. Lewis, 1st Annual Innovative Minds in Prostate Cancer Today (IMPaCT) Meeting, Atlanta, Georgia; September 2007 (poster)

Manuscripts:

"1-^{11}C-Acetate as a PET Radiopharmaceutical for Imaging Fatty Acid Synthase Expression in Prostate Cancer" Amy L. Vāvere, Steven J. Kridel, Frances B. Wheeler and Jason S. Lewis. Journal of Nuclear Medicine, in press.

"Examining the Relationship Between Cu-ATSM Hypoxia Selectivity and Fatty Acid Synthase Expression in Human Prostate Cancer Cell Lines", Amy L. Vāvere and Jason S. Lewis. Nuclear Medicine and Biology, revision submitted.

Training:

Dr. Amy Vavere was a postdoctoral researcher who undertook the majority of the studies described in this report. She was supported in part by an NIH NRSA grant. Following completion of this work she relocated and took a full time position as the Head Radiochemist, Department of Radiological Sciences, St. Jude Children's Research Hospital, Memphis.

CONCLUSION

During this funding period we have shown that, (1) it is not possible to delineate changes in prostate tumor glucose utilization with 2-[^{18}F]Fluoro-2-deoxyglucose (FDG) and microPET following androgen ablation treatment; (2) it is possible to monitor alterations in cellular proliferation with ^{18}F-3'-deoxy-3'-fluorothymidine (^{18}F-FLT) and microPET following treatment; (3) ^{64}Cu-ATSM uptake is affected by the presence of Fatty Acid Synthase (FAS) and, therefore, may not be suitable for the imaging of hypoxia in prostate tumors as the redox balance is changed, and (4) that 1-^{11}C-acetate is a marker for FAS. This work has led to the presentations of eight abstracts at international meetings and two peer-reviewed manuscripts.

Most importantly we have shown that although Cu-ATSM has been a valuable tool as a marker of hypoxia, and it's possible that the nature of its mechanism of retention, though not completely understood, could lead us to answers for the incongruences in its selectivity. The uncertainty lies in the possibility that other physiological changes caused by malignant progression and hypoxia within the cell could also affect this redox balance regardless of oxygen concentration. If the suggested mechanism of Cu-ATSM uptake holds, then reduction, release and ultimate cellular trapping of Cu(I) would be caused by a decrease in the redox potential of the cell. And, although in most cases this is directly due to a change (reduction) in oxygen concentration within the cell, there are many other processes that could also alter the redox potential of this environment. In **prostate tumors**, a reduction of ^{64}Cu-ATSM hypoxia selectivity is demonstrated in a manner that directly correlates to FAS expression. ^{64}Cu-ATSM is a very effective PET agent for clinically delineating many hypoxic human malignancies, but, as with all radiopharmaceuticals, it is not a universal agent. Care should be taken in particular regard to the imaging of prostate tumors.

Also, the data presented herein provides validation for further development of 1-^{11}C-acetate PET imaging as a measure of fatty acid synthesis, and incorporation of the technology into pre-clinical *in vivo* models and clinical studies. These findings are promising as they suggest a possible biomarker for more effective treatments in prostate cancer patients, and possibly others, since FAS expression has shown links to poor prognosis in other cancers as well. Moreover, since FAS inhibitors are being developed as anti-tumor agents, this technology also provides a unique opportunity to monitor the effectiveness and the validation of new FAS inhibitors for translation into a clinical setting.

REFERENCES

1. Lewis JS, McCarthy DW, McCarthy TJ, Fujibayashi Y, Welch MJ. Evaluation of ^{64}Cu-ATSM in vitro and in vivo in a hypoxic tumor model. *J Nucl Med.* 1999;40:177-183.

2. Sramkoski RM, Pretlow TG, 2nd, Giaconia JM, et al. A new human prostate carcinoma cell line, 22Rv1. *In Vitro Cellular & Developmental Biology Animal.* 1999;35:403-409.

3. Dimitrakopoulou-Strauss A, Strauss LG. PET Imaging of Prostate Cancer with ^{11}C-Acetate. *Journal of Nuclear Medicine.* 2003;44:556-558.

4. Hamacher K, Coenen HH, Stocklin G. Efficient sterospecific synthesis of no-carrier-added 2-[18F]-fluoro-2-deoxy-D-glucose using aminopolyether supported nucleophilic substitution. *Journal of Nuclear Medicine.* 1986;27:235-238.

5. Shields AF, Grierson JR, Dohmen BM, et al. Imaging proliferation in vivo with [F-18]FLT and positron emission tomography. *Nature Medicine.* 1998;4:1334-1336.

6. Rasey JS, Grierson JR, Wiens LW, Kolb PD, Schwartz JL. Validation of FLT uptake as a measure of thymidine kinase-1 activity in A549 carcinoma cells. *Journal of Nuclear Medicine.* 2002;43:1210-1217.

7. Dittmann H, Dohmen BM, Kehlbach R, et al. Early changes in [^{18}F]FLT uptake after chemotherapy: an experimental study. *European Journal of Nuclear Medicine and Molecular Imaging.* 2002;29:1462-1469.

8. Vavere AL, Lewis JS. Cu-ATSM: A radiopharmaceutical for the PET imaging of hypoxia. *Dalton Trans.* 2007:(in press).

9. Dearling JLD, Lewis JS, Mullen GED, Rae MT, Zweit J, Blower PJ. Design of hypoxia-targeting radiopharmaceuticals: Selective uptake of copper-64 complexes in hypoxic cells in vitro. *Eur J Nucl Med.* 1998;25:788-792.

10. Fujibayashi Y, Taniuchi H, Yonekura Y, Ohtani H, Konishi J, Yokoyama A. Copper-62-ATSM: A new hypoxia imaging agent with high membrane permeability and low redox potential. *J Nucl Med.* 1997;38:1155-1160.

11. Dehdashti F, Grigsby PW, Mintun MA, Lewis JS, Siegel BA, Welch MJ. Assessing tumor hypoxia in cevical cancer by positron emission tomography with ^{60}Cu-ATSM: relationship to therapeutic response - a preliminary report. *Int J Radiat Biol Phys.* 2003;55:1233-1238.

12. Dehdashti F, Mintun MA, Lewis JS, et al. In vivo assessment of tumor hypoxia in lung cancer with ^{60}Cu-ATSM. *Eur J Nucl Med Mol Imag.* 2003;30:844-850.

13. Dietz DW, Dehdashti FD, Grigsby PW, et al. Tumor hypoxia detected by Positron Emission Tomography with ^{60}Cu-ATSM as a predictor of response and survival in patients undergoing neoadjuvant chemoradiotherapy for rectal aarcinoma: a pilot study. *Dis Colon Rec.*submitted.

14. Burgman P, O'Donoghue JA, Lewis JS, Welch MJ, Humm JL, Ling CC. Cell line-dependent differences in uptake and retention of the hypoxia-selective nuclear imaging agent Cu-ATSM. *Nucl Med Biol.* 2005;32:623-630.

15. O'Donoghue JA, Zanzonico P, Pugachev A, et al. Assessment of regional tumor hypoxia using ^{18}F-fluoromisonidazole and ^{64}Cu(II)-diacetyl-bis(N^4-methylthiosemicarbazone) positron emission tomography: Comparative study featuring microPET imaging, pO_2 probe measurement, autoradiography, and fluorescent microscopy in the R3327-AT and FaDu rat tumor models. *Int J Radiat Biol Phys.* 2005;61:1493-1502.

16. Hochachka PW, Rupert JL, Goldenberg L, Gleave M, Kozlowski P. Going malignant: the hypoxia-cancer connection in the prostate. *BioEssays.* 2002;24:749-757.

17. Brown JM. The hypoxic cell: A target for selective cancer therapy - eighteenth Bruce F. Cain Memorial Award Lecture. *Cancer Res.* 1999;59:5863-5870.

18. Tatum JL, Kelloff GJ, Gillies RJ, et al. Hypoxia: Importance in tumor biology, noninvasive measurement by imaging, and value of its measurement in the management of cancer therapy. *Int J Radiat Biol.* 2006;82:699-757.

19. Gillemin K, Krasnow MA. The hypoxic response: huffing and HIFing. *Cell Death Differentiation.* 1997;89:9-12.

20. Jiang BH, Semenza GL, Bauer C, Marti HH. Hypoxia-inducible factor 1 levels vary over a physiologically relevant range of O_2 tension. *Am J Physiol.* 1996;271:C1172-1180.

21. Höckel M, Vaupel P. Tumor hypoxia: definitions and current clinical, biologic, and molecular aspects. *J Natl Cancer Inst.* 2001;93:266-276.

22. Tannock I, Guttman P. Responses of chinese hamster ovary cells to anticancer drugs under aerobic and hypoxic conditions. *Br J Cancer.* 1981;42:245-248.

23. Teicher BA, Holden SA, Al-Achi SA, Herman TS. Classification of antineoplastic treatments by their differential toxicity toward putative oxygenated and hypoxic tumor subpopulations *in vivo* in the FSaIIC murine fibrosarcoma. *Cancer Res.* 1990;50:3339-3344.

24. Crabtree HG, Cramer W. The action of radium on cancer cells I. II. Some factors determining the susceptibility of cancer cells to radium. *Proc R Soc Ser B.* 1933;113:238-250.

25. Gray LH, Conger AD, Ebert M, Hornsey S, Scott OC. Concentration of oxygen dissolved in tissues at the time of irradiation as a factor in radiotherapy. *Br J Radiol.* 1953;26:638-648.

26. Höckel M, Schlenger K, Aral B, Mitze M, Shäffer U, Vaupel P. Assocaition between tumor hypoxia and malignant progression in advancer cancer of the uterine cervix. *Cancer Res.* 1996;56:4509-4515.

27. Graeber TG, Osmanian C, Jacks T, et al. Hypoxia-mediated selection of cells with diminished apoptotic potential in solid tumours. *Nature (Lond).* 1996;379:88-91.

28. Shweiki D, Itin A, Soffer D, Keshet E. Vascular endothelial growth factor induced by hypoxia may mediate hypoxia-initiated angiogenesis. *Nature (Lond).* 1992;359:843-845.

29. Chao C, Bosch WR, Mutic S, et al. A novel approach to overcome hypoxic tumor resistance: Cu-ATSM-guided intensity-modulated radiation therapy. *Int J Radiat Biol Phys.* 2001;49:1171-1182.

30. Yuan H, Schroeder T, Bowsher JE, Hedlund LW, Wong T, Dewhirst MW. Intertumoral differences in hypoxia selectivity of the PET imaging agent ^{64}Cu(II)-diacetyl-bis(N^4-methylthiosemicarbazone). *J Nucl Med.* 2006;47:989-998.

31. Dearling JLJ, Lewis JS, Mullen GED, Welch MJ, Blower PJ. Copper bis(thiosemicarbazone) complexes as hypoxia imaging agents: structure-activity relationships. *J Biol Inorg Chem.* 2002;7:249-259.

32. Maurer RI, Blower PJ, Dilworth JR, Reynolds CA, Zheng Y, Mullen GED. Studies on the mechanism of hypoxic selectivity in copper bis(thiosemicarbazone) radiopharmaceuticals. *J Med Chem.* 2002;45:1420-1431.

33. Fricke E, Mchtens S, Hofmann M, et al. Positron emission tomography with ^{11}C-Acetate and ^{18}F-FDG in prostate cancer patients. *Eur J Nucl Med Mol Imag.* 2003;30:607-611.

34. Dhanasekaran SM, Barrette TR, Ghosh D, et al. Delineation of prognostic biomarkers in prostate cancer. *Nature.* 2001;412:822-826.

35. Swinnen JV, Roskams T, Joniau S, et al. Overexpression of fatty acid synthase is an early and common event in the development of prostate cancer. *Int J Cancer.* 2002;98:19-22.

36. Welsh JB, Sapinosa LM, Su AI, et al. Analysis of gene expression identifies candidate markers and pharmacological targets in prostate cancer. *Cancer Res.* 2001;61:5974-5978.

37. Menendez JA, Lupu R. Oncologic properties of the endogenous fatty acid metabolism: molecular pathology of fatty acid synthase in cancer cells. *Curr Opin Clin Nutr Metab Care.* 2006;9:346-357.

38. Alo PL, Visca P, G. T, et al. Fatty acid synthase (FAS) predictive strength in poly differentiated early breast carcinomas. *Tumori.* 1999;85:35-40.

39. Alo PL, Visca P, Marci A, Mangoni A, Botti C, Di Tondo U. Expression of fatty acid synthase (FAS) as a predictor of recurrence in stage I breast carcinoma patients. *Cancer.* 1996;77:474-482.

40. Gansler TS, Hardman W, A. HD, Schaffel S, Hennigar RA. Increased expression of fatty acid synthase (OA-519) in ovarian neoplasms predicts shorter survival. *Human Pathol.* 1997;28:686-692.

41. Rashid A, Pizer ES, Moga M, et al. Elevated expression of fatty acid synthase and fatty acid synthetic activity in colorectal neoplasia. *Am J Pathol.* 1997;150:201-208.

42. Wang Y, Kuhajda FP, Li JN, et al. Fatty acid synthase (FAS) expression in human breast cancer cell culture supernatents and in breast cancer patients. *Cancer Lett.* 2001;167:99-104.

43. Rossi S, Graner E, Febbo P, et al. Fatty acid synthase expression defines distinct molecular signatures in prostate cancer. *Mol Cancer Res.* 2003;1:707-715.

44. Myers RB, Oelschlager DK, Weiss HL, Frost AR, Grizzle WE. Fatty acid synthase: An early molecular marker of progression of prostatic adenocarcinoma to androgen independence. *J Urology.* 2001;165:1027-1032.

45. Takahiro T, Shinichi K, Toshimitsu S. Expression of fatty acid synthase as a prognostic indicator in soft tissue sarcomas. *Clin Cancer Res.* 2003;9:2204-2212.

46. Yeh C-W, Chen W-J, Chiang C-T, Lin-Shiau S-Y, Lin J-K. Suppression of fatty acid stnthase in MCF-7 breast cancer cells by tea and tea polyphenols: a possible mechanism for their hypolipidemic effects. *Pharmacogenomics J.* 2003;3:267-276.

47. Kuhajda FP. Fatty-acid synthase and human cancer. New perspectives on its role in tumor biology. *Nutrition (New York).* 2000;16:202-208.

48. Loftus TM, Jaworsky DE, Frehywot GL, et al. Reduced food intake and body weight in mice treated with fatty acid synthase inhibitors. *Science.* 2000;288:2379-2381.

49. Agus DB, Golde DW, Sgouros G, Ballangrud A, Cordon-Cardo C, Scher HI. Positron emission tomography of a human prostate cancer xenograft: association of changes in deoxyglucose accumulation with other measures of outcome following androgen withdrawal. *Cancer Res.* 1998;58:3009-3014.

50. Jadvar H, Xiankui L, Shahinian A, et al. Glucose metabolism of human prostate cancer mouse xenografts. *Mol Imaging.* 2005;4:91-97.

51. Morris MJ, Akhurst T, I. O, et al. Fluorinated deoxyglucose positron emission tomography imaging in progressive metastatic prostate cancer. *Urology.* 2002;59:913-918.

52. Oyama N, Akino H, Suzuki Y, et al. Prognostic value of 2-deoxy-2-[F-18]fluoro-D-glucose positron emission tomography imaging for patients with prostate cancer. *Mol Imaging Biol.* 2002;4:99-104.

53. Oyama N, Akino H, Suzuki Y, et al. The increased accumulation of [^{18}F]fluorodoxyglucose in untreated prostate cancer. *Jap J Clin Oncol.* 1999;29:623-629.

54. Effert PJ, Bares R, Handt S, Wolff JM, Bull U, Jakse G. Metabolic imaging of untreated prostate cancer by Positron Emission Tomography with ^{18}Fluorine-labeled deoxyglucose. *J Urology.* 1996;155:994-998.

55. Hofer C, Laubenbacher C, Block T, Breul J, Hartung R, Schwaiger M. Fluorine-18-fluorodeoxyglucose positron emission tomography is useless for the detection of local recurrence after radical prostatectomy. *Eur Urology.* 1999;36:31-35.

56. Albrecht S, Buchegger F, Soloviev D, et al. ^{11}C-acetate PET in the early evaluation of prostate cancer recurrence. *Eur J Nucl Med Mol Imag.* 2007;34:185-196.

57. Oyama N, Akino H, Kanamaru H, et al. ^{11}C-acetate PET imaging of prostate cancer. *J Nucl Med.* 2002;43:181-186.

58. Oyama N, Miller TR, Dehdashti F, et al. ^{11}C-acetate PET imaging of prostate cancer: detection of recurrent disease at PSA relapse. *J Nucl Med.* 2003;44:549-555.

59. Sandblom G, Sorensen J, Lundin N, Haggman M, Malmstrom P-U. Positron Emission Tomography with C11-acetate for tumor detection and localization in patients with prostate-specific antigen relapse after radical prostatectomy. *Urology.* 2006;67:996-1000.

60. Wachter S, Tomek S, Kurtaran A, et al. ^{11}C-acetate Positron Emission Tomography imaging and image fusion with computed tomography and magnetic resonance imaging in patients with recurrent prostate cancer. *J Clin Oncol.* 2006;24:2513-2519.

61. Wakil SJ. Fatty acid synthase, a proficient multifunctional enzyme. *Biochemistry.* 1989;28:4523-4530.

62. Pizer ES, Pflug BR, Bova GS, Han WF, Udan MS, Nelson JB. Increased fatty acid synthase as a therapeutic target in androgen-independent prostate cancer progression. *Prostate (New York).* 2001;47:102-110.

63. Kuhajda FP, Jenner K, Wood FD, et al. Fatty acid synthesis: a potential selective target for antineoplastic therapy. *Proceedings of the National Academy of Sciences of the United States of America.* 1994;91:6379-6383.

64. Kuhajda FP, Pizer ES, Li JN, Mani NS, Frehywot GL, Townsend CA. Synthesis and antitumor activity of an inhibitor of fatty acid synthase. *Proceedings of the National Academy of Sciences of the United States of America.* 2000;97:3450-3454.

65. Lee JS, Orita H, Gabrielson K, et al. FDG-PET for pharmacodynamic assessment of the fatty acid synthase inhibitor C75 in an experimental model of lung cancer. *Pharmaceutical Res.* 2007;24:1202-1207.

66. Pflug BR, Pecher SM, Brink AW, Nelson JB, Foster BA. Increased fatty acid synthase expression and activity during progression of prostate cancer in the TRAMP model. *Prostate (New York).* 2003;57:245-254.

67. Moerlein SM, Gaehle GG, Welch MJ. Robotic preparation of sodium acetate C-11 injection for use in clinical PET. *Nucl Med Biol.* 2002;29:613-621.

68. Landree LE, Hanlon AL, Strong DW, et al. C75, a fatty acid synthase inhibitor, modulates AMP-activation protein kinase to alter neuronal energy metabolism. *J Biol Chem.* 2004;279:3817-3827.

69. Kridel SJ, Axelrod F, Rozenkrantz N, Smith JW. Orlistat is a novel inhibitor of fatty acid synthase with antitumor activity. *Cancer Res.* 2004;64:2070-2075.

70. Little JL, Wheeler FB, Fels DR, Koumenis C, Kridel SJ. Inhibition of fatty acid synthase induces endoplasmic reticulum stress in tumor cells. *Cancer Res.* 2007;67:1262-1269.

71. Tai Y-C, Ruangma A, Rowland D, et al. Performance evaluation of the microPET Focus: A third-generation microPET scanner dedicated to animal imaging. *J Nucl Med.* 2005;46:455-463.

72. Defrise M, Kinahan PE, Townshend DW, Michel C, Sibomana M, Newport DF. Exact and approximate rebinning algorithms for 3-D PET data. *IEEE Trans Med Imag.* 1997;16:145-158.

73. Shreve P, Chiao PC, Humes HD, Schwaiger M, Gross MD. Carbon-11 acetate PET imaging in renal disease. *J Nucl Med.* 1995;36:1595-1601.

74. Kotzerke J, Volkmer BG, Neumaier B, Gschwend JE, Hautmann RE, Reske SN. Carbon-11 acetate positron emission tomography can detect local recurrence of prostate cancer. *Eur J Nucl Med Mol Imag.* 2002;29:1380-1384.

75. Yoshimoto M, Waki A, Yonekura Y, et al. Characterization of acetate metabolism in tumor cells in relation to cell proliferation: Acetate metabolism in tumor cells. *Nucl Med Biol.* 2001;28:117-122.

76. Swinnen JV, Van Veldhoven PP, Timmermans L, et al. Fatty acid synthase drives the synthesis of phospholipids partitioning into detergent-resistant membrane microdomains. *Biochem Biophys Res Commun.* 2003;302:898-903.

77. Jadvar H, Li X, Park R, Shahinian A, Conti P. Quantitative autoradiography of radiolabeled acetate in mouse xenografts of human prostate cancer. *J Nucl Med.* 2006;47(suppl 1):421P-422P.

78. Bandyopadhyay S, Pai SK, Watabe M, et al. FAS expression inversely correlates with PTEN level in prostate cancer and a PI 3-kinase inhibitor synergizes with FAS siRNA to induce apoptosis. *Oncogene.* 2005;24:5389-5395.

79. Lupu R, Menendez JA. Pharmacological inhibitors of Fatty Acid Synthase (FASN)--catalyzed endogenous fatty acid biosynthesis: a new family of anti-cancer agents? *Curr Pharmacological Biotech.* 2006;7:483-493.

80. Kuhajda FP. Fatty acid synthase and cancer: new application of an old pathway. *Cancer Res.* 2006;66:5977-5980.

81. Knowles LM, Smith JW. Genome-wide changes accompanying knockdown of fatty acid synthase in breast cancer. *BMC Genomics.* 2007;8:doi:10.1186/1471-2164-1188-1168.

82. Hager MH, Soloman KR, Freeman MR. The role of cholesterol in prostate cancer. *Curr Opin Clin Nutr Metab Care.* 2006;9:379-385.

83. Porstmann T, Griffiths B, Chung Y-L, et al. PKB/Akt induces transcription of enzymes involved in cholesterol and fatty acid biosynthesis via activation of SREBP. *Oncogene.* 2005;24:6465-6481.

APPENDIX

Abstracts:

A. ”Correlation of [1-^{11}C] Acetate Uptake to Fatty Acid Synthase Expression in Prostate Tumors.” A.L. Vavere, J.S. Lewis, 16th International Symposium on Radiopharmaceutical Chemistry, Iowa City, Iowa; June, 2005 (oral). J. Label Compd. Radiopharm. 2005: 48: S1-S341

B. ”Hypoxia Marker ^{64}Cu-ATSM Shows Diminished Uptake in Prostate Cancer” A.L. Vavere, J.S. Lewis, 2005 International Chemical Congress of Pacific Basin Societies (Pacifichem), Honolulu, Hawaii; December 2005 (oral).

C. ”Correlation of C-11 Acetate Uptake to Fatty Acid Synthase Expression in Prostate Tumors.” A.L. Vavere, J.S. Lewis. American Association of Cancer Research Pathobiology of Cancer Workshop, Snomass, Colorado; July 2005 (poster).

D. ”Relationship of Cu-ATSM Hypoxia Selectivity and Fatty Acid Synthase Activity in Prostate Tumor Models” A.L. Vavere, J.S. Lewis, Society of Molecular Imaging 5th Annual Meeting, Kona, Hawaii; September 2006 (poster)

E. “1-^{11}C-acetate PET imaging as possible surrogate marker for fatty acid synthase expression in prostate cancer” A.L. Vavere, J.S. Lewis, American Association of Cancer Research 97th Annual Meeting, Washington, D.C.; April 2006 (poster)

F. “Imaging of Prostate Cancer and Response to Therapy using Small Animal Imaging” J.S. Lewis, A.L. Vavere, 11th Prouts Neck Meeting on Prostate Cancer, Maine; November 2006 (oral)

G. ”Diminished Cu-ATSM Hypoxia Selectivity and its Relation to Fatty Acid Synthase Expression in Prostate Tumors” A.L. Vāvere, J.S. Lewis, 17th International Symposium on Radiopharmaceutical Sciences, Aachen, Germany; April 2007 (poster)

H. ”The Consequences of Fatty Acid Synthase in Prostate Tumors: PET Imaging of FAS Expression in Vivo” A.L. Vāvere, S. Kridel, J.S. Lewis, 1st Annual Innovative Minds in Prostate Cancer Today (IMPaCT) Meeting, Atlanta, Georgia; September 2007 (poster)

Manuscripts:

I. “1-^{11}C-Acetate as a PET Radiopharmaceutical for Imaging Fatty Acid Synthase Expression in Prostate Cancer” Amy L. Vāvere, Steven J. Kridel, Frances B. Wheeler and Jason S. Lewis. Journal of Nuclear Medicine, in press, 2007.

J. Examining the Relationship Between Cu-ATSM Hypoxia Selectivity and Fatty Acid Synthase Expression in Human Prostate Cancer Cell Lines”, Amy L. Vāvere and Jason S. Lewis. Nuclear Medicine and Biology, revision submitted.

A. ”Correlation of [1-^{11}C] Acetate Uptake to Fatty Acid Synthase Expression in Prostate Tumors.” A.L. Vavere, J.S. Lewis, 16th International Symposium on Radiopharmaceutical Chemistry, Iowa City, Iowa; June, 2005 (oral). J. Label Compd. Radiopharm. 2005: 48: S1-S341

CORRELATION OF [1-^{11}C] ACETATE UPTAKE TO FATTY ACID SYNTHASE EXPRESSION IN PROSTATE TUMORS

A.L. Vavere, J.S. Lewis.
Division of Radiological Sciences, Washington University School of Medicine, St. Louis, MO, United States.

Although ^{18}F-FDG is routinely used for the detection of many malignancies, visualization of prostate cancer has been troublesome with its relatively slow tumor growth and metabolism and excretion through the nearby bladder. Within the last few years, 1-^{11}C-acetate has been employed for the reliable imaging of prostate cancer using PET (1,2). Prostatic epithelial cells convert from citrate-producing to citrate-oxidizing once they become malignant leading to an increase in the metabolism of acetate.

Fatty acid synthase (FAS) is a multi-functional enzymatic protein involved in many stages of fatty acid biosynthesis. Fatty acids are generally supplied by dietary uptake and therefore FAS is expressed at low levels in most normal tissues except liver, adipose tissue, fetal lung, and the lactating breast. Although it is minimally expressed endogenously, FAS has been found to be over-expressed in prostate carcinomas as well as other cancers (3-5). An increased level of FAS has been found to be indicative of aggressive and late-stage prostatic adenocarcinomas (6). Carbon-14 labeled acetate is routinely used for the monitoring of FAS production in vitro by analysis of its incorporation during lipid biosynthesis (7). The research presented here proposes the use of 1-^{11}C-acetate as a surrogate marker for FAS expression in vivo through PET imaging.

Carbon-11 labeled acetate was prepared by the reaction of ^{11}C-labeled carbon dioxide with a Grignard reagent as previously described (8). Three prostatic carcinomas (CWR22, LAPC-4, and PC-3) were implanted subcutaneously into male athymic mice and allowed to grow until palpable. Small animal PET imaging (MicroPET®, CTI-Concorde Microsystems LLC) was performed 20 minutes post i.v. injection of 350-450 µCi 1-^{11}C-acetate. Post imaging, the mice were euthanized and the tumors excised for subsequent western blot analysis. Regions of interest (ROI) were drawn on the images around the tumors and standardized uptake values (SUVs) were calculated to normalize these values to the injected activity per animal as well as body weight. Tumor tissue was homogenized, the cells were lysed, and BCA analysis was performed to accurately determine protein concentration of the samples. Aliquots were then analyzed by gel electrophoresis and western blot analysis for FAS expression.

Prelimary data shows that SUVs for CWR22 tumors have a 2-fold increase over LAPC-4 tumors, with no visible uptake in the PC-3 tumors which are known to have minimal expression of FAS. This trend was mirrored qualitatively in the intensity of FAS expression by western blot analysis. Further experimental data will serve to validate 1-^{11}C-acetate as a surrogate marker of FAS expression and therefore as a potential prognostic indicator.

We are grateful for financial support from the Department of Defense (W81XWH-04-1-0906). MicroPET imaging was supported by an NIH/NCI SAIRP grant (1 R24 CA83060) and the Small Animal Imaging Core of the Alvin J. Siteman Cancer (NCI Cancer Center Support Grant # 1 P30 CA91842).

References:

1. Oyama N, Miller TR, Dehdashti F et al. *J Nucl Med* 2003; 44(4): 549-555.
2. Fricke E, Machtens S, Hofmann M et al. *Eur J Nucl Med Molec Imag* 2003; 30(4): 607-611.
3. Dhanasekaran SM, Barrette TR, Ghosh D et al. *Nature* 2001; 412: 822-826.
4. Swinnen JV, Roskams T, Joniau S et al. *Int J Cancer* 2002; 98: 19-22.
5. Welsh JB, Sapinoso LM, Su AI et al. *Cancer Res* 2001; 61: 5974-5978.
6. Myers RB, Oelschlager DK, Weiss HL et al. *J Urology* 2001; 165: 1027-1032.
7. Shakir KMM, Sundaram SG, Margolis S. *J Lipid Res* 1978; 19: 433-442.
8. Moerlein SM, Gaehle GG, Brockhorst JL et al. *J Nucl Med* 1995; 36: 157P.

Keywords: Fatty Acid Synthase, microPET, [^{11}C]acetate

B. ”Hypoxia Marker ^{64}Cu-ATSM Shows Diminished Uptake in Prostate Cancer” A.L. Vavere, J.S. Lewis, 2005 International Chemical Congress of Pacific Basin Societies (Pacifichem), Honolulu, Hawaii; December 2005 (oral).

Hypoxia Marker ^{64}Cu-ATSM Shows Diminished Uptake in Prostate Cancer

Androgen ablation therapy for advanced prostate cancers induces a rapid reduction of blood flow to the prostate and prostate tumor tissue and the concomitant onset of a hypoxic environment in these tissues. Cu-ATSM is reduced and retained in hypoxic tissue but rapidly diffuses out of normoxic tissue as an intact complex. Although a 4 fold increase in retention of Cu-ATSM in hypoxic over normoxic tissues is observed 15 minutes after injection in other malignancies with overall uptake at around 90% in hypoxic tissues compared to 25% in normoxic, investigations into its use in prostate cancer had not been reported.

Cu-64-ATSM was produced as previously reported. Prostate cancer cells (PC-3, LNCaP, and 22Rv1) were grown in culture and placed into suspension in serum-free media at a concentration of 5×10^{-6} cells/mL. The suspension (25 mL) was placed in a flask rotating in a water bath heated to 37°C with either moist normoxic (20% O_2, 5% CO_2, 75% N_2) or hypoxic (5% CO_2, 95% N_2) gas. After a 1 hour equilibration time, 25 μCi ^{64}Cu-ATSM was added to the flask followed by aliquot removal of the cells, in triplicate, at various time points between 1 and 60 minutes. The cells were centrifuged to separate the media from the cells and were counted on a gamma counter to assess cellular incorporation of the tracer.

Diminished overall uptake in all tumors was seen with ratios of hypoxic/normoxic uptake of 3.1, 3.2, and 2.3 for LNCaP, 22Rv1, and PC-3 respectively and maximum cellular incorporation was 23%, 62%, and 80%. Other factors such as fatty acid synthase expression and its impact on this decrease in retention are being explored.

We are grateful for financial support from the Department of Defense (W81XWH-04-1-0906) and the National Institutes of Health for an Individual National Research Service Award (F32CA110422-01) for fellowship support of Dr. Vavere.

C. ”Correlation of C-11 Acetate Uptake to Fatty Acid Synthase Expression in Prostate Tumors.” A.L. Vavere, J.S. Lewis. American Association of Cancer Research Pathobiology of Cancer Workshop, Snomass, Colorado; July 2005 (poster).

CORRELATION OF 1-C-11-ACETATE UPTAKE TO FATTY ACID SYNTHASE EXPRESSION IN PROSTATE TUMORS

Amy L. Vāvere* and Jason S. Lewis, Division of Radiological Sciences, Washington University School of Medicine, St. Louis, MO, 63110, USA.

Although ^{18}F-FDG is routinely used for the detection of many malignancies, visualization of prostate cancer has been troublesome with its relatively slow tumor growth and metabolism and excretion through the nearby bladder. Within the last few years, 1-^{11}C-acetate has been employed for the reliable imaging of prostate cancer using PET. Prostatic epithelial cells convert from citrate-producing to citrate-oxidizing once they become malignant leading to an increase in the metabolism of acetate.
Fatty acid synthase (FAS) is a multi-functional enzymatic protein involved in many stages of fatty acid biosynthesis. Fatty acids are generally supplied by dietary uptake and therefore FAS is expressed at low levels in most normal tissues except liver, adipose tissue, fetal lung, and the lactating breast. FAS has been found to be over-expressed in prostate carcinomas as well as other cancers. An increased level of FAS has been found to be indicative of aggressive and late-stage prostatic adenocarcinomas. Carbon-14 labeled acetate is routinely used for the monitoring of FAS production in vitro by analysis of its incorporation during lipid biosynthesis. The research presented here proposes the use of 1-^{11}C-acetate as a surrogate marker for FAS expression in vivo through PET imaging.

Carbon-11 labeled acetate was prepared by the reaction of ^{11}C-labeled carbon dioxide with a Grignard reagent as previously described. Three prostatic carcinomas (CWR22, LAPC-4, and PC-3) were implanted subcutaneously into male athymic mice and allowed to grow until palpable. Small animal PET imaging (MicroPET®, CTI-Concorde Microsystems LLC) was performed 20 minutes post i.v. injection of 350-450 μCi 1-^{11}C-acetate. Post imaging, the mice were euthanized and the tumors excised for subsequent western blot analysis. Regions of interest (ROI) were drawn on the images around the tumors and standardized uptake values (SUVs) were calculated to normalize these values to the injected activity per animal as well as body weight. Tumor tissue was homogenized, the cells were lysed, and BCA analysis was performed to accurately determine protein concentration of the samples. Aliquots were then analyzed by gel electrophoresis and western blot analysis for FAS expression.

Prelimary data shows that SUVs for CWR22 tumors have a 2-fold increase over LAPC-4 tumors, with no visible uptake in the PC-3 tumors which are known to have minimal expression of FAS. This trend was mirrored qualitatively in the intensity of FAS expression by western blot analysis. Further experimental data will serve to validate 1-^{11}C-acetate as a surrogate marker of FAS expression and therefore as a potential prognostic indicator.

We are grateful for financial support from the Department of Defense (W81XWH-04-1-0906). MicroPET imaging was supported by an NIH/NCI SAIRP grant (1 R24 CA83060) and the Small Animal Imaging Core of the Alvin J. Siteman Cancer (NCI Cancer Center Support Grant # 1 P30 CA91842).

D. ”Relationship of Cu-ATSM Hypoxia Selectivity and Fatty Acid Synthase Activity in Prostate Tumor Models” A.L. Vavere, J.S. Lewis, Society of Molecular Imaging, 5th Annual Meeting, Kona, Hawaii; September 2006 (poster)

Relationship of Cu-ATSM Hypoxia Selectivity and Fatty Acid Synthase Activity in Prostate Tumor Models

Category: Oncologic Imaging
Presentation Time: Friday, 5:00 p.m. - 6:00 p.m.
Amy L. Vavere, Jason S. Lewis, Washington University School of Medicine, St. Louis, USA. Contact e-mail: VavereA@mir.wustl.edu
Presentation Number: 575
Poster Board Number: 198

Cu-ATSM, a hypoxia PET imaging agent, is reduced and retained in hypoxic tissue but remains intact and rapidly diffuses out of normoxic tissue. As a defense mechanism in prostate cancer cells, the fatty acid synthesis (FAS) pathway harnesses its oxidizing power for improving the redox balance despite conditions of extreme hypoxia, potentially altering Cu-ATSM hypoxia selectivity. Researchers have shown that C75 inhibits FAS by 89-95%, and in this study it was administered to observe possible changes in Cu-ATSM uptake due to FAS inhibition.

PC-3, LNCaP, and 22Rv1 prostate tumor cells were plated in 6-well plates and grown to ~75% confluence at 37°C and 5% CO_2. Four hours prior to the study, the cells were supplemented with 50 μM C75. ^{64}Cu-ATSM was added to the cells, and the plates were placed in an anoxic gas mixture (5% CO_2 / 95% N_2) to facilitate Cu-ATSM uptake. At various times (15, 32, 64, and 83 minutes) the cells were lysed by addition of 0.15% sodium dodecyl sulfate, after washing in triplicate. Lysis extracts were counted in a γ-counter. Uptake data for all experiments were normalized for the amount of protein present and calculated as the percentage uptake (cell-associated).

Uptake of ^{64}Cu-ATSM increased over time in the C75 treated cells when compared to controls, with differences at 83 minutes of 15, 11, and 26% for PC-3, LNCaP, and 22Rv1 cell lines, respectively. This suggests that ^{64}Cu-ATSM may be an ineffective marker of hypoxia in *prostate* tumor models due to the increased presence of FAS which alters the redox properties of the cell. Further in vitro studies cells in suspension will enable more uniform hypoxic conditions. These findings will be validated in vivo using small animal PET imaging.

We are grateful for financial support from the DOD (PC040435) and NIH (F32CA110422-1).

E. "1-^{11}C-acetate PET imaging as possible surrogate marker for fatty acid synthase expression in prostate cancer" A.L. Vavere, J.S. Lewis, American Association of Cancer Research 97th Annual Meeting, Washington, D.C.; April 2006 (poster)

Oasis, Online Abstract Submission and Invitation System - Program Planner

Abstract Number:	LB-308
Presentation Title:	1-^{11}C-acetate PET imaging as possible surrogate marker for fatty acid synthase expression in prostate cancer
Presentation Start/End Time:	Tuesday, Apr 04, 2006, 1:00 PM - 5:00 PM
Location:	Exhibit Hall, Washington Convention Center
Author Block:	*Amy L. Vavere*, *Jason S. Lewis*. Washington University School of Medicine, St. Louis, MO

Recently, 1-^{11}C-acetate has been utilized for the non-invasive imaging of prostate cancer using Positron Emission Tomography (PET). Prostatic epithelial cells convert from citrate-producing to citrate-oxidizing once they become malignant leading to an increase in the metabolism of acetate. Fatty acid synthase (FAS) is a multi-functional enzymatic protein involved in many stages of fatty acid biosynthesis including the conversion of malonyl-coA and acetate into palmitate. Although it is minimally expressed endogenously, FAS has been found to be over-expressed in prostate carcinomas as well as other cancers and increased levels have been shown to be indicative of aggressive and late-stage prostatic adenocarcinomas. Carbon-14-labeled acetate is routinely used for the monitoring of FAS production in vitro by analysis of its incorporation during lipid biosynthesis. Other researchers have shown that C75, an inhibitor of FAS, reduces acetate metabolism by 89-95% at 4-24 hours post administration. In this study, C75 was used to examine the specificity of 1-^{11}C-acetate for imaging FAS expression.
Intitally, microPET imaging of 1-^{11}C-acetate in 5 prostate tumor models (PC-3, 22Rv1, LNCaP, CWR22, and LAPC-4) resulted in a qualitative correlation between tumor uptake of 1-^{11}C-acetate and FAS expression determined by Western blot analysis. To examine if 1-^{11}C-acetate uptake could be reduced by inhibiting FAS, an additional study was performed with C75. Eight male, PC-3 bearing mice received an i.p. injection of C75 (30 mg/kg) or vehicle control 18 h prior to imaging. MicroPET imaging was performed 20 minutes post i.v. injection of ~200 •Ci 1-^{11}C-acetate followed by a low resolution CT for subsequent co-registration and anatomical reference. Post imaging, the mice were euthanized and the tumors excised for further analysis. Regions of interest (ROI) were drawn on the images around the tumors (excluding any necrotic tissue) and livers. Standardized uptake values (SUVs) were calculated to normalize these values to the injected activity per animal as well as body weight.
Results show tumor SUVs of the C75 treated and control animals to be 0.36 ± 0.14 and 0.24 ± 0.07, respectively. It is important to note that the PC-3 tumors were shown to have the lowest expression of FAS of the prostate models investigated. Preliminary analysis shows that in two of the treated animals, liver uptake was half of that of normal. Analysis of the treatment and imaging of other FAS-expressing prostate tumor models is ongoing. Further experimental data will serve to validate 1-^{11}C-acetate as a surrogate marker of FAS expression and therefore a prognostic indicator of patient survival.
We are grateful for financial support from the DOD (PC040435) and an NIH NRSA (F32CA110422-1) for the salary of ALV.

F. “Imaging of Prostate Cancer and Response to Therapy using Small Animal Imaging” J.S. Lewis, A.L. Vavere, 11th Prouts Neck Meeting on Prostate Cancer, Maine; November 2006 (oral)

Imaging of Prostate Cancer and Response to Therapy using Small Animal Imaging

Jason S. Lewis, PhD and Amy L. Vavere, PhD.

Division of Radiological Sciences
Washington University School of Medicine
St. Louis, MO

Androgen ablation, the standard therapeutic strategy for advanced prostate cancer, induces a rapid reduction of blood flow to prostate and prostate cancer tissues and the concomitant onset of a hypoxia environment in these tissues. The clinical monitoring of the effectiveness of androgen ablation therapy requires a convenient, noninvasive imaging modality that is sensitive to these changes in vasculature and physiology. Positron Emission Tomography (PET) can be used to identify changes in tumor vasculature and physiology, reflecting the consequences of these treatments. Our research program is aimed at using PET to delineate the relationship between androgen ablation and hypoxia (^{64}Cu-ATSM), blood flow (^{64}Cu-PTSM), glucose utilization (^{18}F-FDG), vascular permeability (^{45}Ti-transferrin), cellular proliferation (^{18}F-FLT) and androgen receptor expression (^{18}F-FDHT) in animal models of prostate cancer.

We have also been investigating 1-^{11}C-acetate as a marker for fatty acid synthase (FAS) expression in the same prostate tumor models. Prostatic epithelial cells convert from citrate-producing to citrate-oxidizing once they become malignant leading to an increase in the metabolism of acetate. FAS is a multi-functional enzymatic protein involved in many stages of fatty acid biosynthesis including the conversion of malonyl-coA and acetate into palmitate. Although it is minimally expressed endogenously, FAS has been found to be over-expressed in prostate carcinomas as well as other cancers and increased levels have been shown to be indicative of aggressive and late-stage prostatic adenocarcinomas. Carbon-14 labeled acetate is routinely used for the monitoring of FAS production in vitro by analysis of its incorporation during lipid biosynthesis. Other researchers have shown that C75, an inhibitor of FAS, reduces acetate metabolism by 89-95% at 4-24 hours post administration. We are therefore examining the specificity of 1-^{11}C-acetate for imaging FAS expression in prostate tumors and preliminary analysis shows that 1-^{11}C-acetate may act as a surrogate marker of FAS expression and therefore a prognostic indicator of patient survival.

Funding: United States Department of Defense (PC040435)

G. ”Diminished Cu-ATSM Hypoxia Selectivity and its Relation to Fatty Acid Synthase Expression in Prostate Tumors” A.L. Vāvere, J.S. Lewis, 17th International Symposium on Radiopharmaceutical Sciences, Aachen, Germany; April 2007 (poster)

P350 DIMINISHED CU-ATSM HYPOXIA SELECTIVITY AND ITS RELATION TO FATTY ACID SYNTHASE EXPRESSION IN PROSTATE TUMORS

A.L. VAVERE and J.S. LEWIS

Division of Radiological Sciences, Washington University School of Medicine, St. Louis, MO, USA

Introduction: The validity of Cu-ATSM as a hypoxia imaging agent has been demonstrated in vitro, in vivo, and in humans, but there is concern in regards to its ability to delineate hypoxia in **prostate** tumors. Other groups have reported data in prostate tumor lines that did not support the use of Cu-ATSM, at times finding a negative correlation of uptake to oxygen levels. It is known that other physiological changes caused by hypoxia could affect the cellular redox balance regardless of oxygen concentration. For example, as a defense mechanism in prostate cancer cells, the fatty acid synthesis (FAS) pathway harnesses its oxidizing power for improving the redox balance despite conditions of extreme hypoxia. Although it is minimally expressed endogenously, FAS has been found to be over-expressed in prostate carcinomas. In this study, C75 (an inhibitor of fatty acid synthesis) was used to inhibit FAS activity, thereby overcoming the ability of FAS to offset the redox balance of a hypoxic cell therefore increasing uptake of Cu-ATSM.

Experimental: For each prostate tumor model, cells in suspension were maintained at 37°C in a water bath while constantly humidified by an anoxic gas mixture (95% N_2, 5% CO_2). During a 1 hour equilibration period, one flask was treated with C75 (100 mM) while the other served as a control. After equilibration, 100 μCi ^{64}Cu-ATSM was added to each flask. At various timepoints from 1-60 minutes, 200 mL of cell suspension was removed via pipet in triplicate, and the cells were separated from media and counted in a gamma counter to calculate percent uptake. FAS expression of each tumor line was measured using a FAS-detect™ ELISA kit (FASgen, Inc). These values were normalized by protein concentration as determined by BCA, resulting in a ratio with units of ng FAS/mg protein.

Results and Discussion: Inhibition of FAS with C75 resulted in a dramatic increase in ^{64}Cu-ATSM uptake into prostate tumor cells in vitro under anoxic conditions. The treated cells demonstrated higher uptake values of 20.9 ± 3.27, 103.0 ± 32.6, 144.2 ± 32.3, and 200.1 ± 79.3% over control values for LAPC-4, PC-3, LNCaP, and 22Rv1 prostate tumor cell lines after 15 minutes. Quantification of FAS expression, by ELISA, resulted in values of 0.00438 ± 0.00024, 0.00832 ± 0.00038, 0.01877 ± 0.00092, and 0.02679 ± 0.00224 ng/mg for LAPC-4, PC-3, LNCaP, and 22Rv1, respectively. As expected, a correlation is seen (R^2 = 0.9117) with FAS expression plotted against % change in ^{64}Cu-ATSM uptake with C75 treatment.

Conclusion: Although Cu-ATSM has clinical relevance in the imaging of hypoxia in numerous tumor types, its application to the imaging of prostate cancer may be limited by the cellular expression of FAS.

Acknowledgement: Financial support: DOD (PC040435) and NIH (F32CA110422-1).

Keywords: Cu-ATSM, Fatty Acid Synthase, Hypoxia, C75

”The Consequences of Fatty Acid Synthase in Prostate Tumors: PET Imaging of FAS Expression in Vivo” A.L. Vāvere, S. Kridel, J.S. Lewis, 1st Annual Innovative Minds in Prostate Cancer Today (IMPaCT) Meeting, Atlanta, Georgia; September 2007 (poster)

THE CONSEQUENCES OF FATTY ACID SYNTHASE IN PROSTATE TUMORS: PET IMAGING ITS EXPRESSION IN VIVO

Amy L. Vāvere and Jason S. Lewis*

[1]Division of Radiological Sciences, Washington University School of Medicine, St. Louis, MO, 63110, USA. Email: VavereA@wustl.edu

The validity of Cu-ATSM as a hypoxia imaging agent with Positron Emission Tomography (PET) has been demonstrated in vitro, in vivo, and in humans, but there is concern in regards to its ability to delineate hypoxia in prostate tumors. Other groups have reported data in prostate tumor lines that did not support the use of Cu-ATSM, at times finding a negative correlation of uptake to oxygen levels. It is known that other physiological changes caused by hypoxia could affect the cellular redox balance regardless of oxygen concentration. For example, as a defense mechanism in prostate cancer cells, the fatty acid synthesis (FAS) pathway harnesses its oxidizing power for improving the redox balance despite conditions of extreme hypoxia. FAS is a multi-functional enzymatic protein involved in many stages of fatty acid biosynthesis including the conversion of malonyl-coA and acetate into palmitate. Although it is minimally expressed endogenously, FAS has been found to be over-expressed in prostate carcinomas as well as other cancers and increased levels have been shown to be indicative of aggressive and late-stage prostatic adenocarcinomas. Although it is minimally expressed endogenously, FAS has been found to be over-expressed in prostate carcinomas. In this study, an inhibitor of fatty acid synthesis was used to inhibit FAS activity, thereby overcoming the ability of FAS to offset the redox balance of a hypoxic cell therefore increasing uptake of Cu-ATSM. Inhibition of FAS with C75 resulted in a dramatic increase in ^{64}Cu-ATSM uptake into prostate tumor cells in vitro under anoxic conditions. The treated cells demonstrated higher uptake values of 20.9 ± 3.27, 103.0 ± 32.6, 144.2 ± 32.3, and 200.1 ± 79.3% over control values for LAPC-4, PC-3, LNCaP, and 22Rv1 prostate tumor cell lines. Quantification of FAS expression, by ELISA, resulted in values of 0.00438 ± 0.00024, 0.00832 ± 0.00038, 0.01877 ± 0.00092, and 0.02679 ± 0.00224 ng/μg for LAPC-4, PC-3, LNCaP, and 22Rv1, respectively. As expected, a correlation is seen (R^2 = 0.9117) with FAS expression plotted against % change in ^{64}Cu-ATSM uptake with C75 treatment. We have also been investigating C-11-acetate-PET, as a marker for fatty FAS expression in the same prostate tumor models. Carbon-14 labeled acetate is routinely used for the monitoring of FAS production in vitro by analysis of its incorporation during lipid biosynthesis, so application of C-11-acetate-PET as a non-invasive measure of in vivo FAS levels may hold exceptional promise in the diagnosis and treatment of this disease.

IMPACT: Although Cu-ATSM has clinical relevance in the imaging of hypoxia in numerous tumor types, its application to the imaging of prostate cancer may be limited by the cellular expression of FAS. We are also examining the specificity of 1-C-11-acetate-PET for imaging FAS expression in prostate tumors and preliminary analysis shows that 1-C-11-acetate-PET may act as a surrogate marker of FAS expression and therefore a prognostic indicator of patient survival.

H. “1-^{11}C-Acetate as a PET Radiopharmaceutical for Imaging Fatty Acid Synthase Expression in Prostate Cancer” Amy L. Vāvere, Steven J. Kridel, Frances B. Wheeler and Jason S. Lewis. Journal of Nuclear Medicine, in press.

1-^{11}C-Acetate as a PET Radiopharmaceutical for Imaging Fatty Acid Synthase Expression in Prostate Cancer

Amy L. Vāvere[1], Steven J. Kridel[2], Frances B. Wheeler[2] and Jason S. Lewis[1,3]

[1]Division of Radiological Sciences, Washington University School of Medicine, St. Louis, MO

[2]Department of Cancer Biology, Comprehensive Cancer Center, Wake Forest University School of Medicine, Winston-Salem, North Carolina

[3]Alvin J. Siteman Cancer Center, Washington University School of Medicine, St. Louis, MO

Supported by the United States Department of Defense (PC040435, JSL), the National Institutes of Health (F32 CA110422-03, ALV) and the National Cancer Institute (CA114104, SJK).

Address all correspondence and requests for reprints to:
Jason S. Lewis, Ph.D.
Mallinckrodt Institute of Radiology,
Washington University School of Medicine,
Campus Box 8225
510 S. Kingshighway Blvd.
St. Louis, MO 63110, USA
Tel: (314) 362 4696
Fax: (314) 362 9940
Email: j.s.lewis@wustl.edu

Current Address of First Author (undertook study in-training as Post-Doctoral Researcher):
Amy L. Vāvere, Ph.D.
St. Jude Children's Research Hospital
Mail Stop 752
332 N. Lauderdale St.
Memphis, TN 38105
Tel: (901) 495 2904
Fax: (901) 495 3981
Email: amy.vavere@stjude.org

Running title: 1-^{11}C-acetate and FAS Expression

Word Count: 6,576

ABSTRACT

Although it is accepted that the metabolic fate of 1-^{11}C-acetate is different in tumors than in myocardial tissue due to different clearance patterns, the exact pathway has not been fully elucidated. For decades, fatty acid synthesis has been quantified *in vitro* by the incubation of cells with ^{14}C-acetate. Fatty acid synthase (FAS) has been found to be over-expressed in prostate carcinomas, as well as other cancers, and it's possible that imaging with 1-^{11}C-acetate could be a marker for its expression. **Methods:** *In vitro* and *in vivo* uptake experiments in prostate tumor models with 1-^{11}C-acetate were performed both with and without blocking of fatty acid synthesis with either C75, an inhibitor of FAS, or 5-(Tetradecyloxy)-2-furoic acid (TOFA), an inhibitor of acetyl-CoA carboxylase (ACC). FAS levels were measured by Western blot and immunohistochemical techniques for comparison. **Results:** *In vitro* studies in 3 different prostate tumor models (PC-3, LNCaP, and 22Rv1) demonstrated blocking of 1-^{11}C-acetate accumulation after treatment with both C75 and TOFA. This was further shown *in vivo* in PC-3 and LNCaP tumor-bearing mice after a single treatment with C75. A positive correlation between 1-^{11}C-acetate uptake into the solid tumors and FAS expression levels was seen. **Conclusion:** Extensive involvement of the fatty acid synthesis pathway in 1-^{11}C-acetate uptake in prostate tumors was confirmed, leading to a possible marker for FAS expression *in vivo* by non invasive Positron Emission Tomography (PET) imaging.

Key words: 1-^{11}C-acetate, Fatty Acid Synthase, C75, TOFA

INTRODUCTION

The National Cancer Institute estimates that roughly 219,000 new cases of prostate cancer will occur in 2007 and about 27,000 deaths from this disease (*1*). In the early nineties, early and widespread detection of prostate cancers was made possible by promotion of prostate-specific antigen (PSA) screening in conjunction with digital rectal examination (DRE). Elevated PSA levels are quite high in a patient with prostate cancer, but unfortunately are also caused by benign prostatic hyperplasia, and even inflammation or urinary retention (*2*). Transrectal ultrasound (TRUS) is frequently used to assist surgeons in biopsy and for local staging, CT and MR are commonly used to determine the extent of disease, although structural changes are not always apparent with these modalities (*3*).

^{18}F-fluordeoxyglucose positron emission tomography (^{18}F-FDG PET) has become essential in the diagnosis of many malignancies, but it is not ideal in the detection of prostate cancer. Prostate cancer is one of a handful of tumors with low metabolism and ^{18}F-FDG, being a marker of glucose metabolism, is not highly effective in delineating it from surrounding tissue (*4*). Although FDG has been shown to be effective in the assessment of high grade primary tumors and metastatic disease (*5-9*), other obstacles still leave much to be desired for its use with prostate malignancies, especially at early stages. The bladder clearance of ^{18}F-FDG also poses an obstacle as it is in the same anatomical region as the prostate, and, therefore, the primary tumor. Studies have also shown an inability to differentiate benign hyperplasia in the prostate from malignant disease or post-operative scarring from radical prostatectomy (*10,11*).

Because of the problems associated with ^{18}F-FDG imaging in prostate, alternative modalities must be employed to image prostate cancer. Clinically, 1-^{11}C-acetate has been shown to be an effective tracer for the delineation of prostate cancer and its metastases with PET in humans (*12-16*). Although it is accepted that the metabolic fate of 1-^{11}C-acetate in tumors differs from normal tissue, the exact pathway has not been fully elucidated. Interestingly, fatty acid synthesis has been quantified *in vitro* by the incubation of cells with ^{14}C-acetate.

Fatty acid synthase (FAS) is a multi-functional enzymatic protein that catalyzes fatty acid biosynthesis (*17*). FAS is over-expressed in prostate carcinomas as well as other cancers (*18-22*). On the other hand, FAS levels are low or absent in most normal tissues. FAS levels are associated with tumor aggressiveness in late-stage prostatic adenocarcinomas as well as a prognostic indicator for overall survival (*23*). Previous studies have demonstrated that FAS inhibitors can reduce ^{14}C-acetate incorporation in human tumor cell lines and in human lung xenografts and mouse prostate tumors *ex vivo* (*24-27*). Because of these facts, we hypothesize that FAS is involved with 1-^{11}C-acetate uptake in prostate cancer. The following reports an examination of the mechanism of 1-^{11}C-acetate uptake in prostate tumor models and its implications for tumor progression and patient survival. Understanding the mechanism of 1-^{11}C-acetate uptake and the relation to FAS expression levels could provide a valuable tool to clinicians for the planning and monitoring of treatments due to increased mortality with raised levels of this protein in prostate cancer. It could also be used in validating the translation of novel FAS inhibitors, as anti-cancer agents, into the clinical setting.

MATERIALS AND METHODS

General. All chemicals, unless otherwise stated, were purchased from Sigma-Aldrich Chemical Company, Inc (St. Louis, MO). Radioactive samples were counted in a radioisotope calibrator (Capintec, Inc., Ramsey, NJ) for determination of MBq (mCi) and an automated well scintillation Beckman 8000 gamma counter (Beckman Coulter, Fullerton, CA) for counts per minute. Centrifugation was performed on a Sorvall Superspeed RC-6 Centrifuge (Sorvall, Inc.) refrigerated to 4°C. Male athymic nu/nu mice (<20g, 5-6 weeks old) were purchased from the National Cancer Institute (Frederick, MD). Human prostate carcinoma tumor cell lines PC-3 (AR negative), LNCaP (androgen responsive), and 22Rv1 (androgen resistant) were obtained from American Type Culture Collection (Manassas, VA) and maintained by serial passage in cell culture. Both LAPC-4 (androgen responsive) (Dr. Charles Sawyer at UCLA) and CWR22 (androgen responsive) (Bristol Myers Squibb) tumors were implanted and maintained by animal to animal passage. Carbon-11 labeled acetate was prepared by the reaction of ^{11}C-labeled carbon dioxide with a Grignard reagent as previously described (*28*). Radiochemical purity was always 99% or greater.

***In vitro* Cell Uptake and Inhibition.** PC-3, LNCaP, and 22Rv1 prostate cells were plated in 6-well plates (4.5×10^5, 9×10^5, and 1.2×10^6 cells per well, respectively) 24 hours before the study was initiated. The cells were grown to ~75% confluence at 37°C and 5% CO_2 in appropriate medium and supplemented with 10% heat-inactivated fetal bovine serum. Eighteen hours prior to the uptake experiment, C75 (63.5 μg), an FAS inhibitor (*29*), was added to the growth media (5 mL) in each well in a small amount of

DMSO (10 μL) so that the final concentration in each well was 50 μM (controls received DMSO alone). To initiate the study, the culture medium was removed, and cells were rinsed with phosphate buffered saline (PBS). Approximately 0.37 MBq (10 μCi_ of 1-^{11}C-acetate was added to the cells in 1.0 mL fresh media to initiate tracer uptake (including C75 or DMSO alone to maintain inhibitor concentration). Incubation was terminated at various times (15, 30, or 60 minutes) by removing the radioactive culture medium. Cell monolayers were washed with 2 mL of cold PBS three times to remove any excess culture medium from the extracellular spaces. Lysis of the cells was achieved by addition of 1 mL of 0.25% sodium dodecyl sulfate. Lysis extracts, as well as 1 mL radioactive culture medium as a standard, were counted in a γ-counter and measured for protein content using a standard copper reduction/bicinchoninic acid assay (Pierce Biotechnology, Rockford, IL), with bovine serum albumin as the protein standard. Cellular uptake data for all experiments were normalized for the amount of protein present and calculated as the percentage uptake (cell-associated). A further inhibition study was performed with TOFA, a potent inhibitor of acetyl-CoA carboxylase (ACC), a key enzyme involved in fatty acid biosynthesis (*30*). Procedures were similar to those stated above, with the final concentration of TOFA being 30 μM and the pretreatment occurring 2 hours prior to addition of 1-^{11}C-acetate. The tracer was added directly to the 5 mL of growth media, rather than changing the media, to ensure continued presence of the pretreatment concentration of TOFA.

To compare the abilities of C75 and TOFA to inhibit fatty acid synthesis, PC-3 cells were seeded in 24-well plates at 1×10^5 cells per well. After 48 hours the cells were treated with either C75 (0, 10, 20, 30 or 60 μM) to inhibit FAS or TOFA (0, 10, 20 or 30 μM) to

inhibit ACC for two hours and then 2-^{14}C-acetate (0.037 MBq, 1 μCi) was added for an additional two hours. An additional study was performed in both PC-3 and LNCaP cells, where cells were seeded in 24-well plates at 1×10^5 cells per well. After 48 hours the cells were treated with either C75 (30 μM) to inhibit FAS or TOFA (30 μM) to inhibit ACC for two hours and then 2-^{14}C-acetate (0.037 MBq, 1 μCi) was added for an additional two hours. Control cells received DMSO (0.1 %) only. After the labeling period, the cells were collected, washed and lipids were extracted and quantified by scintillation counting as described previously (*31,32*).

To observe the contribution of the TCA cycle to 1-^{11}C-acetate cellular uptake, an inhibition study with 3-nitroprionic acid, a known inhibitor of succinate dehydrogenase in the TCA cycle, was performed. PC-3 cells plated in 6-well plates 24 hours prior to uptake, were treated with 100 μM 3-nitropropionic acid 2 hours prior to radiotracer uptake, while control cells received vehicle alone. 1-^{11}C-acetate (1.11 MBq, 30 μCi) was added to the wells followed by a 25 minute incubation. Cells were then washed and collected by trypsin/EDTA for counting in the gamma counter and subsequent protein assay for normalization.

Small Animal PET Imaging. All animal experiments were performed in compliance with the Guidelines for the Care and Use of Research Animals established by Washington University's Animal Studies Committee. Single position, whole body imaging was performed using small animal PET (MicroPET®Focus-120 and or 220, CTI-Concorde Microsystems LLC) (*33*). Mice were imaged individually or in pairs in a supine position in

a specially designed bed. Isoflurane (1-2%) was used as an inhaled anesthetic to induce and maintain anesthesia during imaging. The bed was placed near the center of field of view of the PET scanner where the highest image resolution and sensitivity are available. Imaging was performed, 20-min post injection, with a single 10 min static scan. Images were reconstructed by Fourier rebinning followed by two-dimensional Ordered Subset Expectation Maximization (OSEM) (*34*).

PET images were evaluated by analysis of the standardized uptake value (SUV) of the tumor and non-target organ (muscle) using the software ASIPRO (Concorde MicroSystems, Inc.). The average radioactivity concentration within the tumor or tissue was obtained from the average pixel values reported in nCi/cc within a volume of interest (VOI) drawn around the entire tumor or tissue on multiple, consecutive transaxial image slices. SUVs were calculated by dividing this value, the decay-corrected activity per unit volume of tissue (nCi/mL), by the injected activity per unit of body weight (nCi/g). Necrotic tissue was excluded by analysis of the images in comparison to serial slices through the tumor post-mortem. Any necrosis in a tumor was noted and those sections (which also had no uptake) were not included in the overall SUV calculation.

An animal imaging study was performed in 22Rv1, PC-3, CWR22 and LAPC-4 tumor bearing mice, to confirm correlation of uptake of 1-^{11}C-acetate to FAS expression in tumors. Two prostatic carcinoma tumor models were prepared in culture (22Rv1 and PC-3) then harvested for implant by trypsin/EDTA and injected in a volume of 100 μL into the right flank of intact, male nu/nu mice (15-20 g) in the appropriate media at a given concentration (5 x 10^6 cells in Matrigel for 22Rv1 and 3 x 10^6 cells in Kaighn's

modification of Ham's F12 medium for PC-3). CWR22 and LAPC-4 tumors were obtained from animal to animal passage. Tumors were allowed to grow until palpable, and the time varied by model. PET imaging was performed 20-mins post i.v. injection of 14.8-18.5 MBq (400-500 μCi) 1-^{11}C-acetate (100 μL) via the tail vein. The 20-min post injection time point was chosen given the experience of other researchers (*13,14,16*). Post imaging, the mice were euthanized and the tumors excised and flash frozen to -80°C for subsequent Western blot analysis to determine FAS expression. Images were analyzed for determination of SUV and compared to the Western blots.

Western blots. Frozen tumors were thawed over ice, homogenized and the cells lysed with 1X cell lysis buffer (Cell Signaling Technology, Danvers, MA) for determination of protein concentration by BCA protein assay (Pierce, Rockford, IL). 20 μg protein of each sample was run using SDS-PAGE with a 4-20% Tris gradient gel. Standard Western blotting was performed with an anti-FAS primary antibody (rabbit; Novus Biologicals, Littleton, CO) and a goat anti-rabbit secondary antibody (DyLight^{TM}647; Pierce Biotechnology, Rockford, IL). Final detection was achieved by using the enhanced chemiluminescence system (Amersham Life Sciences, Piscataway, NJ) according to the manufacturer's instructions. Prestained standards (Kaleidoscope Prestained Standards 161-0324, BIO-RAD Laboratories, Hercules, CA) were used on each Western blot for reference. Blots were traced and intensity and area values were obtained for each band by densitometry using the Image J software (NIH, Bethesda, MD) to quantify expression.

PET Imaging of FAS Inhibition. Male, nu/nu mice were injected with either PC-3 (3×10^6 cells/100 μL) (n = 3) or LNCaP (1×10^7 cells/100 μL) (n = 4) tumor cells

subcutaneously in the right flank which were allowed to grow until palpable. PET imaging was performed 20 minutes post i.v. injection of 3.7-7.4 MBq (100-200 μCi) 1-^{11}C-acetate (100 μL) followed by a low resolution CT scan for subsequent co-registration and anatomical reference. Following imaging, all mice received an i.p. injection of C75 at 30 mg/kg dissolved in DMSO/RPMI 1640 media (<2% DMSO). Eighteen hours post treatment, the mice were imaged again following the same protocol. Post imaging, the mice were euthanized and the tumors excised and formalin fixed for staining and immunohistochemical analysis.

Immunohistochemistry. Following PET imaging to observe inhibition of 1-^{11}C-acetate uptake in prostate tumors by blocking of FAS, immunohistochemical techniques were employed to demonstrate the extent of protein expression. Tumors from the *in vivo* inhibition study were formalin fixed, paraffin embedded, sliced and placed on slides for immunohistochemical analysis by the Histology Core at Washington University, while also staining one slide per section with hemotoxylin and eosin to confirm tissue viability. Slides were baked for 30 minutes at 60°C and then soaked in two fresh soaks of xylene for 3 minutes each, hydrated in two soaks of 100% ethanol for 2 minutes each, two times with 95% ethanol for 2 minutes each, two times with 70% ethanol for 2 minutes each, and one time with 50% ethanol for two minutes. Slides were then rinsed in doubly distilled water and placed in 3 washes of PBS buffer for before blocking with a protein block (Dako) in a humidified chamber for 30 minutes at room temperature. After aspiration of the blocking solution, the slides were incubated with the FAS primary antibody (1:1000; Anti-FASN [M] antibody 34-6E7; FASGen, Inc, Baltimore, Md) overnight in a humidified chamber at 4°C and then rinsed again with PBS buffer. The

slides were then incubated with secondary goat anti-mouse antibody labeled with biotin (1:200; ImmunoPure GAM IgG, Pierce) for 30 minutes and rinsed with PBS buffer followed by incubation for 30 minutes with ABC Vector Elite solution diluted in 0.5M NaCl. The slides were rinsed three times in 0.1M Tris buffer, pH 7.4 and then incubated in DAB and chromogen (DAB+ Kit, Dako) for 10 minutes. After repeated rinsing with tap water, the slides were counterstained with Mayer's Hematoxylin for 40 seconds minutes and washed with tap water. Dipping 10 times in Bluing Reagent preceded dehydration and cover-slipping of the slides using Permount. Slides were observed and compared (10×) to the H&E stained slides under a Nikon Eclipse E600W microscope fitted with a Nikon DXM1200F digital camera. As a result of the protocol, FAS protein should appear brown in color.

Statistics. Statistically significant differences between mean values were determined using analysis of variance (ANOVA) coupled to Scheffe's test or, for statistical classification, a Student's t-test was performed.

RESULTS

Inhibition of fatty acid synthesis reduces 1-^{11}C-acetate *in vitro* uptake. To confirm the hypothesis that 1-^{11}C-acetate uptake in tumors is related FAS expression, an *in vitro* blocking study was performed. Cells were pretreated with for 18 hours with C75, a known inhibitor of FAS, prior to uptake of 1-^{11}C-acetate to determine if uptake could be blocked. All cells showed a linear increase in uptake over time in both the C75 treated

and control tumor cells. In all cases the uptake in the control cells was consistently higher throughout the duration of the study. By 30 min, the C75 treated cells showed inhibition of uptake by 26.4% ($p = 0.0005$) in the PC-3 cell line, and 16.7% ($p = 0.0010$) and 26.9% ($p = 0.0007$) for LNCaP and 22Rv1, respectively (Fig. 1A). Cell viability was measured by trypan blue staining. An average of 95% viability was measured for each of the cell lines, with no decrease in overall cell number due to the presence of C75 (data not shown).

The role of acetyl Co-A carboxylase (ACC) in 1-^{11}C-acetate uptake was also determined by treating cells with TOFA, a potent inhibitor of ACC; ACC is the rate limiting enzyme in the fatty acid synthesis pathway. After pretreatment with TOFA, cell uptake of 1-^{11}C-acetate was significantly reduced, more so than with C75 (Fig. 1B). The percentage of blocking increased over time in all cases, with values of 29.8 ± 5.75%, 67.4 ± 9.22%, and 34.7 ± 9.31% for PC-3, LNCaP, and 22Rv1, respectively, at 30 minutes. To demonstrate that TOFA is a more potent inhibitor of FA synthesis than C75 a dose-response comparison between TOFA and C75 in PC-3 cells was performed (Fig. 2A and 2B). It is evident that even at concentrations of 10 μM, TOFA has a significantly more pronounced effect on FA synthesis than C75 (10 μM: 10.7 ± 0.59 % vs. 84.9 ± 2.47%). An additional one-point study comparing PC-3 cells with LNCaP cells was undertaken to show that this relationship was observed in more than one cell line. It was shown that 30 μM C75 inhibited about 30% of FA activity in both PC-3 and LNCaP cells while TOFA inhibited FA synthesis about 75-80% (both after a 2 hour treatment) (Fig. 2C). These data demonstrate that 1-^{11}C-acetate uptake is directly related to the degree of FAS inhibition in prostate tumor cell lines.

PET imaging demonstrates an *in vivo* correlation between 1-^{11}C-acetate uptake and FAS expression. To test the hypothesis that 1-^{11}C-acetate may be imaging FAS expression *in vivo*, an imaging study was performed, with excision of the tumors post imaging for further analysis of FAS levels by Western blot. 1-^{11}C-acetate PET imaging of 4 prostate tumor models (PC-3, 22Rv1, CWR22, and LAPC-4) was performed (Fig. 3A-C). Regions of interest (ROIs) were drawn on the images around the tumors, excluding any necrotic tissue. Standardized uptake values (SUVs) at 20 mins post injection were calculated to normalize these values (nCi/cc) to the injected activity per animal (nCi), as well as body mass (g). Imaging SUVs were 0.11 ± 0.01 for LAPC-4 (n = 2), 0.26 ± 0.06 for CWR-22 (n = 2), and 0.18 ± 0.02 for 22Rv1 (n = 3). In this case, the PC-3 tumors (n = 2) could not be delineated from the surrounding tissue and, therefore, no SUVs were calculated. Visual inspection of the Western blot results revealed obvious differences in the intensity of the band near 250 kDa (FAS = 267 kDa) with PC-3 showing the lowest levels of expression, 22Rv1 and LAPC-4 with significantly more intensity than PC-3, and CWR22 being the highest of those examined (Fig. 3D). Densitometry analysis confirmed this trend quantitatively. The relative values of expression were averaged for each tumor type resulting in 2354.1 ± 22.8, 9640.9 ± 2552.3, 11160 ± 25.0, and 15798 ± 4057.6 for PC-3, LAPC-4, 22Rv1, and CWR22, respectively. Comparison of the average SUVs from the PET data with Western blot analysis of the homogenized tumor tissue resulted in a correlation (R^2 = 0.974) between tumor uptake of 1-^{11}C-acetate and FAS expression (Fig. 3E).

Small animal PET imaging of FAS inhibition (C75 blocks 1-^{11}C-acetate uptake *in vivo*). Because the *in vitro* results confirmed that 1-^{11}C-acetate uptake could be diminished by inhibition of FAS, a similar study was pursued *in vivo*. PC-3 (as the low-expressing control) and LNCaP tumor-bearing mice were imaged with 1-^{11}C-acetate before and after treatment with C75 so that each mouse would serve as its own control (Fig. 4A). In 6 out of the 7 image sets analyzed, tumor uptake of 1-^{11}C-acetate decreased following a single treatment with C75. LNCaP tumors showed an average decrease in uptake of 12.3%, with PC-3 SUVs reduced by an average of 49.4% (Fig. 4B). Reasoning for the significant difference in the effect of FAS inhibition on acetate uptake ($p = 0.013$) between the two tumor types was explored by immunohistochemical analysis of FAS expression (Fig 4C). Visual inspection of the FAS stained slides clearly demonstrated a much higher abundance of the protein in the LNCaP tumors when compared to PC-3 in all cases. H&E stains of all tumor slides confirmed viability of the tissue. The brown staining also co-localized in the same areas as the hemotoxylin stain on subsequent slides, indicating protein-rich portions (data not shown).

DISCUSSION

1-^{11}C-acetate was first examined as a possible tracer for malignancies by Shreve et al. in 1995 (*35*) and has since been extensively investigated in prostate cancer and its metastases (*12-16*). Direct comparisons by researchers have shown greater sensitivity for detection over standard use of ^{18}F-FDG (*4,13*). Most recent work has demonstrated 1-^{11}C-acetate as a useful tool for detecting recurrent disease at PSA relapse in many cases (*12,14,15,36*) and even better results when paired with CT and MRI for

anatomical reference and observation of structural changes (*16*). Despite these findings, no definitive explanation for increased uptake has been made.

Acetate can be metabolized by several distinct pathways in cells. Of course, acetate can be metabolized through the TCA cycle. In tumor cells, acetate can also be used as substrate or substrate precursor during fatty acid synthesis. Acetate can be converted to malonyl-CoA by ACC. FAS then uses malonyl-CoA and acetyl-CoA, as substrates for FA synthesis. Acetyl-CoA and malonyl-CoA also provide substrate for fatty acid elongation in the mitochondria and ER, respectively. In addition, acetate is a precursor for cholesterol synthesis. As a result, 1-^{11}C-acetate incorporation could be affected by multiple pathways. Considering that FAS and the fatty acid synthesis pathway are highly expressed and active in multiple cancers, prostate cancer in particular, this pathway could be a major determinant of 1-^{11}C-acetate uptake in prostate tumors.

Researchers have postulated that increased acetate uptake in malignancies may be due to increased lipid biosynthesis. Accordingly, one study recently observed the uptake and metabolism of ^{14}C-acetate into four non-prostate tumor cell lines (LS174T: human colon adenocarcinoma, RPMI2650: human nasal septum tumor, A2780: human ovary carcinoma, and A375: human malignant melanoma) and one fibroblast model (*37*). They demonstrated that all malignant lines examined had significantly higher uptake over the fibroblasts and that the acetate incorporated into the lipid soluble fractions, and primarily Phosphatidylcholine (PC). Interestingly, Swinnen *et al.* have demonstrated that FAS-derived palmitate primarily partitions to detergent-insoluble lipid fractions where PC is the primary constituent (*38*). Similarly, uptake of 2-^{14}C-acetate has also been measured

in CWR22 and PC-3 tumors in castrated and noncastrated mice (*39*). The authors found that acetate uptake correlated with androgen receptor expression, suggesting that acetate uptake can be affected by androgen. FAS has been shown to be overexpressed in prostate cancer (*18-22*), however, specific examination of FAS levels in correlation to 1-^{11}C-acetate uptake by PET have yet to be reported. Since high levels of FAS expression have also been found to be an indicator of a poor prognosis in patients with prostate cancer, resulting in a 4.45-fold higher risk of death (*40*), we hypothesized that a non-invasive imaging method such as 1-^{11}C-acetate-PET for the determination of FAS in tumors could provide clinicians with an additional tool for individualized therapy.

In this current study, pharmacological inhibition of the FAS pathway was used to demonstrate the specificity of 1-^{11}C-acetate for imaging FAS expression by blocking the protein. C75-treated cells showed a significant decrease in cellular accumulation of 1-^{11}C-acetate when compared to controls, but still showed an appreciable amount of cellular uptake (Fig 1A). It is likely that either all of the FAS was not blocked or other pathways described above are also involved. Inhibition of fatty acid synthesis with TOFA, a pharmacological inhibitor of ACC, the rate-limiting enzyme involved in fatty acid biosynthesis, also had significant impact of the cellular accumulation of 1-^{11}C-acetate (Fig. 1B). The demonstration that TOFA is a more efficient inhibitor of fatty acid synthesis than C75 (Fig. 2A-C) correlates well with differences in 1-^{11}C-acetate uptake. Furthermore, because blockade of the two key enzymes involved in fatty acid synthesis affected acetate uptake, our data demonstrate that a large portion of 1-^{11}C-acetate tumor uptake and retention is related to the fatty acid synthesis pathway.

Demonstrating that *in vivo* uptake of 1-^{11}C-acetate in four prostate tumor models correlated with FAS levels (Fig. 3), it is evident that FAS is at least involved in 1-^{11}C-acetate uptake *in vivo*, the first time this relationship has been demonstrated. After showing that 1-^{11}C-acetate cellular uptake can be diminished with FAS inhibition *in vitro* and that uptake correlates to FAS expression levels *in vivo*, we performed an FAS blocking study *in vivo* with C75 (Fig. 4). With each mouse serving as its own control, specific changes in overall tumor uptake were calculated and showed a small average change in the LNCaP mice (~12%) and a larger effect in the PC-3 model (~49%). LNCaP has a higher expression of FAS (Fig 4C), therefore the amount of C75 given is likely to show less of an effect than in PC-3 where its lower expression of FAS would result in a more extreme response with the same amount of C75.

Inhibition of FAS with C75, Orlistat, triclosan, and many other compounds has led to promising *in vitro* and *in vivo* results confirming FAS as a viable target for cancer therapies (*41,42*). Although FAS represents an important therapeutic target, there has been no *in vivo* demonstration that FAS inhibitors significantly block fatty acid synthesis in tumors. One study with [^{18}F]fluorodeoxyglucose (FDG-PET) to monitor the effects of C75 on tumor glucose metabolism in a rodent model of human A549 lung cancer was recently reported (*26*). It was shown that a transient, reversible decrease in glucose metabolism and tumor metabolic volume after C75 was noted after treatment, with the peak effect seen at 4 h. This, however, was an indirect measure of fatty acid synthesis, while the use 1-^{11}C-acetate shows a direct measurement. The data presented herein provide validation for further development of 1-^{11}C-acetate PET imaging, as a measure of fatty acid synthesis, and incorporation of the technology into pre-clinical *in vivo*

models and clinical studies. Such information could provide important validation of FAS inhibitors efficacy and represents a unique tool in aiding the translation of new FAS inhibitors for the treatment of cancer into the clinical setting.

As mentioned earlier, acetate can be metabolized by other pathways as well. The TCA cycle is a major factor in acetate metabolism throughout the body and its presence in the cells needs to be considered. In one experiment, 3-nitropropionic acid (a known inhibitor of the TCA cycle) was added during cell uptake and showed a reduction of 1-^{11}C-acetate uptake of 14.3 ± 3.7% in the PC-3 model (data not shown). It has been shown that siRNA mediated knockdown of FAS in MDA-MB-435 mammary carcinoma cells can also affect expression of genes related to the TCA cycle and glycolysis and may also influence acetate metabolism indirectly (*43*). This supports in part, the idea that TCA could be a major contributor to the retention of 1-^{11}C-acetate and is regulated by the FA synthesis pathway. Given the role of cholesterol in prostate cancer (*44*), and that in some cell lines increased FA synthesis has been shown to be accompanied by an increase in cholesterol synthesis (*45*), further studies on the ability of the cholesterol synthesis pathway to regulate PET imaging of 1-^{11}C-acetate uptake in prostate cancer may also be warranted. On the other hand, the data presented herein clearly identify FAS and the fatty acid synthesis pathway as an important determinant of 1-^{11}C-acetate uptake in PET imaging of prostate cancer.

CONCLUSION

These findings are promising as they suggest a possible biomarker for more effective treatments in prostate cancer patients, and possibly others, since FAS expression has

shown links to poor prognosis in other cancers as well. Moreover, since FAS inhibitors are being developed as anti-tumor agents, this technology also provides a unique opportunity to monitor the effectiveness and the validation of new FAS inhibitors for translation into a clinical setting.

ACKNOWLEDGEMENTS

The authors thank Amanda Roth, Nicole Fettig, Margaret Morris, Lori Strong and Susan Adams for technical support. Thanks also to the cyclotron facility staff for radiopharmaceutical production. We also thank Drs. Nobuyuki Oyama and Gordon Parry for their helpful discussions. We are grateful for financial support (JSL) from the Department of Defense (PC 040435) and the NIH for salary support of ALV (F32CA110422-03) and support to SJK (CA 114104).

REFERENCES

1. Jemal A, Siegel R, Ward E, Murray T, Xu J, Thun MJ. Cancer Statistics, 2007. *CA: A Cancer J Clinicians.* 2007;57:43-66.

2. Gretzer MB, Partin AW. PSA markers in prostate cancer detection. *Urol Clin N Am.* 2003;30:677-686.

3. Akin O, Hricak H. Imaging of prostate cancer. *Radiol Clin N Am.* 2007;45:207-222.

4. Fricke E, Mchtens S, Hofmann M, et al. Positron emission tomography with ^{11}C-Acetate and ^{18}F-FDG in prostate cancer patients. *Eur J Nucl Med Mol Imaging.* 2003;30:607-611.

5. Agus DB, Golde DW, Sgouros G, Ballangrud A, Cordon-Cardo C, Scher HI. Positron emission tomography of a human prostate cancer xenograft: association of changes in deoxyglucose accumulation with other measures of outcome following androgen withdrawal. *Cancer Res.* 1998;58:3009-3014.

6. Jadvar H, Xiankui L, Shahinian A, et al. Glucose metabolism of human prostate cancer mouse xenografts. *Mol Imaging.* 2005;4:91-97.

7. Morris MJ, Akhurst T, I. O, et al. Fluorinated deoxyglucose positron emission tomography imaging in progressive metastatic prostate cancer. *Urology.* 2002;59:913-918.

8. Oyama N, Akino H, Suzuki Y, et al. Prognostic value of 2-deoxy-2-[F-18]fluoro-D-glucose positron emission tomography imaging for patients with prostate cancer. *Mol Imaging Biol.* 2002;4:99-104.

9. Oyama N, Akino H, Suzuki Y, et al. The increased accumulation of [^{18}F]fluorodoxyglucose in untreated prostate cancer. *Jap J Clin Oncol.* 1999;29:623-629.

10. Effert PJ, Bares R, Handt S, Wolff JM, Bull U, Jakse G. Metabolic imaging of untreated prostate cancer by Positron Emission Tomography with ^{18}Fluorine-labeled deoxyglucose. *J Urology.* 1996;155:994-998.

11. Hofer C, Laubenbacher C, Block T, Breul J, Hartung R, Schwaiger M. Fluorine-18-fluorodeoxyglucose positron emission tomography is useless for the detection of local recurrence after radical prostatectomy. *Eur Urology.* 1999;36:31-35.

12. Albrecht S, Buchegger F, Soloviev D, et al. ^{11}C-acetate PET in the early evaluation of prostate cancer recurrence. *Eur J Nucl Med Mol Imag.* 2007;34:185-196.

13. Oyama N, Akino H, Kanamaru H, et al. ^{11}C-acetate PET imaging of prostate cancer. *J Nucl Med.* 2002;43:181-186.

14. Oyama N, Miller TR, Dehdashti F, et al. ^{11}C-acetate PET imaging of prostate cancer: detection of recurrent disease at PSA relapse. *J Nucl Med.* 2003;44:549-555.

15. Sandblom G, Sorensen J, Lundin N, Haggman M, Malmstrom P-U. Positron Emission Tomography with C11-acetate for tumor detection and localization in patients with prostate-specific antigen relapse after radical prostatectomy. *Urology.* 2006;67:996-1000.

16. Wachter S, Tomek S, Kurtaran A, et al. ^{11}C-acetate Positron Emission Tomography imaging and image fusion with computed tomography and magnetic resonance imaging in patients with recurrent prostate cancer. *J Clin Oncol.* 2006;24:2513-2519.

17. Wakil SJ. Fatty acid synthase, a proficient multifunctional enzyme. *Biochemistry.* 1989;28:4523-4530.

18. Dhanasekaran SM, Barrette TR, Ghosh D, et al. Delineation of prognostic biomarkers in prostate cancer. *Nature.* 2001;412:822-826.

19. Swinnen JV, Roskams T, Joniau S, et al. Overexpression of fatty acid synthase is an early and common event in the development of prostate cancer. *Int J Cancer.* 2002;98:19-22.

20. Welsh JB, Sapinosa LM, Su AI, et al. Analysis of gene expression identifies candidate markers and pharmacological targets in prostate cancer. *Cancer Res.* 2001;61:5974-5978.

21. Pizer ES, Pflug BR, Bova GS, Han WF, Udan MS, Nelson JB. Increased fatty acid synthase as a therapeutic target in androgen-independent prostate cancer progression. *Prostate (New York).* 2001;47:102-110.

22. Rossi S, Graner E, Febbo P, et al. Fatty acid synthase expression defines distinct molecular signatures in prostate cancer. *Mol Cancer Res.* 2003;1:707-715.

23. Myers RB, Oelschlager DK, Weiss HL, Frost AR, Grizzle WE. Fatty acid synthase: An early molecular marker of progression of prostatic adenocarcinoma to androgen independence. *J Urology.* 2001;165:1027-1032.

24. Kuhajda FP, Jenner K, Wood FD, et al. Fatty acid synthesis: a potential selective target for antineoplastic therapy. *PNAS.* 1994;91:6379-6383.

25. Kuhajda FP, Pizer ES, Li JN, Mani NS, Frehywot GL, Townsend CA. Synthesis and antitumor activity of an inhibitor of fatty acid synthase. *PNAS.* 2000;97:3450-3454.

26. Lee JS, Orita H, Gabrielson K, et al. FDG-PET for pharmacodynamic assessment of the fatty acid synthase inhibitor C75 in an experimental model of lung cancer. *Pharmaceut Res.* 2007;24:1202-1207.

27. Pflug BR, Pecher SM, Brink AW, Nelson JB, Foster BA. Increased fatty acid synthase expression and activity during progression of prostate cancer in the TRAMP model. *Prostate (New York).* 2003;57:245-254.

28. Moerlein SM, Gaehle GG, Welch MJ. Robotic preparation of sodium acetate C-11 injection for use in clinical PET. *Nucl Med Biol.* 2002;29:613-621.

29. Loftus TM, Jaworsky DE, Frehywot GL, et al. Reduced food intake and body weight in mice treated with fatty acid synthase inhibitors. *Science.* 2000;288:2379-2381.

30. Landree LE, Hanlon AL, Strong DW, et al. C75, a fatty acid synthase inhibitor, modulates AMP-activation protein kinase to alter neuronal energy metabolism. *J Biol Chem.* 2004;279:3817-3827.

31. Kridel SJ, Axelrod F, Rozenkrantz N, Smith JW. Orlistat is a novel inhibitor of fatty acid synthase with antitumor activity. *Cancer Res.* 2004;64:2070-2075.

32. Little JL, Wheeler FB, Fels DR, Koumenis C, Kridel SJ. Inhibition of fatty acid synthase induces endoplasmic reticulum stress in tumor cells. *Cancer Res.* 2007;67:1262-1269.

33. Tai Y-C, Ruangma A, Rowland D, et al. Performance evaluation of the microPET Focus: A third-generation microPET scanner dedicated to animal imaging. *J Nucl Med.* 2005;46:455-463.

34. Defrise M, Kinahan PE, Townshend DW, Michel C, Sibomana M, Newport DF. Exact and approximate rebinning algorithms for 3-D PET data. *IEEE Trans Med Imag.* 1997;16:145-158.

35. Shreve P, Chiao PC, Humes HD, Schwaiger M, Gross MD. Carbon-11 acetate PET imaging in renal disease. *J Nucl Med.* 1995;36:1595-1601.

36. Kotzerke J, Volkmer BG, Neumaier B, Gschwend JE, Hautmann RE, Reske SN. Carbon-11 acetate positron emission tomography can detect local recurrence of prostate cancer. *Eur J Nucl Med Mol Imag.* 2002;29:1380-1384.

37. Yoshimoto M, Waki A, Yonekura Y, et al. Characterization of acetate metabolism in tumor cells in relation to cell proliferation: Acetate metabolism in tumor cells. *Nucl Med Biol.* 2001;28:117-122.

38. Swinnen JV, Van Veldhoven PP, Timmermans L, et al. Fatty acid synthase drives the synthesis of phospholipids partitioning into detergent-resistant membrane microdomains. *Biochem Biophys Res Commun.* 2003;302:898-903.

39. Jadvar H, Li X, Park R, Shahinian A, Conti P. Quantitative autoradiography of radiolabeled acetate in mouse xenografts of human prostate cancer. *J Nucl Med.* 2006;47(suppl 1):421P-422P.

40. Bandyopadhyay S, Pai SK, Watabe M, et al. FAS expression inversely correlates with PTEN level in prostate cancer and a PI 3-kinase inhibitor synergizes with FAS siRNA to induce apoptosis. *Oncogene.* 2005;24:5389-5395.

41. Lupu R, Menendez JA. Pharmacological inhibitors of Fatty Acid Synthase (FASN)--catalyzed endogenous fatty acid biosynthesis: a new family of anti-cancer agents? *Curr Pharm Biotechno.* 2006;7:483-493.

42. Kuhajda FP. Fatty acid synthase and cancer: new application of an old pathway. *Cancer Res.* 2006;66:5977-5980.

43. Knowles LM, Smith JW. Genome-wide changes accompanying knockdown of fatty acid synthase in breast cancer. *BMC Genomics.* 2007;8:doi:10.1186/1471-2164-1188-1168.

44. Hager MH, Soloman KR, Freeman MR. The role of cholesterol in prostate cancer. *Curr Opin Clin Nutr Metab Care.* 2006;9:379-385.

45. Porstmann T, Griffiths B, Chung Y-L, et al. PKB/Akt induces transcription of enzymes involved in cholesterol and fatty acid biosynthesis via activation of SREBP. *Oncogene.* 2005;24:6465-6481.

FIGURE CAPTIONS

FIGURE 1. (A) *In vitro* cell association of 1-^{11}C-acetate at 30 min in PC-3, LNCaP, or 22Rv1 prostate cancer cells with and without 18 h prior treatment with C75, a FAS inhibitor. (*p = 0.001, **p = 0.0007, ***p = 0.0005)**;** (B) *In vitro* cell association of 1-^{11}C-acetate at 30 min in PC-3, LNCaP or 22Rv1 prostate cancer cells with and without 2 h prior treatment with TOFA, an ACC inhibitor to block the fatty acid synthesis pathway. (*p = 0.0025, **p = 0.0008, ***p = 0.0001). Error bars are ± SD.

FIGURE 2. A dose-response comparison of the relative effects of (A) C75 and (B) TOFA on FA synthesis in PC-3 cells, performed with ^{14}C-acetate. (C) Comparison of FA synthesis inhibition with 30 μM of C75 or TOFA in PC-3 and LNCaP cells. Error bars are ± SD.

FIGURE 3. Representative transaxial and coronal PET image slices of LAPC-4 (A), CWR22 (B), and 22Rv1 (C) tumor-bearing mice at 20 minutes post i.v. injection of 14.8-18.5 MBq (400-500 μCi) 1-^{11}C-acetate. Arrows mark tumor location. PC-3 tumors were not visualized. (D) Western blot of tumor lysates to show qualitative levels of FAS expression. Visual inspection of the Western blot results revealed obvious differences in the intensity of the band near 250 kDa (standard band denoted by black arrow; FAS = 267 kDa) with PC-3 showing relatively non-existent bands, 22Rv1 and LAPC-4 with significantly more intensity, and CWR22 being the highest of those examined. Multiplication of the area of the band by its intensity (after subtraction of background intensity) gave a relative value of expression for the sample analyzed. (E) SUV values of

1-^{11}C-acetate uptake in prostate tumor models versus the relative FAS expression (by Western blot) of these samples shows a direct correlation (R^2 = 0.974). Error bars are ± SD.

FIGURE 4. (A) Representative image slices of a LNCaP tumor-bearing mouse post i.v. injection of 3.7-7.4 MBq (100-200 μCi) 1-^{11}C-acetate. Arrows mark tumor location. (B) Overall change in Standardized Uptake Value (SUV) in solid PC-3 and LnCaP tumors in mice pre- and post-treated with C75. Error bars are ± SD. (C) Representative immunohistochemical staining of harvested prostate tumors for FAS (brown) showing a strong reactivity in the LNCaP, while PC-3 has almost none. 10× magnification. Three 3 slices per tumor were analyzed.

Fig. 1

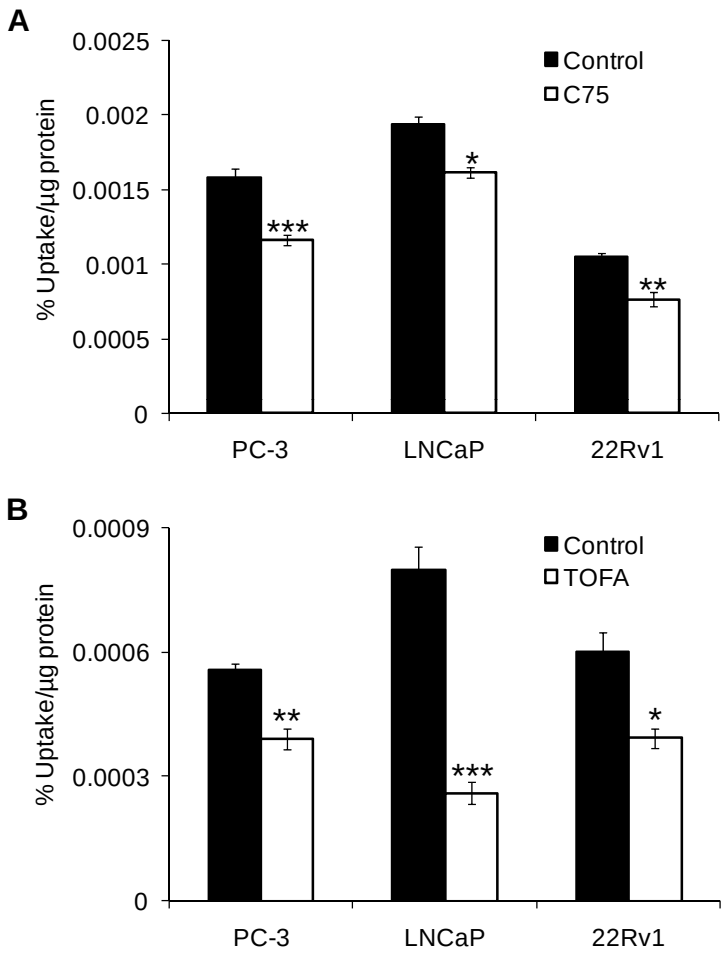
A
0.0025
0.002
0.0015
0.001
0.0005
0
% Uptake/µg protein
Control
C75
***
*
**
PC-3
LNCaP
22Rv1
B
0.0009
0.0006
0.0003
0
% Uptake/µg protein
Control
TOFA
**
***
*
PC-3
LNCaP
22Rv1

Fig. 2

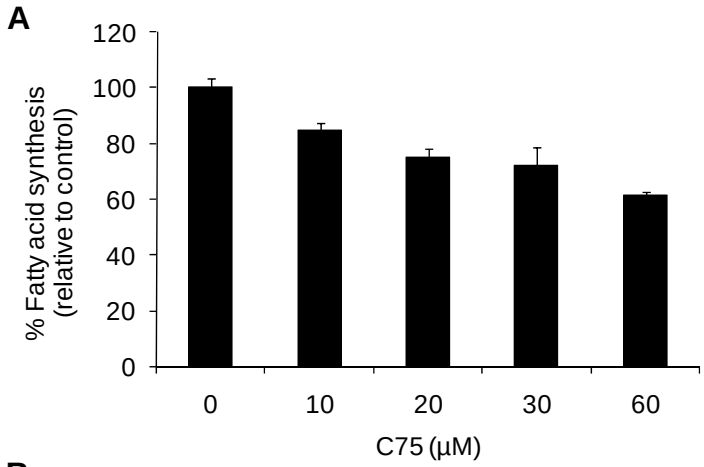
A
120
100
80
60
40
20
0
% Fatty acid synthesis (relative to control)
0
10
20
30
60
C75 (μM)

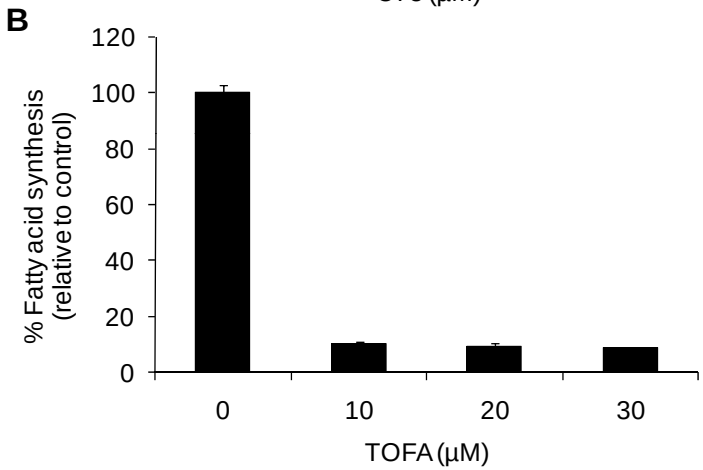
B
120
100
80
60
40
20
0
% Fatty acid synthesis (relative to control)
0
10
20
30
TOFA (μM)

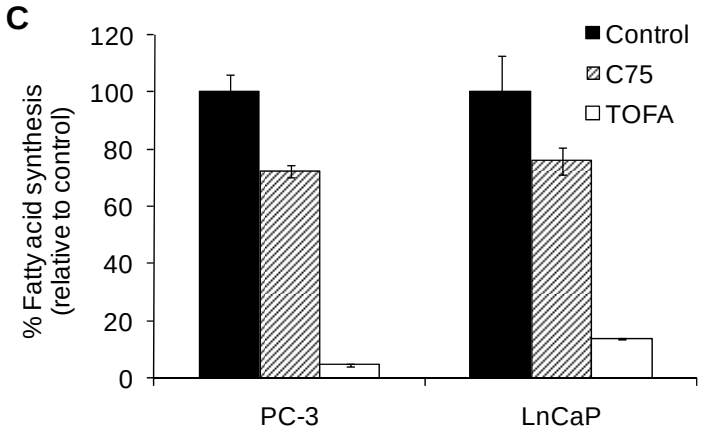
C
120
100
80
60
40
20
0
% Fatty acid synthesis (relative to control)
Control
C75
TOFA
PC-3
LnCaP

Fig. 3

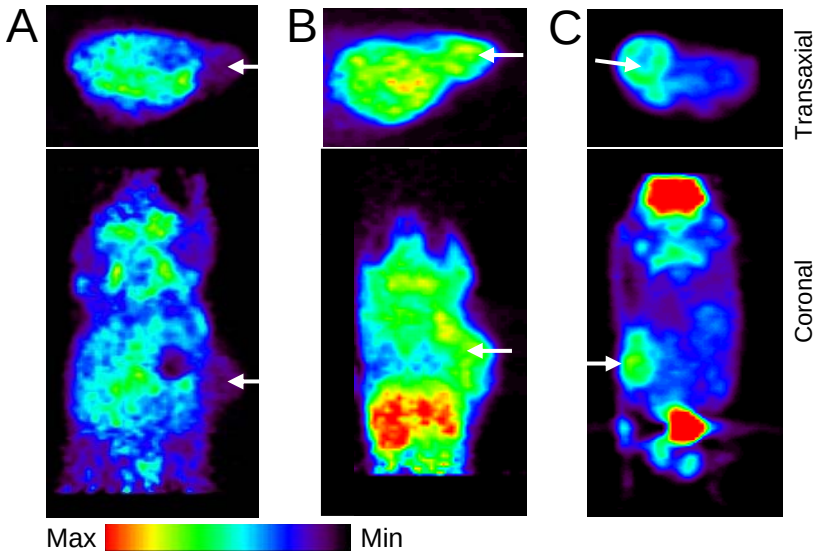
A
B
C
Transaxial
Coronal
Max
Min

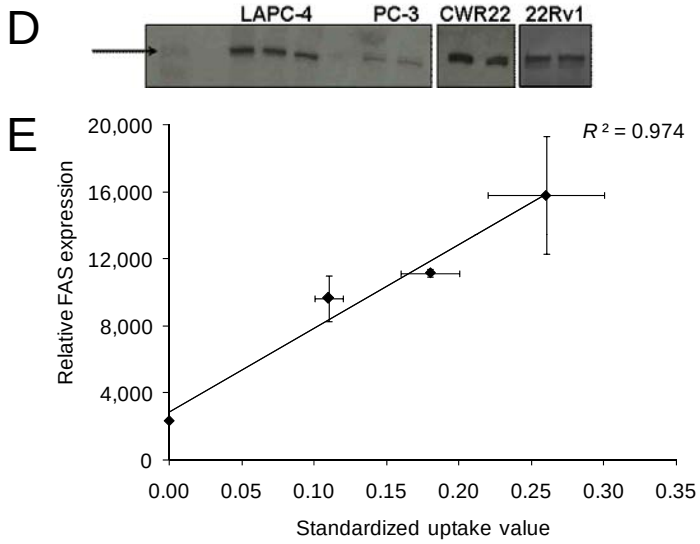
D
LAPC-4
PC-3
CWR22
22Rv1
E
R² = 0.974
Relative FAS expression
20,000
16,000
12,000
8,000
4,000
0
0.00
0.05
0.10
0.15
0.20
0.25
0.30
0.35
Standardized uptake value

Fig. 4

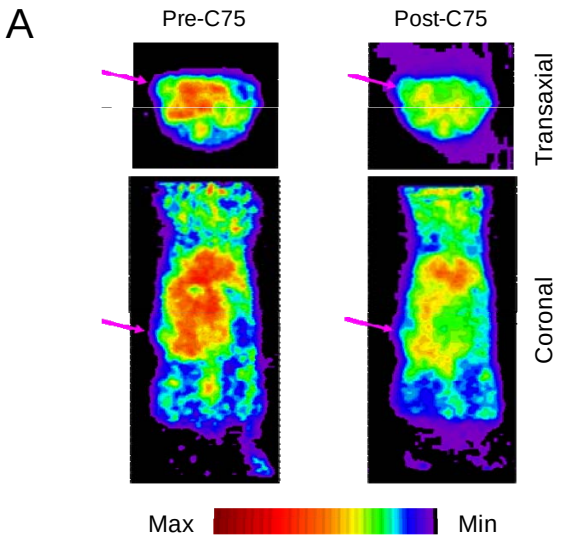
A
Pre-C75
Post-C75
Transaxial
Coronal
Max
Min

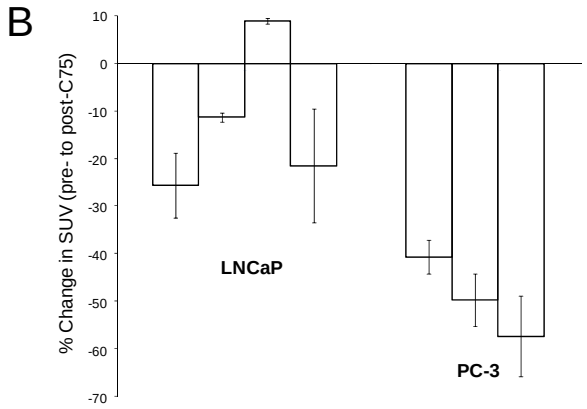
B
% Change in SUV (pre- to post-C75)
10
0
-10
-20
-30
-40
-50
-60
-70
LNCaP
PC-3

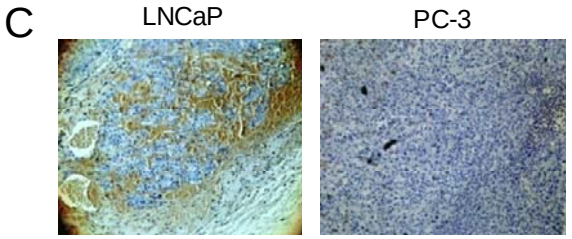
C
LNCaP
PC-3

I. “Examining the Relationship Between Cu-ATSM Hypoxia Selectivity and Fatty Acid Synthase Expression in Human Prostate Cancer Cell Lines”, Amy L. Vāvere and Jason S. Lewis. Nuclear Medicine and Biology, revision submitted

Examining the Relationship Between Cu-ATSM Hypoxia Selectivity and Fatty Acid Synthase Expression in Human Prostate Cancer Cell Lines

Amy L. Vāvere[1] and Jason S. Lewis[1,2]

[1] Division of Radiological Sciences, Washington University School of Medicine, St. Louis, MO, 63110, USA

[2] Alvin J. Siteman Cancer Center, Washington University School of Medicine, St. Louis, MO, 63110, USA

Short title: Cu-ATSM and FAS in prostate cancer

Keywords: Fatty Acid Synthase, Cu-ATSM, PET, prostate cancer

Address all correspondence and requests for reprints to:
Jason S. Lewis, Ph.D.
Mallinckrodt Institute of Radiology,
Washington University School of Medicine,
Campus Box 8225
510 S. Kingshighway Blvd.
St. Louis, MO 63110, USA

Tel: (314) 362 4696
Fax: (314) 362 9940
Email: j.s.lewis@wustl.edu

This work was supported by the United States Department of Defense (PC040435) and fellowship support from a National Institutes of Health NRSA (F32CA110422-03).

ABSTRACT

Introduction. PET imaging with Cu-ATSM for delineating hypoxia has provided valuable clinical information, but investigations in animal models of prostate cancer have shown some inconsistencies. As a defense mechanism in prostate cancer cells, the fatty acid synthesis pathway harnesses its oxidizing power for improving the redox balance despite conditions of extreme hypoxia, potentially altering Cu-ATSM hypoxia-selectivity.

Methods. Human prostate tumor cultured cell lines (PC-3, 22Rv1, LNCaP, and LAPC-4), were treated with an FAS inhibitor (C75, 100 μM) under anoxia. ^{64}Cu-ATSM uptake into these treated cells, and non-treated anoxic cells, was then examined. Fatty acid synthase (FAS) expression level in each cell line was subsequently quantified by ELISA. An additional study was performed in PC-3 cells to examine the relationship between the restoration of ^{64}Cu-ATSM hypoxia-selectivity and the concentration of C75 (100, 20, 4, or 0.8 μM) administered to the cells.

Results. Inhibition of fatty acid synthesis with C75 resulted in a significant increase in ^{64}Cu-ATSM retention into prostate tumor cells *in vitro* under anoxia over 60 mins. Inhibition studies demonstrated higher uptake values of 20.9 ± 3.27, 103.0 ± 32.6, 144.2 ± 32.3, and 200.1 ± 79.3% at 15 mins over control values for LAPC-4, PC-3, LNCaP, and 22Rv1 cells, respectively. A correlation was seen (R^2 = 0.911) with FAS expression plotted against % change in ^{64}Cu-ATSM uptake with C75 treatment.

Conclusions. Although Cu-ATSM has clinical relevance in the PET imaging of hypoxia in many tumor types, its translation to the imaging of prostate cancer may be limited by the over-expression of FAS associated with prostatic malignancies.

INTRODUCTION

The onset of hypoxia in malignant tissues is fairly universal, though not homogeneous, and is associated and influenced by a myriad of complicated processes. It is thought that since tumor cells are metabolically more active and proliferative than normal cells, they drain the surrounding tissue and blood supply of oxygen faster than it is supplied [1-3]. Tumors with increased levels of hypoxia afford resistance to traditional radiation therapy, as well as reducing the effects of many chemotherapeutic agents [4-7]. Measuring tissue oxygenation is no trivial task. The most common method, the use of an Eppendorf O_2 probe to measure oxygen tension, is effective but also quite invasive. Although the values obtained through this method have been predictive of metastatic potential and patient response to treatment [8-10], the technical difficulties of this technique make it generally undesirable.

In recent years, investigations into alternative, non-invasive methods for measuring pO_2 have been pursued by numerous researchers [2]. The use of PET imaging in conjunction with radiolabeled molecules that undergo chemical changes in the presence or absence of oxygen has led to a few promising tracers. ^{18}F-MISO (^{18}F-fluormisonidazole) exploits a simple chemical cycle whereby it takes the place of oxygen as an electron acceptor and is reduced and trapped. In the presence of oxygen, the initially reduced compound returns to its original state by receiving an additional electron from oxygen in a futile cycle. Imaging with ^{18}F-MISO has proved somewhat successful as a measure of oxygen levels, however the contrast between hypoxic and normoxic tissues is minimal (tumor to blood ratio > 1.2) [11-15]. ^{18}F-FAZA (^{18}F-fluoroazomycin arabinoside) has also been investigated as an alternative to ^{18}F-MISO with faster background clearance while

maintaining hypoxia selectivity [16, 17]. A recent pilot study showed promising results for clinical imaging in head and neck cancer patients [18].

Copper(II)-diacetyl-bis(N^4-methylthiosemicarbazone), Cu-ATSM, labeled with a positron emitting isotope of copper (^{60}Cu, ^{61}Cu, ^{62}Cu or ^{64}Cu) has been shown, *in vitro* and *in vivo*, to be selective for hypoxic tissue [19-21]. The clinical use of Cu-ATSM for delineating hypoxic human tumors using PET has provided valuable information in cervical, lung and rectal cancers [22-24]. Although a rapid >4-fold increase in retention of Cu-ATSM in hypoxic over normoxic cells was observed with overall retention at around 90% in hypoxic compared to 25% in normoxic cells [20, 25], these investigations did not include the use of prostate tumor cell lines. Burgmann *et al.* reported diminished hypoxic selectivity of Cu-ATSM *in vitro* in a rat prostate cancer cell line, R3327-AT [26]. In their analysis of 6 different cell lines ratios of hypoxic or anoxic uptake of ^{64}Cu-ATSM to normoxic uptake showed that the retention into the two prostate lines were consistently the lowest of the six lines examined. The same group also reported *in vivo* imaging studies comparing ^{64}Cu-ATSM and ^{18}F-MISO in two animal models of cancer [27]. In the FaDu human squamous cell carcinoma tumor model, the early (~1-4 h) and late (~19 h) ^{64}Cu-ATSM images were similar and were in general accordance with ^{18}F-MISO scans. However, their data did not support using Cu-ATSM as an indicator of hypoxia at early timepoints in the R3327-AT prostate model, with a negative correlation with ^{18}F-MISO at 1 hour after administration. Therefore, although the use of Cu-ATSM has been validated *in vitro* and *in vivo* in multiple tumor models and clinically in various human cancers, there is a concern that its ability to delineate hypoxia in **prostate** tumors may be suspect. In this work, we aimed to investigate and to begin to explain the causes

for the reduction of Cu-ATSM hypoxia-selectivity in prostate tumor lines. Given that the mechanism of Cu-ATSM hypoxia-selectivity is reliant on a chemical reduction of Cu(II) and that in prostate cancer the fatty acid synthesis pathway harnesses its oxidizing power for improving the redox balance (i.e., lower NADH/NAD+ ratios) despite conditions of extreme hypoxia [28], we wanted to explore these relationships as a potential reason for the lack of Cu-ATSM hypoxia-selectivity in prostate tumors.

METHODS

All chemicals, unless otherwise stated, were purchased from Sigma-Aldrich Chemical Company, Inc (St. Louis, MO). All solutions were prepared using distilled, deionized water (>18 MΩ resistivity) by passing through a Milli-Q filtration system (Millipore Corp., Milford, MA). Radioactive samples were counted in a radioisotope calibrator (Capintec, Inc., Ramsey, NJ) for determination of mCi and an automated well scintillation Beckman 8000 gamma counter (Irvine, CA) for counts per minute. ^{64}Cu was produced at Washington University School of Medicine on a CS-15 biomedical cyclotron using previously published methods [29] and ^{64}Cu-ATSM was prepared as previously described [21]. Human prostate carcinoma tumor cell lines PC-3, LNCaP, and 22Rv1 were obtained from American Type Culture Collection (Manassas, VA) and LAPC-4 cells were a gift from Dr. Charles Sawyers at UCLA. Cells were maintained by serial passage in cell culture. LAPC-4 was shown in our laboratories to have relatively low FAS expression compared with the other prostate tumor cell lines and was therefore chosen as a ‘negative’ control.

***In vitro* ^{64}Cu-ATSM uptake.** A comparison of ^{64}Cu-ATSM uptake under anoxic and normoxic conditions was made in three prostate cell lines – 22Rv1, LNCaP, and PC-3. The apparatus and methods used in the *in vitro* uptake study are based on those previously described in the literature [20]. Viability of the cells was measured with a hemocytometer utilizing trypan blue staining. Briefly, two three-neck flasks containing cells in suspension were immersed in a 37°C water bath by a rod connected to a stand rotating on an external orbital mixer. An anoxic (5% CO_2, 95% N_2) and normoxic (20% O_2, 5% CO_2, 95% N_2) gas mixture were humidified and brought to 37°C before being passed continuously through each of the flasks. 30-50 mL of cell suspension (1×10^6 cells/mL) was added to each flask and given 1 hour to equilibrate to the environment. After equilibration, 100 μCi ^{64}Cu-ATSM was added to each of the flasks in a small amount (~5 μL) of ethanol. At 1, 5, 15, 30, 45, and 60 minutes, 200 μL of cell suspension was removed *via* pipet and placed in a 1.5 mL Eppendorf tube which was immediately centrifuged for 30 s at 3000 rpm to pellet the cells. 180 μL of the supernatant was then pipetted off and deposited in a separate tube. This was done in triplicate at each timepoint. All pellet and supernatant samples were counted on a gamma counter. Percent uptake was calculated as activity in the pellet (corrected for remaining supernatant) divided by the sum of the pellet and supernatant.

C75 treatment studies were performed in four prostate cell lines – 22Rv1, LNCaP, PC-3, and LAPC-4 following similar methods. In this case, both flasks were under anoxic conditions, while one flask received C75 for FAS inhibition. During the hour of equilibration, C75 was added to the cells (in 10 μL or less of DMSO) so that the final concentration in the flask was 100 μM, while the other flask received DMSO alone. At 1,

5, 15, 30, 45, and 60 minutes the same procedure of sample collection and analysis was performed.

FAS expression by ELISA. FAS expression of each tumor line was quantified using a FAS-detect™ ELISA kit (FASgen, Inc.) based on a two-site ELISA technique to quantitatively measure FAS in human serum. Cells were pelleted and lysed by addition of 1 mL of cell lysis buffer containing protease inhibitors and incubated on ice for 30 minutes. The cell debris was then repelleted and the final supernatant was analyzed. Results were compared to a standard curve of varying concentrations of FAS to determine the concentration in ng/mL. These values were normalized by protein concentration as determined by using a standard copper reduction/bicinchoninic acid assay (Pierce) with bovine serum albumin as the standard, resulting in a ratio with units of ng FAS/μg protein.

***In vitro* C75 dose response on ^{64}Cu-ATSM uptake.** These *in vitro* studies were performed using the same apparatus and methods as previously described in the initial *in vitro* experiments. In this study however, various amounts of C75 were added to the cells (in 10 μL or less of DMSO) so that the final concentration of C75 in each flask was 100, 20, 4, or 0.8 μM.

RESULTS

For each cell line, two three-neck flasks containing cells (35 mL) in suspension were placed under anoxic and normoxic conditions with or without pretreatment with C75 (100 μM). Uptake of ^{64}Cu-ATSM was measured over time to determine if FAS inhibition (by

C75) restored the cells' ability to trap Cu-ATSM under low oxygen conditions. Inhibition of FAS with C75 resulted in a dramatic increase in ^{64}Cu-ATSM retention into prostate tumor cells *in vitro* under anoxic conditions (Fig. 1). The treated cells demonstrated higher uptake values at 15 minutes of 20.93 ± 3.271, 103.0 ± 32.57, 144.2 ± 32.28, and 200.1 ± 79.27 % over control values for LAPC-4, PC-3, LNCaP, and 22Rv1 cell lines, respectively. These values would later be correlated to FAS expression of each cell line.

Ratios of anoxic to normoxic ^{64}Cu-ATSM uptake demonstrate the selectivity of the tracer in a particular model, and so these were also compared over the 60 minute experiment (Fig. 2, 15 min data shown). The value obtained for the retention of ^{64}Cu-ATSM into EMT-6 murine mammary carcinoma cells at 15 min is included for comparison [25]. The 15 minute time point was chosen since Cu-ATSM in these cells was shown to plateau at this point (Fig. 1). Similar kinetics were shown in Lewis et al., [25] and Dearling et al., 1998 [20]. Also given that this is entirely an *in vitro* study, the potential blood flow issues associated with *in vivo* studies was not felt to be a factor. It is also worth pointing out that in the human ^{60}Cu-ATSM studies uptake in tumors [22, 23] resulted in high contrast levels between hypoxic and normoxic tissues by as little as 10-15 minutes post injection, and yielded clinically relevant information about tumor oxygenation that was predictive of tumor behavior and response to therapy. In this current study, values in all three of the cell lines examined under normoxic conditions, were lower than the EMT-6 ratios suggesting that visualization of solid tumors, derived from these prostate cancer cell lines may be difficult due to normoxic background retention in the surrounding tissue.

Samples of each cell line were analyzed to determine if relative amounts of FAS were related to the magnitude of Cu-ATSM retention at 15 min post-incubation. Quantification of FAS expression, by ELISA, resulted in values of 0.00438 ± 0.00024, 0.00832 ± 0.00038, 0.01877 ± 0.00092, and 0.02679 ± 0.00224 ng FAS/μg total protein for LAPC-4, PC-3, LNCaP, and 22Rv1, respectively. As expected, a correlation is seen (R^2 = 0.911) with FAS expression plotted against the change in hypoxic retention resulting from inhibition of FAS (Fig. 3).

The dose response effect of C75 on the restoration of hypoxic retention of Cu-ATSM was measured in PC-3 cells utilizing the same cell suspension apparatus and anoxic gas mixture. During a 1-hour equilibration period, the four flasks were treated with varying concentrations of C75 (100, 20, 4, or 0.8 μM). Confirming the effect of FAS inhibition on ^{64}Cu-ATSM uptake, the experiment showed increasing retention directly related to C75 concentration with values of 0.0037 ± 0.0037, 0.0030 ± 0.0031, 0.0026 ± 0.0026, and 0.0024 ± 0.0025 % uptake/μg protein for 100, 20, 4, and 0.8 μM respectively at 15 mins (Fig. 4).

DISCUSSION

Low oxygen levels are a hallmark of malignant processes, leading to a cascade of oncogenic properties that support tumor growth and invasion [1-3, 30, 31]. Existing in this harsh environment, the cells go into survival mode and do not easily respond to DNA damaging chemotherapeutics or agents that promote apoptosis [6, 7]. In the absence of oxygen, the damaging radicals created by traditional radiation therapy recombine resulting in little damage to the target tissue [3-5]. Levels of tumor hypoxia

have also been correlated to overall patient survival and tumor aggressiveness [1, 2, 32-34].

^{64}Cu-ATSM [19], which targets hypoxia as opposed to metabolism, has already been confirmed as a clinically important PET agent in the prediction of prognosis in several cancers. It has been shown to be a useful clinical PET imaging tracer that can distinguish responders to conventional therapies from non-responders in patients with lung [23], cervical [22], rectal [24] and head and neck (data not published) cancer. It has also been suggested as a potential tool for radiation oncologists to tailor the radiation dose based on hypoxic regions, giving the resistant regions an increased dose [35].

Recently, Yuan *et al*, showed that the regional ^{64}Cu-ATSM retention in two tumors types (R3230Ac and 9L) correlated closely with intrinsic markers for hypoxia, but in a third tumor type (FSA) a correlation was not observed [36]. The suggested reason for this low correlation between Cu-ATSM uptake and hypoxic distribution was the differing redox statuses of the tumor types. FSA tumors may have a lower-than-average redox potential with high concentrations of electron donors. If the speculated mechanism of Cu-ATSM uptake holds, then reduction, release and ultimate cellular trapping of Cu(I) would be caused by a decrease in the redox potential of the cell [19, 21, 26, 37, 38]. In the FSA tumor line, the lower-than-average redox potential caused reduction and trapping of ^{64}Cu-ATSM in both hypoxic and normoxic areas. It was also suggested that the higher perfusion levels surrounding the hypoxic regions of the FSA tumor could contribute to the higher level of retention of Cu-ATSM in normoxic FSA cells. *In vitro* and *in vivo* experiments have also revealed inconsistencies in the hypoxic selectivity of Cu-ATSM in

prostate cancer models [26, 27]. Although a very limited number of other tumor cell lines such as FSA have shown inconsistencies, prostate tumors clearly stand out as the primary tumor type that Cu-ATSM hypoxia-selectivity is reduced to low or even undetectable levels [26, 27]. This current study was undertaken in human prostate tumor lines to better examine the reasons for the lack of hypoxia-selectivity of Cu-ATSM in prostate tumors.

Biologically, prostate tumors have some unique characteristics when compared to other malignancies. Prostate cancer is known to have low metabolism, and the most common PET tracer for detecting malignancies, ^{18}F-FDG, is not effective in delineating it from surrounding tissue [39] and also goes to sites of inflammation. Fatty acid synthase (FAS) is a multi-functional enzymatic protein involved in many stages of fatty acid synthesis and has been found to be overexpressed in prostate carcinomas as well as other cancers [40-48]. It is an androgen-regulated enzyme that is overexpressed in the vast majority of prostate tumors and its expression defines distinct molecular signatures in prostate cancer [49]. An increased level of FAS has been found to be indicative of aggressive and late-stage prostatic adenocarcinomas [50] as well as a prognostic indicator for overall survival [51].

As a defense mechanism in prostate cancer cells, the fatty acid synthesis pathway harnesses its oxidizing power for improving the redox balance (i.e., lower NADH/NAD$^+$ ratios) despite conditions of extreme hypoxia [28]. This pathway is able to consume reducing equivalents (i.e., NADPH) as part of its normal processes. Under hypoxic conditions, anaerobic glycolysis creates excessive levels of lactate, which limits the

respiratory chain and reduces its oxidizing power. The relationship between the fatty acid synthesis pathway and prostate tumors has been superbly reviewed by Hochachka et al., [28]. In regards to the hypoxia-selectivity of Cu-ATSM, it has been shown that Cu-ATSM enters all cells by passive diffusion, and under normoxic conditions freely exits the cell. Under hypoxic or anoxic conditions, the redox potential of the cell is altered such that the Cu(II) in the complex is reduced to Cu(I) and the complex falls apart [21, 26, 37, 38]. This retention mechanism is reliant on the reduction of the Cu(II) to Cu(I), and if cellular reducing equivalents such as NADPH are consumed by the overexpression of the fatty acid synthesis pathway this chemical reduction, even under conditions of hypoxia, is unlikely to take place.

Analysis of the hypoxic selectivity of the four human prostate models studied shows diminished selectivity when compared to EMT-6 mammary carcinoma (Fig. 2). By dividing the anoxic uptake by the normoxic uptake, a relative selectivity is calculated. Values of approximately 1.5-3.8, which were found in this study, are consistently lower than many other cell lines described in the literature [26]. In Burgman's study, MCF-7, FSaII, and FaDu cell lines show selectivity of between 7 and 10, with R3327-AT showing no hypoxia selectivity at all [26]. Interestingly, cancers of the breast [44, 45, 48], colon [47] and ovary [46] are also known to demonstrate *elevated* levels of FAS. Given that in the Burgmann study [26] MCF7 cells demonstrated high hypoxia-selectivity for Cu-ATSM and they are known to express high levels of FAS [52], additional pathways may be involved in reducing Cu-ATSM hypoxia-selectivity that are not explained entirely by the presence of over-expression of FAS. However, it is important also to discuss what is meant by the term of 'overexpression' or "express high levels'. Even though the literature

often uses these terms, they must be placed in context; in this current study we chose to compare four human prostate cancer cells lines that were shown to have *relatively* low or high expression to one another. It is has been shown that the overexpression of FAS in precursor prostate tumors is significantly higher than that of other tumor types such as breast [53]. Therefore, even though breast cancer and other malignancies are known to have higher levels FAS than surrounding normal tissue, whether or not this overexpression is at a level that will prevent Cu-ATSM reduction in hypoxic cells has yet to be determined. A full comparative and exhaustive study is therefore required in other cell types (e.g., breast tumor lines) before similar conclusions about the relationship of FAS expression and Cu-ATSM hypoxia-selectivity can be made for those tumor types.

C75 is a small molecule that binds to and inhibits mammalian FAS and inhibits fatty acid synthesis in human cancer cells. Researchers have shown that C75 inhibits FAS by 89-95% [54]. In this study, C75 was used to inhibit FAS activity in prostate tumor cell lines by blocking this enzymatic cycle's ability to offset the redox balance of a hypoxic cell, therefore, increasing retention of Cu-ATSM under hypoxic conditions. Typically a blocking study is designed to inhibit uptake of the radiotracer; in this case we were attempting to block the FAS so that it is unable to 'stabilize' the redox environment of the cell. Its inhibition should allow the anticipated retention of Cu-ATSM in hypoxic regions of the tumor. *In vitro* results in all cell lines demonstrate that FAS has a significant impact on the retention of ^{64}Cu-ATSM into human prostate tumor cells under oxygen-limited conditions. Inhibition of FAS with a single 1 hour treatment of C75 (50 μM) resulted in increased retention of Cu-ATSM in all four tumor lines tested *in vitro* (Fig.1), but to a limited extent in the low-FAS-expressing LAPC-4. Results also showed that a linear

change in uptake correlated directly to the cellular expression of FAS (Fig 3.). To demonstrate that restoration of retention is directly related to FAS inhibition, a dose response experiment was undertaken (Fig. 4).

CONCLUSION

Cu-ATSM has been a valuable tool as a marker of hypoxia, and it's possible that the nature of its mechanism of retention, though not completely understood, could lead us to answers for the incongruences in its selectivity. The uncertainty lies in the possibility that other physiological changes caused by malignant progression and hypoxia within the cell could also affect this redox balance regardless of oxygen concentration. If the suggested mechanism of Cu-ATSM uptake holds, then reduction, release and ultimate cellular trapping of Cu(I) would be caused by a decrease in the redox potential of the cell. And, although in most cases this is directly due to a change (reduction) in oxygen concentration within the cell, there are many other processes that could also alter the redox potential of this environment. In prostate tumors, a reduction of ^{64}Cu-ATSM hypoxia selectivity is demonstrated in a manner that directly correlates to FAS expression. ^{64}Cu-ATSM is a very effective PET agent for clinically delineating many hypoxic human malignancies, but, as with all radiopharmaceuticals, it is not a universal agent. Care should be taken in particular regard to the imaging of prostate tumors.

ACKNOWLEDGEMENTS

The authors thank Susan Adams for cell preparation. We also thank Drs. Nobuyuki Oyama and Steven Kridel for their helpful discussions. Thanks also to the cyclotron

facility staff for radionuclide production. We are grateful for financial support from the Department of Defense (PC040435) and the NIH for salary support for ALV (F32CA110422-03).

REFERENCES

[1] Brown JM. The hypoxic cell: A target for selective cancer therapy - eighteenth Bruce F. Cain Memorial Award Lecture. Cancer Res 1999;59:5863-5870.

[2] Tatum JL, Kelloff GJ, Gillies RJ, Arbeit JM, Brown JM, Chao KSC, Chapman JD, Eckelman WC, Fyles AW, Giaccia AJ, Hill RP, Koch CJ, Krishna MC, Krohn KA, Lewis JS, Mason RP, Melillo G, Padhani AR, Powis G, Rajendran JG, Reba R, Robinson SP, Semenza GL, Swartz HM, Vaupel P, Yang D, Croft B, Hoffman J, Liu G, Stone H and Sullivan D. Hypoxia: Importance in tumor biology, noninvasive measurement by imaging, and value of its measurement in the management of cancer therapy. Int J Radiat Biol 2006;82:699-757.

[3] Höckel M and Vaupel P. Tumor hypoxia: definitions and current clinical, biologic, and molecular aspects. J Natl Cancer Inst 2001;93:266-276.

[4] Crabtree HG and Cramer W. The action of radium on cancer cells I. II. Some factors determining the susceptibility of cancer cells to radium. Proc R Soc Ser B 1933;113:238-250.

[5] Gray LH, Conger AD, Ebert M, Hornsey S and Scott OC. Concentration of oxygen dissolved in tissues at the time of irradiation as a factor in radiotherapy. Br J Radiol 1953;26:638-648.

[6] Tannock I and Guttman P. Responses of chinese hamster ovary cells to anticancer drugs under aerobic and hypoxic conditions. Br J Cancer 1981;42:245-248.

[7] Teicher BA, Holden SA, Al-Achi SA and Herman TS. Classification of antineoplastic treatments by their differential toxicity toward putative oxygenated

and hypoxic tumor subpopulations *in vivo* in the FSaIIC murine fibrosarcoma. Cancer Res 1990;50:3339-3344.

[8] Brizel DM, Scully SP, Harrelson JM, Layfield LJ, Bean JM, Prosnitz LR and Dewhirst MW. Tumor oxygenation predicts for the likelihood of distant metastases in human soft tissue sarcoma. Cancer Res 1996;56:941-943.

[9] Gatenby RA, Kessler HB, Rosenblum JS, Coia LR, Moldofsky PJ, Hartz WH and Broder GJ. Oxygen distribution in squamous cell carcinoma metastases and its relationship to outcome of radiation therapy. Int J Radiat Oncol Biol Phys 1988;14:831-838.

[10] Nordsmark M, Bentzen SM, Rudat V, Brizel D, Lartigau E, Stadler P, Becker A, Markus A, Molls M, Dunst J, Terris DJ and Overgaard J. Prognostic value of tumor oxygenation in 397 head and neck tumors after primary radiation therapy. An international multi-center study. Radiother Oncol 2005;77:18-24.

[11] Rajendran JG and Krohn KA. Imaging hypoxia and angiogenesis in tumors. Radiologic Clin N Am 2005;43:169-187.

[12] Nunn A, Linder K and Strauss HW. Nitroimidazoles and imaging hypoxia. Eur J Nucl Med 1995;22:265-280.

[13] Rajendran JG, Mankoff DA, O'Sullivan F, Peterson LM, Schwartz DL, Conrad EU, Spence AM, Muzi M, Farwell DG and Krohn KA. Hypoxia and glucose metabolism in malignant tumors: evaluation by [^{18}F]Fluoromisonidazole and [^{18}F]Fluorodeoxyglucose positron emission tomography imaging. Clin Cancer Res 2004;10:2245-2252.

[14] Rajendran JG, Wilson DC, Conrad EU, Peterson LM, Bruckner JD, Rasey JS, Chin LK, Hofstrand PD, Grierson JR, Eary JF and Krohn KA. [^{18}F]FMISO and

[^{18}F]FDG PET imaging in soft tissue sarcomas: correlation of hypoxia, metabolism and VEGF expression. Eur J Nucl Med Mol Imaging 2003;30:695-704.

[15] Cherk MH, Foo SS, Poon AM, Knight SR, Murone C, Papenfuss AT, Sachinidis JI, Saunder TH, O'Keefe GJ and Scott AM. Lack of correlation of hypoxic cell fraction and angiogenesis with glucose metabolic rate in non–small cell lung cancer assessed by ^{18}F-fluoromisonidazole and ^{18}F-FDG PET. J Nucl Med 2006;47:1921-1926.

[16] Piert M, Machulla H-J, Picchio M, Reischl G, Ziegler S, Kumar P, Wester H-J, Beck R, McEwan AJB, Wiebe LI and Schwaiger M. Hypoxic-specific tumor imaging with ^{18}F-fluoroazomycin arabinoside. J Nucl Med 2005;46:106-113.

[17] Sorger D, Patt M, Kumar P, Wiebe LI, Barthel H, Seese A, Dannenberg C, Tannapfel A, Kluge R and Sabri O. [^{18}F]Fluoroazomycinarabinofuranoside (^{18}FAZA) and [^{18}F]Fluoromisonidazole (^{18}FMISO): A comparative study of their selective uptake in hypoxic cells and PET imaging in experimental rat tumors. Nucl Med Biol 2003;30:317-326.

[18] Souvatzoglou M, Grosu AL, Roper B, Krause BJ, Beck R, Reischl G, Picchio M, Machulla H-J, Wester H-J and Piert M. Tumour hypoxia imaging with [^{18}F]FAZA PET in head and neck cancer patients: a pilot study. Eur J Nucl Med Mol Imag 2007:DOI: 10.1007/s00259-007-0424-3.

[19] Vavere AL and Lewis JS. Cu-ATSM: A radiopharmaceutical for the PET imaging of hypoxia. Dalton Trans 2007:(in press).

[20] Dearling JLD, Lewis JS, Mullen GED, Rae MT, Zweit J and Blower PJ. Design of hypoxia-targeting radiopharmaceuticals: Selective uptake of copper-64 complexes in hypoxic cells in vitro. Eur J Nucl Med 1998;25:788-792.

[21] Fujibayashi Y, Taniuchi H, Yonekura Y, Ohtani H, Konishi J and Yokoyama A. Copper-62-ATSM: A new hypoxia imaging agent with high membrane permeability and low redox potential. J Nucl Med 1997;38:1155-1160.

[22] Dehdashti F, Grigsby PW, Mintun MA, Lewis JS, Siegel BA and Welch MJ. Assessing tumor hypoxia in cevical cancer by positron emission tomography with ^{60}Cu-ATSM: relationship to therapeutic response - a preliminary report. Int J Radiat Biol Phys 2003;55:1233-1238.

[23] Dehdashti F, Mintun MA, Lewis JS, Bradley J, Govindan R, Laforest R, Welch MJ and Siegel BA. In vivo assessment of tumor hypoxia in lung cancer with ^{60}Cu-ATSM. Eur J Nucl Med Mol Imag 2003;30:844-850.

[24] Dietz DW, Dehdashti FD, Grigsby PW, Malyapa RS, Myerson RJ, Picus J, Ritter J, Lewis JS, Welch MJ and Siegel BA. Tumor hypoxia detected by Positron Emission Tomography with ^{60}Cu-ATSM as a predictor of response and survival in patients undergoing neoadjuvant chemoradiotherapy for rectal aarcinoma: a pilot study. Dis Colon Rec:submitted.

[25] Lewis JS, McCarthy DW, McCarthy TJ, Fujibayashi Y and Welch MJ. Evaluation of ^{64}Cu-ATSM in vitro and in vivo in a hypoxic tumor model. J Nucl Med 1999;40:177-183.

[26] Burgman P, O'Donoghue JA, Lewis JS, Welch MJ, Humm JL and Ling CC. Cell line-dependent differences in uptake and retention of the hypoxia-selective nuclear imaging agent Cu-ATSM. Nucl Med Biol 2005;32:623-630.

[27] O'Donoghue JA, Zanzonico P, Pugachev A, Wen B, Smith-Jones P, Cai S, Burnazi E, Finn R, Burgman P, Ruan S, Lewis JS, Welch MJ, Ling CC and Humm JL. Assessment of regional tumor hypoxia using ^{18}F-fluoromisonidazole and ^{64}Cu(II)-diacetyl-bis(N^4-methylthiosemicarbazone) positron emission tomography: Comparative study featuring microPET imaging, pO_2 probe measurement, autoradiography, and fluorescent microscopy in the R3327-AT and FaDu rat tumor models. Int J Radiat Biol Phys 2005;61:1493-1502.

[28] Hochachka PW, Rupert JL, Goldenberg L, Gleave M and Kozlowski P. Going malignant: the hypoxia-cancer connection in the prostate. BioEssays 2002;24:749-757.

[29] McCarthy DW, Shefer RE, Klinkowstein RE, Bass LA, Margenau WH, Cutler CS, Anderson CJ and Welch MJ. Efficient production of high specific activity ^{64}Cu using a biomedical cyclotron. Nucl Med Biol 1997;24.

[30] Gillemin K and Krasnow MA. The hypoxic response: huffing and HIFing. Cell Death Differentiation 1997;89:9-12.

[31] Jiang BH, Semenza GL, Bauer C and Marti HH. Hypoxia-inducible factor 1 levels vary over a physiologically relevant range of O_2 tension. Am J Physiol 1996;271:C1172-1180.

[32] Höckel M, Schlenger K, Aral B, Mitze M, Shäffer U and Vaupel P. Assocaition between tumor hypoxia and malignant progression in advancer cancer of the uterine cervix. Cancer Res 1996;56:4509-4515.

[33] Graeber TG, Osmanian C, Jacks T, Housman DE, Koch CJ, Lowe SW and Giaccia AJ. Hypoxia-mediated selection of cells with diminished apoptotic potential in solid tumours. Nature (Lond) 1996;379:88-91.

[34] Shweiki D, Itin A, Soffer D and Keshet E. Vascular endothelial growth factor induced by hypoxia may mediate hypoxia-initiated angiogenesis. Nature (Lond) 1992;359:843-845.

[35] Chao C, Bosch WR, Mutic S, Lewis JS, Dehdashti FD, Mintun MA, Demsey JF, Perez CA, Purdy JA and Welch MJ. A novel approach to overcome hypoxic tumor resistance: Cu-ATSM-guided intensity-modulated radiation therapy. Int J Radiat Biol Phys 2001;49:1171-1182.

[36] Yuan H, Schroeder T, Bowsher JE, Hedlund LW, Wong T and Dewhirst MW. Intertumoral differences in hypoxia selectivity of the PET imaging agent ^{64}Cu(II)-diacetyl-bis(N^4-methylthiosemicarbazone). J Nucl Med 2006;47:989-998.

[37] Dearling JLJ, Lewis JS, Mullen GED, Welch MJ and Blower PJ. Copper bis(thiosemicarbazone) complexes as hypoxia imaging agents: structure-activity relationships. J Biol Inorg Chem 2002;7:249-259.

[38] Maurer RI, Blower PJ, Dilworth JR, Reynolds CA, Zheng Y and Mullen GED. Studies on the mechanism of hypoxic selectivity in copper bis(thiosemicarbazone) radiopharmaceuticals. J Med Chem 2002;45:1420-1431.

[39] Fricke E, Mchtens S, Hofmann M, van den Hoff J, Bergh S, Brunkhorst T, Meyer GJ, Karstens JH, Knapp WH and Boerner AR. Positron emission tomography with ^{11}C-Acetate and ^{18}F-FDG in prostate cancer patients. Eur J Nucl Med Mol Imag 2003;30:607-611.

[40] Dhanasekaran SM, Barrette TR, Ghosh D, Shah R, Sooryanarayana V, Kurachi K, Pienta KJ, Rubin MA and Chinnaiyan AM. Delineation of prognostic biomarkers in prostate cancer. Nature 2001;412:822-826.

[41] Swinnen JV, Roskams T, Joniau S, Van Poppel H, Oyen R, Baert L, Heyns W and Verhoeven G. Overexpression of fatty acid synthase is an early and common event in the development of prostate cancer. Int J Cancer 2002;98:19-22.

[42] Welsh JB, Sapinosa LM, Su AI, Kern SG, Wang-Rodriguez J, Moskaluk CA, Frierson HF and Hampton GM. Analysis of gene expression identifies candidate markers and pharmacological targets in prostate cancer. Cancer Res 2001;61:5974-5978.

[43] Menendez JA and Lupu R. Oncologic properties of the endogenous fatty acid metabolism: molecular pathology of fatty acid synthase in cancer cells. Curr Opin Clin Nutr Metab Care 2006;9:346-357.

[44] Alo PL, Visca P, G. T, Mangoni A, Lenti L, Monaco S, Botti C, Serpieri DE and Di Tondo U. Fatty acid synthase (FAS) predictive strength in poly differentiated early breast carcinomas. Tumori 1999;85:35-40.

[45] Alo PL, Visca P, Marci A, Mangoni A, Botti C and Di Tondo U. Expression of fatty acid synthase (FAS) as a predictor of recurrence in stage I breast carcinoma patients. Cancer 1996;77:474-482.

[46] Gansler TS, Hardman W, A. HD, Schaffel S and Hennigar RA. Increased expression of fatty acid synthase (OA-519) in ovarian neoplasms predicts shorter survival. Human Pathol 1997;28:686-692.

[47] Rashid A, Pizer ES, Moga M, Milgraum LZ, Zahurak M, Pasternack GR, Kuhajda FP and Hamilton SR. Elevated expression of fatty acid synthase and fatty acid synthetic activity in colorectal neoplasia. Am J Pathol 1997;150:201-208.

[48] Wang Y, Kuhajda FP, Li JN, Pizer ES, Han WF, Sokoll LJ and Chan DW. Fatty acid synthase (FAS) expression in human breast cancer cell culture supernatents and in breast cancer patients. Cancer Lett 2001;167:99-104.

[49] Rossi S, Graner E, Febbo P, Weinstein L, Bhattacharya N, Onody T, Bubley G, Balk S and Loda M. Fatty acid synthase expression defines distinct molecular signatures in prostate cancer. Mol Cancer Res 2003;1:707-715.

[50] Myers RB, Oelschlager DK, Weiss HL, Frost AR and Grizzle WE. Fatty acid synthase: An early molecular marker of progression of prostatic adenocarcinoma to androgen independence. J Urology 2001;165:1027-1032.

[51] Takahiro T, Shinichi K and Toshimitsu S. Expression of fatty acid synthase as a prognostic indicator in soft tissue sarcomas. Clin Cancer Res 2003;9:2204-2212.

[52] Yeh C-W, Chen W-J, Chiang C-T, Lin-Shiau S-Y and Lin J-K. Suppression of fatty acid stnthase in MCF-7 breast cancer cells by tea and tea polyphenols: a possible mechanism for their hypolipidemic effects. Pharmacogenomics J 2003;3:267-276.

[53] Kuhajda FP. Fatty-acid synthase and human cancer. New perspectives on its role in tumor biology. Nutrition (New York) 2000;16:202-208.

[54] Loftus TM, Jaworsky DE, Frehywot GL, Townsend CA, Ronnett GV, Lane MD and Kuhajda FP. Reduced food intake and body weight in mice treated with fatty acid synthase inhibitors. Science 2000;288:2379-2381.

Figure Captions.

Figure 1. Uptake of ^{64}Cu-ATSM into prostate tumor cells (in suspension) under anoxic conditions (5% CO_2 + 95% N_2) treated with C75 (dashed) and compared to control (solid). (n = 3 at each timepoint)

Figure 2. Ratios of anoxic to normoxic ^{64}Cu-ATSM uptake in prostate cancer cells lines at 15 mins demonstrating differing selectivity of the tracer in different models. The value obtained for the retention of ^{64}Cu-ATSM into EMT-6 murine mammary carcinoma cells at 15 mins is included for comparison [25].

Figure 3. Correlation of FAS expression as determined by ELISA to % change in ^{64}Cu-ATSM uptake between C75 treated (100 μM) and control cells under anoxic conditions (5% CO_2, 95% N_2) at 15 min post-incubation. Points on the graph represent LAPC-4, PC-3, LNCaP, and 22Rv1 from left to right. (n = 3 at each timepoint)

Figure 4. Dose response of ^{64}Cu-ATSM uptake at 15 mins (under anoxic conditions) in PC-3 cells following FAS inhibition by C75. p = 0.0026 (100-20), p = 0.0002 (20-4).

FIGURE 1

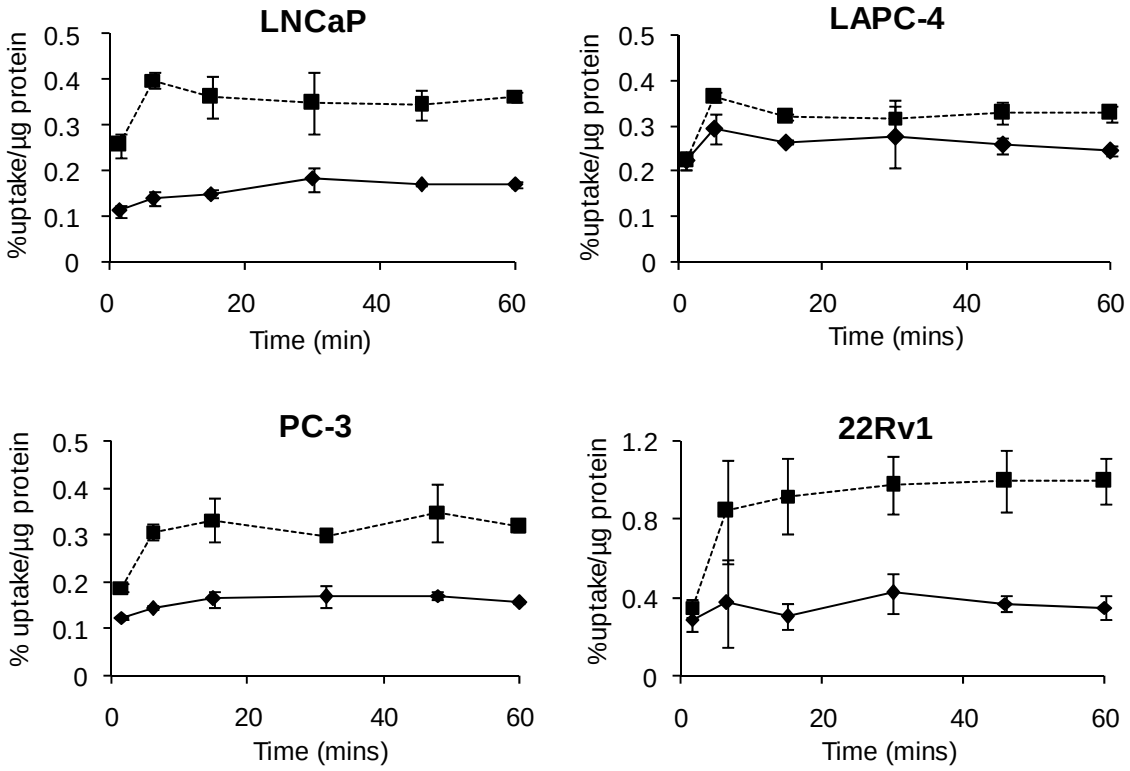
LNCaP
%uptake/µg protein
0.5
0.4
0.3
0.2
0.1
0
0
20
40
60
Time (min)
LAPC-4
%uptake/µg protein
0.5
0.4
0.3
0.2
0.1
0
0
20
40
60
Time (mins)
PC-3
% uptake/µg protein
0.5
0.4
0.3
0.2
0.1
0
0
20
40
60
Time (mins)
22Rv1
%uptake/µg protein
1.2
0.8
0.4
0
0
20
40
60
Time (mins)

FIGURE 2

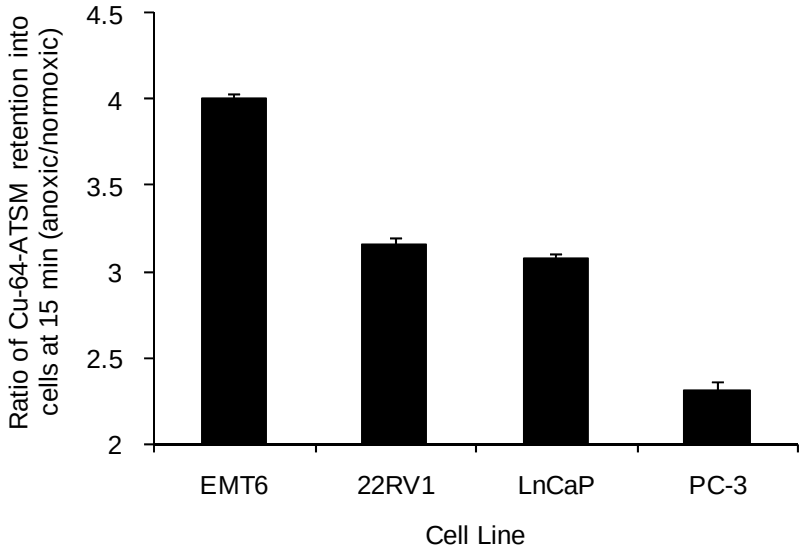
Ratio of Cu-64-ATSM retention into cells at 15 min (anoxic/normoxic)
4.5
4
3.5
3
2.5
2
EMT6
22RV1
LnCaP
PC-3
Cell Line

FIGURE 3

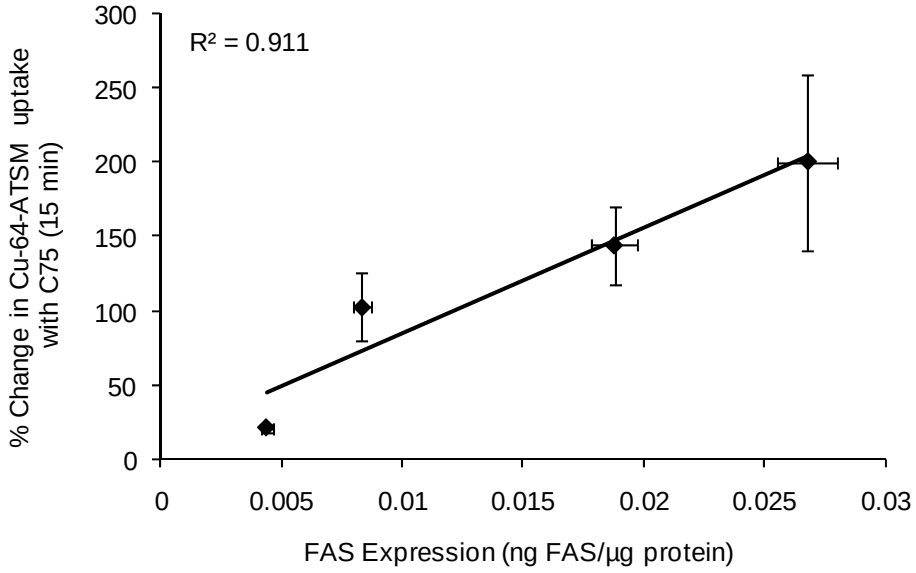
R² = 0.911
% Change in Cu-64-ATSM uptake with C75 (15 min)
300
250
200
150
100
50
0
0
0.005
0.01
0.015
0.02
0.025
0.03
FAS Expression (ng FAS/µg protein)

FIGURE 4

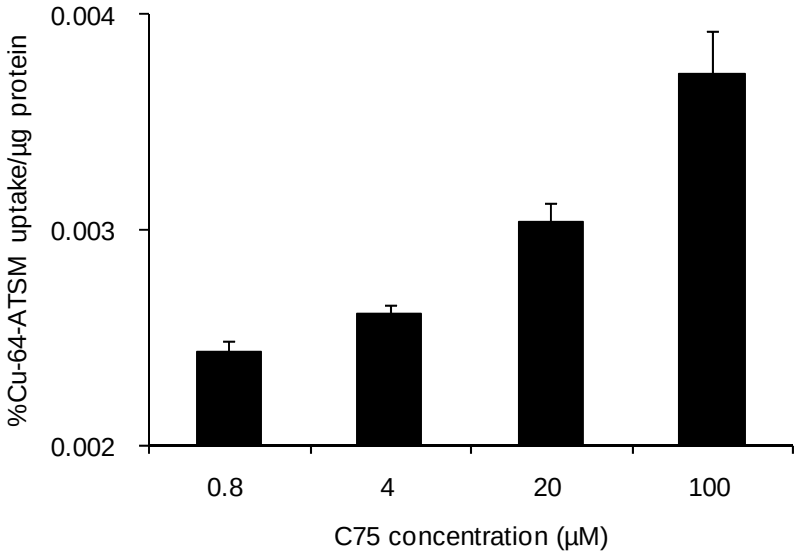
0.004
0.003
0.002
%Cu-64-ATSM uptake/µg protein
0.8
4
20
100
C75 concentration (µM)